DELIVERY OF MONOCLONAL ANTIBODIES FROM MICROENCAPSULATED CELLS

Assem Ashimova

A thesis submitted in partial fulfillment of the requirement of Nazarbayev University for the degree of Doctor of Philosophy in Science, Engineering and Technology

Supervisory committee:
Dr. Gonzalo Hap Hortelano, Nazarbayev University
Dr. Jeannette Kunz, Nazarnayev University
Dr. Gorka Orive, University of the Basque Country

February 2023

Declaration

I declare that the research contained in this thesis, unless otherwise formally indicated within the text, is the original work of the author. The thesis has not been previously submitted to this or any other university for a degree and does not incorporate any material already submitted for a degree.

Signed: 

Dated: February 21, 2023

ABSTRACT

The use of monoclonal antibodies (mabs) is a promising therapeutic approach for the prophylaxis and treatment of a wide range of illnesses, including cancer, autoimmune, and infectious disorders. They currently rank among the most widely used drugs in the pharmaceutical sector. The area of medicine where mabs are most extensively employed is oncology. Unfortunately, the complicated and costly nature of mab design, mab secretion, and purification are prohibitive and pose a hurdle to product development and pre-clinical modification, which is a significant obstacle to the use of mab therapy in clinical practice. Additionally, parenteral mab administration also poses clinical difficulties. Patients experience mild-to-moderate injection site and infusion-related responses, despite mab therapy having a low overall reactogenicity.

Here, we proposed that mabs might be efficiently given by allogeneic cells that produce mabs and are encapsulated to increase cell viability and safeguard against host immunological reactions. Various illnesses, such as diabetes mellitus, anemia, cancer, and neurodegenerative disease, have been successfully treated in animal models and people through the delivery of therapeutic drugs by microencapsulated single-cell populations. A single injection of microcapsules is anticipated to be effective since the microcapsules can be tailored to last for the duration necessary for the treatment by altering the concentration of alginate and the cross-linking of alginate with PLL. While preventing immune cells from attacking the enclosed cells, the biocompatible membrane permits a bidirectional flow of nutrients, oxygen, and waste products. When a slow, continuous mab release over a lengthy period of time is necessary, cell encapsulation-aided mab delivery is preferable to bolus mab injection.

Therefore, in this pre-clinical model, we investigated the feasibility of mab administration utilizing an enclosed cell culture that expresses mab. Until now, transformed hybridoma cells have been used to produce and secrete mabs. The novelty of this study is the use of non-professional immune cells, such as murine G8 myoblasts and human HEK293 (human embryonic kidney cells) cells, to secrete mabs. These cells were transfected with plasmids that encode the heavy and light chains of human IgG specific for antigens relevant in treating cancer and COVID-19 and then enclosed in alginate microcapsules. Afterward, immunocompetent (C57/BL6J) mice were intraperitoneally implanted with the microcapsules, and changes in the level of circulating mab were evaluated. Western blotting, ELISA, and microscopy were used to characterize the mab both *in vitro* and *ex vivo*. Co-transfected G8 cells secreted intact IgG at sustained levels similar to transfected HEK293 cells. Partial characterization of the secreted mab was performed. Mice implanted with

microcapsules containing G8 cells secreting mab induced the detection of blood mab for 40 days. This study shows the feasibility of cell microencapsulation for the systemic delivery of intact mab. This method has potential significant therapeutic applications that call for further investigation.

ACKNOWLEDGMENTS

Special thanks to Nazarbayev University for the opportunity to work with the leading edge in exciting research resources and for the unique atmosphere provided here.

Firstly, I would like to express my sincere gratitude to my lead supervisor Professor *Gonzalo Hortelano* for giving me the opportunity to be part of his research group, for his patience and motivation, for gently guiding me through this journey, creating a friendly and professional atmosphere, positive and kind attitude and for endless support in every aspect of my research and Ph.D. life.

I would greatly like to thank my external supervisor, *Professor Gorka Orive,* for giving me an opportunity to visit his laboratory at the University of Basque Country and for taking the time to review my work and providing valuable comments and professional advice.

I would also like to extend my gratitude to *Dr. Jeannette Kunz,* who agreed to co-supervise me, share her immense expertise, and promptly respond to my questions.

I express my deepest gratitude to *Professor Luis R. Rojas-Solorzano* for his positive attitude, genius support, and help to Ph.D. students at Nazarbayev University.

I want to give special thanks and gratitude to our former lab member, *Baur Negmetzhanov,* for his support starting from day one. His strong management skills and support have been an invaluable experience and motivation for me.

I special thank *Sergey Yegorov* for sharing his invaluable knowledge and experience, for critical reviews of experiments and manuscripts, and for his valuable time and patience.

My deepest thanks also go to *Askhat Myngbay,* who helped me design and troubleshoot the experiments.

I greatly appreciate my colleagues and study team members sharing the laboratory experience during my Ph.D. journey. It was a great pleasure to work with great young researchers and colleagues who became my friends: *Balnur Zhaisanbayeva, Aigul Raimbekova, Yeldar Baiken, Ainur Zhulamanova, Madina Satayeva, Ulpan Kart, Samat Bayakhmetov, Bimarzhan Assatova,*

Akbayan Yerishova, Angelina Verloka. I'm grateful to them for making these years an interesting and exciting journey.

I very much appreciate the help of our collaborators from the National Center of Biotechnology, Karaganda Medical University, and National Laboratory Astana, especially *Yuliya Safarova,* for helping with *in vivo* experiments.

I greatly thank the members of my thesis examination committee: *Professor Enrico Marsili, Professor Ferdinand Molnar, and Professor Konstantinos Kostas.*

I also want to thank the Thesis Examination Arrangement committee members: *Professor Konstantinos Kostas, Professor Damira Kanayeva,* and *Professor Daniele Tosi.*

I also thank my best friend, Zhadyra Yerkesh, who supported me throughout these years despite being in different countries.

I especially thank my amazing husband and partner, my best friend *Yelaman Konysbek,* who motivated and fully supported me throughout this Ph.D. adventure and life.

Finally, I want to express my endless love and sincere appreciation to my family, my lovely father, *Nurzhan Suleimenov* and mother, *Meirash Suleimenova*, to my sisters *Yenlik Ashimova* and *Khorlan Ashimova* and brother *Abay Ashimov*. None of my achievements would have been possible without their lifelong support, prayers, care, and sacrifices for educating and preparing me for my future.

This Ph.D. thesis is lovingly dedicated to my parents.

TABLE OF CONTENTS

THESIS OUTPUTS

PUBLISHED ARTICLES:

1. **Ashimova A**, Myngbay A, Yegorov S, Negmetzhanov B, Kadyrova I, Yershova A, Kart U, Miller MS, Hortelano G. Sustained Delivery of a Monoclonal Antibody against SARS-CoV-2 by Microencapsulated Cells: A Proof-of-Concept Study. *Pharmaceutics*. 2022; 14(10):2042. https://doi.org/10.3390/pharmaceutics14102042
2. **Ashimova**, **A.N.,** Yegorov, S., Negmetzhanov, B. and Hortelano, G., 2019. Cell Encapsulation Within Alginate Microcapsules: Immunological Challenges and Outlook. *Frontiers in Bioengineering and Biotechnology*, *7*, p.380.
3. Kadyrova I, Yegorov S, Negmetzhanov B, Kolesnikova Y, Kolesnichenko S, Korshukov I, Akhmaltdinova L, Vazenmiller D, Stupina Y, Kabildina N, **Ashimova A**, Raimbekova A, Turmukhambetova A, Miller MS, Hortelano G, Babenko D. High SARS-CoV-2 seroprevalence in Karaganda, Kazakhstan before the launch of COVID-19 vaccination. PLoS One. 2022 Jul 27;17(7):e0272008. doi: 10.1371/journal.pone.0272008. PMID: 35895743; PMCID: PMC9328563.

AWARDS:

Laureate of the “Daryn” State Youth Prize in the Science nomination, Kazakhstan, December 2020

LIST OF TABLES

LIST OF FIGURES

domain (RBD) ELISA and standardized to the non-transfected supernatant readout.

Figure 24. SARS-CoV-2 monoclonal antibody secretion in G8 cells co-transfected with the CR3022 heavy and light chains.

Figure 25. Western blotting of supernatants from control (non-transfected) G8 cells (a) and commercial BEI CR3022 mab (b).

Figure 26. SARS-CoV-2 monoclonal antibody secretion in HEK293 cells co-transfected with the CR3022 heavy and light chains.

Figure 27. Purified cell culture supernatants and the BEI CR3022 mab were denatured prior to Western blotting.

Figure 28. Representative ELISA plot of S-IgG binding for G8 cell supernatants untransfected, transfected, encapsulated cells to compare with the human plasma of a patient with COVID-19.

Figure 29. Alginate microcapsules containing G8 cells. Images were taken using light (at ×4 and ×10 magnification) and scanning electron microscopy (at ×800 magnification).

Figure 30. Representative output from the automated cell counter shows the cells' count and viability from retrieved microcapsules.

Figure 31. Supernatants obtained from non-encapsulated and encapsulated G8 cells consistently secreting CR3022 48 hours after the last culture media change.

Figure 32 A, B) Changes in the levels of circulating SARS-CoV-2 mab following the administration of microcapsules. Results from the RBD-IgG ELISA were shown as OD450 readings (A) and mab concentration adjusted to mouse plasma implanted with the CR3022-naïve G8 microcapsules (B).

Figure 32 C) SARS-CoV-2 monoclonal antibody (CR3022) identification in mice after implantation for more than 40 days. Experiments were conducted in triplicate, and error bars indicate standard deviation.

Figure 33. Neutralization assay showing partial neutralization.

Figure 34. ELISA measurement of the mouse anti-CR3022 antibody response.

Figure 35. G8 cell-containing alginate microcapsules were removed from the peritoneal cavity after 40 dpi.

Figure 36. Pre-implantation and post-retrieval levels of CR3022 secretion (RBD-binding mab per capsule) at day 40.

Figure 37. Alginate microcapsules washing steps. When time is not indicated, a brief wash period followed by suction of solution was used.

Figure 38. OD values of *in vitro* expression of human FIX from A) G8, B) C2C12 cells, C) Pos/Neg controls.

Figure 39. Images of alginate microcapsules containing cells after retrieval from mice.

Figure 40. Mouse antibodies level to human FIX.

LIST OF ABBREVIATIONS

Ab - Antibody

ACE2 - Angiotensin-converting enzyme 2

ADCC - Antibody-dependent cellular cytotoxicity

Ag – Antigen

APA - Alginate-PLL-alginate microcapsules

ATP - Adenosine triphosphate

BME - β-Mercaptoethanol

Ca^{2+} - Calcium ions

CDC - Complement dependent cytotoxicity

CDR - Complementary-determining region

CD20 - Cluster of differentiate 20

DAMPs - Damage-associated molecular patterns

DEAE - Diethyl aminoethyl

Dpi- Days post-implantation

EGFR - Epidermal growth factor receptor

EMA -European Medicines Agency

Escherichia coli- E. coli

EUA - Emergency use authorization

FcR - Fc Receptors

FDA - Food and Drug Administration

Fv - Fragment variable

h – Hour

HA - Hyaluronic acid

HAMA - Human anti-mouse antibody

HEK293 - Human embryonic kidney cells

HGPRT - Hypoxanthine-guanine-phosphoribosyltransferase

hIgG - Human immunoglobulin

HMGB - High mobility group box

HNSCC - Head and neck squamous cell carcinoma

HC – Heavy chain

Ig - Immunoglobulin

IVIG - Intravenous immunoglobulin G

LC – Light chain

mA – Milliampere

mab - Monoclonal antibody

NK - Natural killer

OD - Optical density

Opti-MEM - Modified Eagle's Minimum Essential Medium

PEG - Polyethylene glycol

PLL - Poly-L-lysine

PLO - Poly-L-ornithine

PrEP - Pre-exposure prophylaxis

PVDF - Polyvinylidene difluoride

RA - Rheumatoid arthritis

RBD - Receptor-binding Domain

RT - Room temperature

S protein - Spike protein

SARS-CoV-2 - Severe acute respiratory syndrome coronavirus 2

scFv - Single-chain variable fragment

TL9 - Toll-like receptor 9

TMPRSS2 - Transmembrane serine protease

TNF-α -Tumor necrosis factor alpha

Tregs - Regulatory T cells

UV – Ultraviolet

US -The United States

V - Variable

w/v - Weight/volume

CHAPTER 1

1.1 INTRODUCTION

Monoclonal antibodies (mabs) are among the most promising therapeutic products in the pharmaceutical industry and medicine. Antibodies have overtaken prescription pharmaceuticals as the industry's top sellers in the last five years, and by 2020, biologics accounted for eight of the top 10 bestselling drugs globally. The US Food and Drug Administration (US FDA) has authorized 79 therapeutic mabs, all currently available. Nonetheless, the complicated and costly features of mab manufacturing, where mab manufacture and purification are notoriously expensive and offer difficulty for product development and pre-clinical modification, is a substantial obstacle to applying mab therapy in clinical practice. In order to increase cell survival and protect against host immunological reactions, this study proposed that mabs might be efficiently supplied by encapsulated allogeneic cells that express mabs.

The biocompatible membrane permits a bidirectional flow of nutrients, oxygen, and waste products by preventing immune cells from attacking the enclosed cells. The microcapsules can be engineered by adjusting the concentration of alginate and the cross-linking of alginate with PLL to last for the length of time desired for the treatment so that a single injection of microcapsules is expected to be effective. When a stable, progressive mab release is required, cell encapsulation-aided mab delivery is preferable to bolus mab injection. Previous research demonstrated mab delivery from hybridoma cell lines. With this method, therapeutic amounts of mab were delivered over an extended period of time to numerous animal models. Unfortunately, hybridoma cells, murine cells produced by fusing a B lymphocyte and a malignant myeloma cell, cannot be used for human implantation. As demonstrated in this study, the potential therapeutic range of encapsulated technology to deliver mab is expanded by the capability of using encapsulated genetically altered cells that are not expert antibody-secreting cells. The novelty of this thesis is based on examining whether encapsulated non-professional immune cells such as myoblasts can produce and release mabs levels against SARS-CoV-2 *Spike* protein, CD20, and EGFR antigens, at clinically relevant levels. This study aimed to prove that it was possible to maintain functioning mabs in genetically modified encapsulated cells in a pre-clinical animal model.

1.2. THESIS HYPOTHESIS

The hypothesis of this thesis is that non-immune cells can be genetically engineered to secrete and deliver functional and clinically relevant levels of monoclonal antibodies through alginate microcapsules.

1.3. SPECIFIC AIMS

AIM I: DELIVERY OF MONOCLONAL ANTI-EGFR AND ANTI-CD20 ANTIBODIES FROM MICROENCAPSULATED CELLS. More specifically:

A. Design and synthesis of DNA coding for monoclonal antibodies against EGFR and CD20 antigens of cancer

B. Characterization of secreted monoclonal antibodies in transfected cells

C. Delivery of monoclonal antibodies from microencapsulated cells

AIM II: DELIVERY OF FUNCTIONAL MONOCLONAL ANTI-SARS-COV-2 ANTIBODIES FROM MICROENCAPSULATED CELLS. More specifically:

A. DNA plasmid coding for the constant and variable regions of the heavy and light chains of monoclonal antibodies against SARS-CoV-2 Spike protein

B. Characterization of secreted monoclonal antibodies in transfected cells

C. Delivery of monoclonal antibodies from microencapsulated cells

D. Functional characterization of secreted monoclonal antibodies

AIM III: MODULATION OF IMMUNE RESPONSE. More specifically:

A. Characterization of secreted hFIX, Fc, and mIL-10 proteins in transfected cells

C. *In vivo* delivery of monoclonal antibodies from microencapsulated cells

D. Characterization of immune response to immune modulators

1.4 THESIS ORGANIZATION

The Ph.D. thesis consists of six chapters.

Chapter 1 is the introduction that outlines the thesis, thesis hypothesis, and specific aims.

Chapter 2 presents a broad literature review of the appropriate research work presented in the thesis. The first part supports the topics that include the IgG structure, classification, cost, production, and purification methods. In contrast, the second section discusses the main targets of mabs against cancer or other infectious diseases. The third section presents the cell encapsulation strategy for drug delivery, which comprises the different cell sources and biomaterials for capsule formation. The literature review ends with the immunology part describing the immune responses elicited by antigens.

Chapter 3 addresses Aim 1 by describing *in vitro* experiments toward developing monoclonal antibodies against cancer. The chapter describes in detail all the methods for the mab DNA design, synthesis, and characterization of mabs against EGFR and CD20 antigens, cell culture, and mab secretion from free and encapsulated cells.

Chapter 4 focuses on Aim 2 by describing *in vitro* and *in vivo* experiments and the findings from these studies. The chapter describes in detail all the methods for the mab DNA vectors, synthesis, and characterization of mab against SARS-CoV-2. This chapter also describes cell culture and mab secretion from free and encapsulated cells. Finally, the delivery of mab from encapsulated cells implanted in mice is described.

Chapter 5 presents efforts toward modulating the immune responses to transgenes delivered through alginate microcapsules *in vivo* through the co-delivery of an antigen and immunomodulatory molecules from genetically engineered encapsulated cells.

Chapter 6 offers conclusions from the results of this thesis and discusses potential directions for future research.

CHAPTER 2

LITERATURE REVIEW

2.1 Immunoglobulin

The scientific concept of the "magic bullet" was established by Paul Ehrlich, who, in 1890, anticipated that antibodies could be used to deliver chemically combined poisonous agents to specific cell types and that it might be possible to kill the particular disease-causing organism while causing no harm to the body itself [1]. Later, in 1975, George Köhler and César Milstein described the hybridoma technology, which enables the continuous cultivation of antibody-secreting cells with a determined specificity. Antibodies, also recognized as immunoglobulins (Ig), are glycoproteins produced in large quantities by B-cells. Antibodies play a crucial function in the immune system as a part of adaptive immunity, specifically by recognizing and neutralizing immunogenic foreign pathogens such as bacteria or viruses, as well as other disease-causing organisms [2]. Each antibody is generated due to the immune system's reaction to a specific antigen. Antigens include peptides, carbohydrates, fats, and DNA, which cause the immune system to respond, leading to the growth of lymphocytes and particular antibodies produced by those antigens. The antigen receptor for the cells in the B-cell receptor, B-cell membrane-bound immunoglobulin. Spatial complementarity interactions occur between antibodies and antigens (lock and key). The parts of the antigen that the antibody recognizes are known as epitopes [3].

2.1.1 Antibodies structure and function

Immunoglobulins are sizeable globular plasma proteins secreted mainly by B-cells and act primarily as a defense against antigens. They are the most abundant proteins in plasma and are essential components of the immune system [4]. Circulating antibodies can effectively identify, kill, or neutralize foreign pathogens. They also cause apoptosis by interacting with specific cell surface molecules [5].

Human IgG has a molecular weight of approximately 150, 000 daltons and a size of about 10 nm [3]. It is a roughly Y"-shaped glycoprotein composed of 4 polypeptide chains: 2 equal heavy chains (HC, MW-approximately 50-70 kDa) and 2 similar light chains (LC, MW-approximately 25 kDa), which are connected by interdomain disulfide bonds and non-covalent hydrophilic and hydrophobic connections [6]. Covalent binding between sulfhydryl groups of cysteine molecules and non-

covalent bonds hold two HCs together [7]. Both heavy and light chains have the variable (V) and constant (C) regions at the N- and C-termini, respectively. In contrast to the LC, which has one constant (CL) and one variable domain (VL), the HC has four parts: three constants (CH1, CH2, and CH3) and one variable (VH). The constant regions serve as the structure's backbone [6].

Each antibody molecule contains three distinct functional fragments: two antigen-binding fragments (Fab region) and one fragment crystallizable region (Fc region) [6]. These two parts are connected by a hinge region, which provides conformational flexibility in antibodies after adhering to antigens or when the substance moves through the body. Each region of the antibody serves a distinct purpose. The Fab region functions as an antigen-binding site, allowing specific antigens to be recognized. Antibody specificity toward antigens is caused by the antigen-binding site, especially the complementary-determining regions (CDR) of the N-terminal Ig region in both the HC and LC [8]. The CDRs are divided by systemically conserved regions that form a β-sheet structure presenting these loops on the surface of the variable domain [9]. Each variable domain contains three CDR loops, which are responsible for an antibody-antigen specificity [10]. They are identified as L1, L2, L3, H1, H2, and H3 [11]. The Fc region, which forms the base of a "Y" structure, determines the effector capabilities of antibodies, for example, complement activation connection with Fc receptors (FcRs) and the generation of a corresponding immune response to a given antigen [12]. When an antibody binds to a specific antigen, it activates the conventional route of complement-dependent cytotoxicity (CDC) as well as antibody-dependent cellular cytotoxicity (ADCC). The cytolytic action of effector cells whose surface antigens are bound to specific antibodies is ADCC. ADCC is important in the clinical impact of anti-tumor mabs like Herceptin and Rituximab [13].

2.1.2 Classification and functions of immunoglobulin isotypes

Immunoglobulins are divided into 5 significant isotypes depending on the arrangement of their heavy chain, with some having multiple subtypes. Immunoglobulin A (IgA), Immunoglobulin D (IgD), Immunoglobulin E (IgE), Immunoglobulin M (IgM), and Immunoglobulin G are the five major types of immunoglobulin (IgG). There are different forms of HCs indicated by Greek letters: μ, γ, ε, α, and δ, which define the antibody type, especially IgM, IgG, IgE, IgG, and IgD [14]. Also, there are two varieties of LC: kappa and lambda. There is just one form of LC produced by each B-cell. The ratio of the two types of LC varies between species. Each LC class has two regions: a constant domain (CL) and a variable domain (VD).

In contrast, the HC subclasses IgA, IgD, and IgG have 3 constant (C) and 1 variable (V) domain. IgE and IgM have four constant domains and one variable domain. "Y" shaped macromolecules

have a monomeric basic structure. IgD, IgE, and IgG antibody isotypes are monomers, whereas IgA is a dimer and IgM is a pentamer [6]. IgM's pentametric structure is helpful because it has a low affinity. Still, as a pentamer, it can bind to many instances of the target protein on the antigen at the same time, resulting in avidity [15]. Each immunoglobulin isotype's structure and functions are highly variable [14].

IgM

IgM is the most abundant immunoglobulin, and it is expressed in early B-cell development as a component of the adaptive humoral immune response of the organism to an outside infection [16]. IgM is a heterotetramer with a molecular mass of approximately 990 kDa [17] that is made up of five or, in rare cases, six subunits. IgM accounts for about 15% of normal adult immunoglobulin. These molecules form pentamers, which makes them particularly effective at activating the complement system [18].

Disulfide linkages that are covalently formed between the Fc domains of IgM molecules and between the single cross-linking joining (J) chain and IgM Fc regions stabilize pentameric IgM. The J chain is a small 15 kDa polypeptide linker that promotes mucosal surface secretion and regulates IgA and IgM formation [19]. This chain is formed in the cells that secrete IgA. Even though monomeric IgM has a weak antibody-binding potential due to immaturity, the multivalent structure of the molecule provides a strong avidity of pentameric antibodies.

IgD

IgD is a monomeric immunoglobulin isotype found in low concentrations in blood serum, accounting for around 0.25% of all antibodies. The immunoglobulin isotype has a molecular weight of 185 kDa and a half-life of 2.8 days, comparable to IgE [20]. It also comprises two of the same heavy polypeptide chains of the delta class, and two conform light polypeptide chains. When a B-cell departs the bone marrow and populates secondary lymphoid organs, the IgD molecule is expressed. When B-cells reach maturity, they co-express surface IgD and IgM and take a role in B-cell receptor activation. It has also been discovered that IgD binds to basophils and mast cells, causing them to develop antibacterial factors that are useful in allergic reactions [21].

IgA

IgA is a type of immunoglobulin involved in mucosal surface immunity and serves as an important first-line defense against toxins, viruses, and bacteria. IgA levels in mucosal surfaces and secretions,

such as tears, saliva, sweat, and colostrum, are higher than in all other antibody isotypes combined [22]. IgA has two subclasses (IgA1 and IgA2) with different hinge regions, with IgA1 having a more extended hinge region than IgA2. It is possible to produce monomeric and dimeric versions of IgA [23]. A dimeric form of IgA called secretory IgA (sIgA) is made up of two or more monomeric IgA molecules that are covalently bound together by the J peptide and a second polypeptide chain called the secretory component (SC), which is obtained from the polymeric-Ig receptor (pIgR) found in endosomes [24].

IgE

IgE is a large, globular protein found only in mammals that are linked to type I hypersensitivity and allergic response. IgE has a structure similar to IgG, but it lacks a hinge region, and it features an additional interstrand disulfide among its CH2 domains, creating its CH3 and CH4 areas more similar to IgG's CH2 and CH3 regions [25]. IgE has the shortest half-life and is the less plentiful of the antibody isotypes, having a concentration of approximately 150 ng/mL in human plasma contrary to 10 mg/mL IgG in an average individual [26]. IgE binds to two different types of receptors. The FcRI is a strong affinity IgE receptor that was found on mast cells, eosinophils, basophils, and Langerhans cells and was involved in allergic responses. The second is low-affinity FcRII, which is secreted only on B-cells and also helps to regulate IgE levels [27].

IgG

The most prevalent antibody isotype within the human body is IgG. And that accounts for approximately 75% of the total antibody circulating mass. IgG possesses the greatest serum half-life among any immunoglobulin isotype, lasting about 15-25 days [28]. As previously stated, IgG consists of two identical heavy chains (50-70 kDa) and two similar light chains (25 kDa), yielding a molecule of about 150 kDa. Four linked gene codes IgG HCs, resulting in the subclasses IgG1, IgG2, IgG3, and IgG4 [28]. They are distinct in terms of the hinge and constant regions. The IgG`s Fc domain can interact with FcRs normally secreted via cytotoxic cell lines (macrophages and NK cells) [29], resulting in different effector functions for different subclasses. The FcR is in charge of cell-mediated recognition of antibody-antigen complexes. IgG1 and IgG3 isotypes activate the complement system more efficiently and bind to macrophages and monocytes more effectively [30]. The IgG4 antibody is a blocking antibody for anaphylactic sensitization reactions [31]. IgG2 antibody has the minor effector function but is primarily responsible for anticarbohydrate IgG responses to bacterial capsular polysaccharides [28].

2.1.3 Monoclonal antibodies in the clinic

Because mabs can be targeted towards antigens on cell surfaces, using them in clinics is one method of combating cancer and other diseases. Mabs can attack cancer cells directly or as carriers for other compounds used for treatment or diagnosis. Because of their immune system functions, antibodies can be used in clinical diagnostics, therapeutic applications, and medical research. In the clinic, mabs are safe and effective in the course of treating a broad spectrum of diseases involving cancer and other autoimmune illnesses [32]. Muromonab-CD3 (Orthoclone OKT3), the initial pharmaceutical mouse anti-human mab, was certified by the US FDA in 1986 to treat leukemia [33]. Approximately 100 therapeutic mabs have been approved by the US FDA or the European Medicines Agency (EMA) between 1986 and December 2019 [34].

Mabs are currently among the most popular medications in the pharmaceutical industry. However, oncology is the field of medicine where mabs are already widely used to treat a variety of cancers (lymphoma, myeloma, glioblastoma, melanoma, neuroblastoma, lung, breast, colorectal, head and neck, and ovarian cancers). A pioneering mab against cancer was Rituximab (Rituxan), a chimeric anti-CD20 mab, which was authorized to be used in medicine in 1997 [35]. The vast majority of mabs are designed to combat multiple diseases [36]. More than 570 mabs are currently being tested in clinical studies (Phase I, Phase I/II, and Phase II), with six novel therapeutic mabs approved in 2019 [37]. Mabs can be used alone or in combination with cytokines, toxins, radioisotopes, or other active substances during therapy and diagnosis of cancer [38]. Herceptin (Trastuzumab), a treatment for metastatic breast cancer, is an example of a successful combination of a cytotoxic drug and an antibody that recognizes receptors on cancer cells. Herceptin is a mab that has been humanized and suppresses the growth of cancer cells by binding to the HER2 receptors [39]. Also, mab therapy is a method of treating complex diseases in rheumatoid arthritis (RA) and other inflammatory disorders [40]. Several clinical trials have shown that blocking the inflammation-promoting cytokine molecule tumor necrosis factor-alpha (TNF-α) with anti-TNF antibodies is a long-term effective therapy [41,42]. Adalimumab (Humira) is the best-selling mab in the world that inhibits TNF. In 2002, it was licensed for medical usage in the US[43].

Coronavirus disease 2019 (COVID-19) mab therapy is well tolerated and poses few risks. The most frequent adverse outcomes recorded are responses at the site of injection and responses from infusions. Infusion-related reactions are common with drugs such as rituximab, and possible side effects might occur after giving mabs [44,45]. An infusion response might include flushing, fever/chills, back discomfort, stomach pain, pruritus, or skin irritations, among other symptoms. Typically reactions associated with infusion appear 30-60 minutes after the injection is started. Most

infusion-related responses are self-limiting and manageable by halting the infusion and treating the signs. When the symptoms have subsided, the infusion can be reintroduced more gradually [46]. Responses to infusions happened in 1% of the patients who received sotrovimab. Diarrhea was the most commonly reported side effect (1%) [47]. Mabs are an effective treatment option for mild to severe COVID-19 infection in non-hospitalized patients. However, throughout the global pandemic, mabs were in limited availability. Individuals who are more likely to require hospitalization or die as a result of COVID-19, such as the elderly and those with chronic illnesses, are prioritized by federal guidelines.

2.1.4 Development of therapeutic antibodies

Muromonab-CD3 is a murine immune system-produced anti-human protein. When the first therapeutic mab Muromonab-CD3 was injected into a human, the host responded with an immunogenic response, including anaphylactic shock. The human Fc region was substituted for the murine sequences in one solution to the immunogenicity problem [48]. As a result, several mab groups based on protein origin were developed: human mabs, murine mabs, humanized mabs, and chimeric mabs [49]. Mabs are named after their specific structure, and the suffix of the mabs name indicates the manufacturing method.

Murine antibodies are entirely composed of rodent host proteins. Murine antibodies played a vital role in the creation of therapeutic antibodies. On the other hand, treatments using murine antibodies were ineffective and had numerous drawbacks. This is because after receiving these mabs intravenously, patients developed a human anti-mouse antibody (HAMA) response. HAMA reactions have been identified in about 50% of cases following one dose of murine mabs, which exceeds 90% of developing HAMA after two or three additional shots [50,51]. As a result, engineering clinically interesting murine mabs into those that function more like human Ig is advantageous. To accomplish this, important occurrences from the human heavy chain backbone were transferred to the structure of the xenogeneic murine antibodies, preserving the Ag-binding properties. Both chimeric and humanized mabs can be given to patients for long periods without causing a clinically significant immune response [52]

Chimeric antibodies contain genetic materials from various species, accounting for roughly two-thirds of human protein. The constant regions of mouse mab, for example, could be replaced by another species, such as a human [53]. A chimeric antibody's structure is composed of approximately 70% human material [54]. Chimeric antibodies were first developed in 1980, and recombinant DNA

was investigated. Abciximab, the initial chimeric antibody, was authorized by the US FDA in 1994 to inhibit platelet aggregation by blocking platelet glycoprotein IIb/IIIa receptors [55].

Humanized antibodies are non-human antibodies that have been genetically engineered to be more similar to antibodies produced naturally in humans [56]. Only about 5-10% of these mabs are from other species. Humanized antibodies have several advantages over murine mabs, including lower immunogenicity, human effector mechanisms, and longer half-life of serum [57]. The first humanized mab, daclizumab, was approved by the US FDA in 1997. Daclizumab is a mab that prevents the body from rejecting the transplanted organ.

Fully human antibodies, which lack murine sequences, were created by expressing isolated human variable domain genes in *Escherichia coli* (*E. coli)* [58,59]. Transgenic mouse expression or phage display, in which a collection of human antibodies are displayed on the exterior of the phage and then chosen and boosted in *E. coli*, are the primary methods for producing these antibodies.

2.1.5 Hybridoma Technology

The scientists César Milstein and George Köhler 1975 achieved one of science's most significant breakthroughs when they successfully fused short-lived B-cells that produce antibodies with a myeloma cell line that has been immortalized, creating a hybridoma [2]. Cloning and testing these hybridoma cells would follow the mass mab production on a large scale. This endeavor won the two scientists the Nobel Prize in 1980. The findings demonstrated the ability to isolate different hybrid lines that produce antibodies directed against the same antigen but with various effector functions. The idea behind this technology is that the cells produced by this fusion will have characteristics of both parental cells. They can produce specific antibodies against an antigen used for donor immunization from spleen cells, and they obtain cancerous capacity for immortal multiplication *in vitro* or *in vivo* from myeloma cells. The myelomas used for the fusion are pre-selected to ensure that they lack the hypoxanthine-guanine-phosphoribosyltransferase (HGPRT) gene and are not secreting antibodies. To select fused cells, HAT medium (hypoxanthine-aminopterin-thymidine) is used. Unfused myeloma cells cannot use the de novo or salvage pathways to produce nucleotides due to the absence of the HGPRT gene, and non-fused B-cells possess a brief lifespan [60]. This technique is still widely used to produce antibodies more than 45 years after it was discovered.

The therapeutic action of mabs is exerted over a period of time, such as the targeting of specific tumor cells with mabs. Thus, ideally, the delivery of mabs will be done in a sustained manner. Currently, repeated bolus administrations are required. Therefore, alternative delivery strategies are

desirable. Gene therapy could provide an answer to this challenge. However, *in vivo,* delivery of vectors coding for mabs could face immunological and/or safety concerns. Transplantation of cells secreting functional mabs could be considered but transplanted cells would also face immune rejection. The use of microencapsulated allogeneic cells could overcome cell rejection.

Another knowledge gap is the fact that only lymphocytes or tumor-derived hybridomas have been used for the expression and secretion of mabs. This thesis aimed to bridge this gap by proposing the use of safe non-professional immune cells such as myoblasts. In contrast to proliferative cells such as fibroblasts, encapsulated myoblasts have been shown to restrict their proliferation and remain viable for months.

2.1.6 Recombinant production host systems

There are numerous options available when it comes to selecting a host for the creation of a particular recombinant protein. Because it has a wide range of expression systems and is simple to cultivate, the *E. coli* bacterium is typically the launching point for any cloning and expression effort [61]. However, there is no standard host system for expression that is effective for all proteins. Despite being more complicated and expensive, mammalian cell culture is frequently the only option for synthesizing big proteins that demand much post-translational glycosylation. As a result, the first factor to consider when choosing the best production host must be the product's glycosylation. The second criterion is frequently annual production requirements. Lower production quantities and, as a result, higher investment prices are associated with higher titers. Because host development times vary so greatly between hosts, the preference for expression host frequently establishes time to market. Each system has a unique set of benefits and drawbacks. Aside from titer and capacity for post-translational modifications, technical considerations include induction methods and host protease activity. Various additional factors must be considered when aiming for industrial production, such as the royalty burden of the host cell and vector, material expenses, regulatory concerns regarding the host cell and vector, dangerous byproducts, and reproducibility.

Escherichia coli - bacteria

Even though there are numerous alternatives for producing pharmaceuticals and other recombinant proteins, *E. coli* remains the most commonly used since it provides a quick and cost-effective manufacturing option [62]. The main advantages of *E. coli*, according to Sarramegna et al., [63], are the affordable production costs, the recombinant protein's characteristics, and its speedy generation.

The propensity to create inclusion bodies, however, can lead to issues in the production of recombinant proteins because the proteins must be neatly folded for sufficient biological activity. *E. coli* cannot carry out post-translational modifications and lacks a secretion system that allows for for the efficient release of proteins into the culture medium. *E. coli* is an excellent option if no post-translational modifications are needed. Commercial production of several recombinant hormones, such as insulin and interferons, takes place in *E. coli* [64].

Using phage display technology, researchers have demonstrated the quick isolation and characterization of peptides [65], proteins [66], and antibodies as therapeutic candidates for pharmaceutical research programs [67]; describe a method for isolating antigen-specific antibodies without using conventional hybridoma technology. To isolate antibodies via phage display, antibody expression on filamentous plant tips is exposed to immobilized antigen via a procedure called "biopanning." Immune libraries and nonimmune or naive antibody libraries are two types of immunoglobulin gene libraries [68].

Yeasts

Using modified *Saccharomyces cerevisiae*, at least 10 authorized biopharmaceuticals are produced. Among them are especially insulin and growth hormones. Furthermore, *Saccharomyces cerevisiae* is used to make the great majority of vaccines that are currently available on the market. The most significant of them are recombinant hepatitis B vaccinations [64]. Given its ability to reach high cell densities, ease of control, and ability to undergo posttranslational protein changes, *Pichia pastoris* would make a suitable host [69]. Post-translational modifications carried out by yeast cells are distinct from those made by cells in mammals [70]. Compared to mammalian cell systems, yeasts grow quicker and create more protein. Yeasts may have the disadvantage of producing unwanted glycosylated recombinant proteins, though the amount of glycosylation depends on the strain and expression method. *Pichia pastoris* glycosylation levels are often lower than in *Saccharomyces cerevisiae*[71].

Mammalian cells

Hybridoma cells and murine myeloma cell lines are additional mammalian cell types used in the development of biopharmaceuticals [72]. Only mammalian cell cultures can synthesize large macromolecules that require specific glycosylation. Additionally, mammalian cell cultures are used to produce every antibody-based product. Farid [73] claims that the mass of mabs are fabricated in

stirred tank bioreactors by batch or fed-batch cultivation of mammalian cell systems. Typically, the filtration and chromatography processes are used to purify mabs [73,74].

2.1.7 Purification of Immunoglobulins

Immunoglobulins are rigid molecules that can preserve biological function even after short-term pH extremes and long-term storage at -20°C. Because crude antibody preparations might pose issues with specific test techniques, separating antibodies from serum, cell culture lysates, or supernatants is commonly necessary. The sort of purification technology employed is typically defined by the degree of purity necessary for the specific use of the antibody.

At specific salt concentrations, hydrophobic interactions between molecules eventually result in immunoglobulin precipitation as the salt concentration rises. Utilizing ammonium sulfate as an initial clean-up step is typical before isolating comparatively pure immunoglobulin fractions. Purification of crude antibody preparations has also been documented utilizing separation methods using chromatography, such as anion-exchange diethylaminoethyl (DEAE) columns, that take advantage of antibodies' essential character [75].

IgG may be isolated using proteins A and G columns. Protein G interacts more strongly with immunoglobulin molecules, such as mouse IgG, than Protein A. Proteins A and G are readily linked to sepharose, providing vital support with a high immunoglobulin capacity and little nonspecific binding. The bound antibody may be eluted to high/low pH solutions after the crude antibody preparation has been applied to such column supports and washed to remove non-specifically bound protein.

The antigen of interest (such as 4'-amino warfarin) is covalently coupled to a solid support (such as Sepharose-4B) using affinity-purification techniques, which offer a convenient way to produce high-purity antigen-specific antibody preparations because both non-specific immunoglobulin and extraneous non-specific protein are eluted. A combination of buffers with a low pH and a high salt content can then be used to release the bound antibody.

2.1.8 Cost of mabs

The commercial success of mabs has been directly correlated with their clinical success. As pharmaceutical firms continue to aggressively engage in therapeutic mab research and development (R&D), it is anticipated that mabs will be the primary growth area of the prescription pharmaceutical industry between 2008 and 2020, driven by higher sales of both current products and future products [36].

The mabs market has increased between 7.2% and 18.3 % annually since 2013 at a pace. At this time, a quicker approval rate and a robust pipeline would also support market expansion. By taking this into account and basing their projections on the market's present worth, they assumed increasing annually by 10%, or 15%, which led to a forecast between US$137 and US$200 billion in value by 2022 [76]. Only 7% of the revealed production locations are in Asia, which produces most of the world's mabs, followed by the US and the EU. Within the European Union and the United States, 11 biosimilars that target the top five mabs are currently being used for therapeutic purposes.

Concerning 34% mab-indication combinations, the annual cost of treatment exceeded $100,000; the most expensive was eculizumab, and the least costly was denosumab ($2465), which is used to prevent fractures. Oncology or hematology had the highest median annual cost of care for mabs, with immunology coming in second at $53,969. 43 oncology and hematology mab-indication combinations cost more than $100,000 per year of therapy for 29 (67%) of them. Combinations of mab indications in oncology and hematology accounted for more than 85% of those priced at $100,000 or more, even though they only made up 43 of the 107 combinations of mab indications authorized during the last 20 years overall [76].

For mabs approved for "other" cancer types, such as neuroblastoma, glioblastoma, metastatic renal cell carcinoma, and urothelial carcinoma, the median yearly cost of therapy was $167,152. Head, neck, or lung cancer had the highest median treatment price ($163,746). For example, Rituximab needs 8–16 doses of 375 mg/m^{-2}, totaling 6–12 g for each patient (see http://www.rituxan.com), to be clinically effective, according to the majority of trials [48].

Because of this, vast cultures of mammalian cells must be used to produce therapeutic antibodies, followed by time-consuming purification processes conducted under Good Manufacturing Practice guidelines. As a result, producing therapeutic antibodies is very expensive, which restricts the useage these drugs. Several different manufacturing and purification techniques in plants and microorganisms are now being explored, which could result in considerable advancement shortly [77].

2.2 Targets

2.2.1 Epidermal growth factor receptor (EGFR)

Many epithelial cancers have an overexpression of the tyrosine kinase receptor known as the epidermal growth factor receptor (EGFR), which is an ErbB family member [78]. Its structure consists of a tyrosine kinase domain flanked by a carboxy-terminal tail containing tyrosine autophosphorylation sites, a short transmembrane segment, and an extracellular cysteine-rich

ligand-binding domain [79]. EGF, TGF-, Epigen, Amphiregulin, Epiregulin, and Betacellulin are the six known ligands for EGFR [80]. When a ligand binds to the receptor, it undergoes a conformational change, enabling the carboxy-terminal tail's tyrosine residues to dimerize and undergo autophosphorylation. This causes intracellular signaling to begin by binding cytoplasmic proteins to phosphotyrosine-binding domains. Several downstream pathways are activated when different docking proteins bind to the receptor. Using EGFR as a drug target prevents tumor growth, proliferation, and migration by blocking signaling pathways.

Anti-EGFR agents with clinical activity and approval for cancer treatment include mabs against the receptor extracellular domain and ATP-competitive tyrosine kinase inhibitors [78,81]. Therapeutic antibodies targeting the ErbB family have proven to be the most effective in patients with solid malignancies [82]. Anti-EGFR antibodies enhanced responses, disease management, and survival in patients with colorectal cancer who have wild-type KRas [83]. Hence the US FDA allowed their use for patients with unmutated KRas.

Cetuximab is the most widely used EGFR-specific mab and has thus been studied for its use in various tumors associated with abnormal EGFR expression. Because EGFR deregulation promotes tumorigenesis, angiogenesis, and metastasis formation, it is frequently overexpressed in many epithelial tumors, including 80-100% of head and neck cancers and 22-75% of colon cancers [84].

The US FDA approved Cetuximab in 2004 for EGFR-positive metastatic colorectal carcinoma. This decision was based on clinical phase II and III studies in CRC patients that reported reaction times of 9-12% for monotherapy with Cetuximab and 17-25% for the Cetuximab and irinotecan combination therapy. Considering the stated seven-day half-life of Cetuximab, it is suggested that patients begin their treatment with a 400 mg/m^2 starting dose and then receive weekly infusions of 250 mg/m^2. The positive effects of Cetuximab in people with head and neck squamous cell carcinoma (HNSCC) were demonstrated, guiding the approval of Cetuximab for HNSCC in 2006 [85].

The most common side effects associated with Cetuximab treatment were skin-related toxicities, typically limited to grade 1 or 2 skin rash and occurring in 86% of treated patients. Severe side effects (grade 3 or 4) were observed in 10-15% of patients, with no reports of life-threatening side effects. Other dermatological side effects, such as erythema and acne, also occurred. These side effects, which may be related to endogenous EGFR expression in keratinocytes and skin fibroblasts, are treatable symptomatically. Additional side effects, such as severe infusion reaction, IgE against oligosaccharides, and hypomagnesemia, were occasionally observed but were easily managed.

Cetuximab can eliminate EGFR-overexpressing tumor cells. Overall, the safety profile of

Cetuximab therapy, with only minor side effects, suggests that this antibody could mediate the elimination of cells engineered with a truncated EGFR. There is no reason to believe that potential side effects will be more severe in immunocompromised cell graft recipients than in immunocompetent tumor patients.

2.2.2 CD20

A group of cell surface markers known as clusters of differentiation (CD) can be used to differentiate between various B-cell maturational stages. All B-cell surfaces express CD20, an activated-glycosylated phosphoprotein that starts to build up during the pro-B phase and continues to do so until the cell reaches maturity. This protein enhances B-cell immune responses to T-independent antigens and is known to have no natural ligands [86]. Due to its high levels of expression in the majority of B-cell malignancies and the fact that it is not internalized or shed from the plasma membrane as a result of mab treatment, it serves as an ideal target for mabs. As a result, it may last a long time on the cell surface, resulting in a sustained immunological response from complements and macrophages [87]. For the last three decades, mabs targeting CD20 have been used in clinics, with constant structural modifications [88].

Rituximab is a CD20-specific humanized antibody. To treat cancer, it was the first therapeutic antibody to be approved. Several 1-3 phase clinical trials have demonstrated its efficacy against chronic lymphocytic leukemia/small lymphocytic lymphoma (CLL/SLL) and Hodgkin's lymphoma, and autoimmune adverse effects like RA, autoimmune hemolytic and anemia immune thrombocytopenia [89]. Ofatumumab, another anti-CD20 mab, appeared to have more stable CD20 binding, a slower off-rate, and greater complement-dependent cytotoxicity than rituximab. It has been demonstrated that ofatumumab mediates CDC against Raji cells that are resistant to Rituximab and CLL cells that express little CD20 because it binds a different CD20 epitope than Rituximab [90]. Twelve antibodies have received FDA approval for treating different hematological malignancies and solid tumors. Early and late-stage clinical studies also evaluate a significant number of additional therapeutic antibodies.

2.2.3 SARS-CoV-2

Severe acute respiratory syndrome coronavirus 2 (SARS-CoV-2), a novel strain, first appeared in Wuhan, China, in December 2019. Until March 2020 COVID-19 had spread like a pandemic, causing millions of deaths and devastating economic pressure on healthcare systems around the globe [91]. In addition to causing severe respiratory symptoms, SARS-CoV-2 infection can also

result in sepsis, kidney, liver, cardiac damage, and other complications. Although there are some less common COVID-19 signs like diarrhea, a loss of smell and taste, and skin rash, the most affected organ is the lungs. This is because Angiotensin-converting enzyme 2 (ACE2), which is widely expressed in tissues like the heart, kidneys, lungs, and intestines, serves as a host receptor for the *spike* protein of both SARS-CoV-1 and SARS-CoV-2. However, the majority of ACE2-expressing cells are alveolar epithelial type II cells.

In contrast to the SARS-CoV-1 outbreak in 2002-2003 (774 death), the SARS-CoV-2 global pandemic has already demonstrated enormously high death rates being over 7M [92]. Such incomparable statistical data is explained by the higher infectivity of SARS-CoV-1 and more effective capabilities of immunity evasion. Coronaviruses are single-stranded RNA-enveloped viruses. They're made up of structural proteins: nucleocapsid, envelope, and *spike*. In most cases, the S-protein is referred to as *Spike* in the literature. Since it also occurs in influenza, HIV, and Ebola viruses, coronaviruses are not the only source of this condition. The S-protein has a size range of 180–200 kDa, is typically found in trimers, and is highly conserved (76%) in both SARS-CoV-1 and SARS-CoV-2 [93]. Nevertheless, those two viruses' Receptor-binding Domain (RBD) differs significantly from one to the other (74% and 50%, respectively), noting extensive mutagenesis. Two subunits make up the protein: S1 and S2. In conclusion, S1 primarily binds to the host receptor, whereas S2 allows fusion and subsequent infection. The host serine protease transmembrane serine protease 2 (TMPRSS2) cleaves between S1 and S2 to signal the start of the infection. S1 is significant for pathogenicity because it contains RBD [94]. In contrast to other coronaviruses that cause SARS, the RBD of SARS-CoV-2 has more residues (22) that interact with the host receptor and a greater surface area that penetrates the host cell throughout receptor interaction. Second, there are essential mutations in the SARS-CoV-2 RBD, like F486 (which results in strong hydrophobic interaction with ACE-2 Y83) and E484 (formation of strong ionic interaction with ACE2 K31) [93]. S-protein has emerged as a crucial component in the creation of SARS-CoV-2 vaccines as a result of its functional significance in locating RBD. Although some COVID-19 vaccine developers utilize the live-attenuated approach, some of those vaccines did not induce T-cell immunity. A few SARS-CoV-2 vaccines, on the other hand, that used genetic engineering to introduce the S-protein to the host cell have been shown to induce cellular and humoral immunity that is RBD-reactive. For example, Johnson & Johnson, Oxford-AstraZeneca, and Sputnik V use attenuated adenoviral vectors with the gene encoding for S-protein insertion. mRNA of the S-protein that is enclosed in a lipid nanoparticle is used by Pfizer-BioNTech and Moderna, respectively. As of July 2021, the Vaccines of Pfizer-BioNTech, Moderna, and Johnson&Johnson are issued as emergency use

authorization (EUA) by the US FDA.

As of July 2021, Remdesivir is the only antiviral medication that the US FDA has approved [95]. It is prescribed to patients exclusively in conditions competent to inpatient hospital care to adults and children over the age of 12 and weighing more than 40 kilograms. Remdesivir, a phosphoramidite prodrug of a monophosphate nucleoside analog, inhibits viral RNA-dependent RNA polymerase (RdRp), preventing virus replication. Remdesivir mimics adenosine triphosphate (ATP) and subsequently competes with it during the assembly of the RdRp complex, which results in the termination of RNA synthesis. The study has shown that COVID-19 patients' recovery time was 1.5 times faster with Remdesivir compared to placebo (10 and 15 days, respectively). Those receiving Remdesivir experienced adverse reactions in 24.6% of cases, while those receiving a placebo doing so in 31.6% of cases [96].

As of December 2022, FDA has approved 3 commercial mabs (bamlanivimab plus etesevimab, casirivimab plus imdevimab, sotrovimab, and bebtelovimab) to treat patients at high risk who have mild to moderate COVID-19 cases to obtain EUA [97]. Only one anti-SARS-CoV-2 mab product—tixagevimab with cilgavimab (Evusheld) is now approved for use as pre-exposure prophylaxis (PrEP). One of the mabs that proved their efficacy is the combination of casirivimab and imdevimab (Trade name REGEN-COV) [98]. Those are two Fc-unmodified recombinant human immunoglobulins G-1 mabs. Clinically they are employed as intravenous or subcutaneous injections. A controlled, placebo-controlled, randomized clinical trial has shown that the therapy reduced the COVID-19 hospitalization rates in high-risk patients by 70% compared to the placebo [99]. Importantly, casirivimab and imdevimab are not to be prescribed to hospitalized patients due to COVID-19 or to individuals who need oxygen or mechanical ventilation. This is because the data has demonstrated worse clinical outcomes in those patients. Casirivimab and imdevimab (both independently and in combination) retain the capability of neutralizing the *spike* proteins of some SARS-CoV-2 variants in vesicular stomatitis virus and virus-like particles (VSV/VLP) experiments. However, it is unclear whether this data will result in better clinical outcomes [100].

Sotrovimab is a human immunoglobulin G-1 mab with two heavy-chain polypeptides and two light-chain polypeptides and is also produced by Chinese Hamster Ovary cells. It was isolated from a patient's plasma who recovered from SARS-CoV-1 and was proven to work for SARS-CoV-2. It attaches to the *spike* protein RBD's highly conserved epitope region. Kd of Sotrovimab-RBD interaction is 0.21 nM [101]. Although sotrovimab does not prevent the RBD-ACE2 interaction directly, it inhibits the step occurring before the membrane fusion between the viral and host. The placebo-controlled, double-blinded, randomized trial demonstrated that Sotrovimab reduces the risk

of hospitalization by 85% in high-risk patients with mild to moderate COVID-19 clinical picture [47] who do not require supplemental oxygen and/or mechanical ventilation. Analogically, safety is still being determined.

Bamlanivimab and etesevimab are neutralizing mabs that bind to the S-protein of SARS-CoV-2. They block *spike* protein-ACE2 interaction. On June 25, 2021, the US FDA announced a pause on the nationwide distribution of bamlanivimab and etesevimab. This is because bamlanivimab and etesevimab are inactive against dominating variants [102].

2.3 Cell Encapsulation

Novel biomaterial-based platforms have benefited millions of patients as biomedicine has developed, enabling earlier diagnosis, less invasive and quick surgeries, and shorter hospital stays. Cell microencapsulation is a technique that enables the implantation of allogeneic and xenogeneic cells while protecting them from the host immune system using a semipermeable membrane that only permits the diffusion of gases, nutrients, and therapeutics but not of cells of the immune system [103]. Algire was the first to describe a transparent chamber for an *in vivo* therapeutic approach in 1943 [104], and he was the first who reports that encapsulating allo- and xenogenic tissues before actual transplantation reduced membrane overgrowth and emphasized the value of biocompatibility. T.M.S. Chang, in 1964 suggested to use of an ultra-thin polymeric membrane to encapsulate transplanted cells for immune protection, coining the term "artificial cells" to describe this idea of bioencapsulation [105].

Over the next 15 years, significant progress has been made in understanding the biological and chemical conditions for effective cell encapsulation techniques. With the help of alginate/poly-l-lysine-coated microcapsules, Lim and Sun were able to extend the viability of pancreatic islets in 1980 [106]. During 15 weeks in a rodent model, implanted microcapsules continued to function. Later, more research was conducted on diabetes [107]. When cells were implanted inside biocompatible, semi-permeable microcapsules, therapeutic proteins were continuously delivered to the patient. According to Chang, encapsulated cells have a wide range of uses. The cell encapsulation method has been investigated in the past to deliver therapeutics for a variety of other conditions, such as central nervous system delivery [108,108–111], cancer [112], metabolic disorders [112–114], and anemia [115] among multiple other conditions. As a result, several biotechnology firms have formed to create encapsulation devices [116]. There have been concurrent studies of a number of implantation sites, such as the intraperitoneal [117], intratumoral [118], intrathecal [108], and intraocular [119].

In one of the earliest clinical studies to employ cell encapsulation, type 1 diabetic patients' insulin independence was sustained for nine months following intraperitoneal injection of human islets in capsule form [120]. Seven type 1 diabetic patients who underwent encapsulated islet transplantation in a different study were able to maintain stable insulin independence [121]. The long-term survival and functionality of transplanted encapsulated islets were shown by Elliott et al. in a 41-year-old diabetic patient [117]. Mesenchymal stem cells were co-encapsulated with pig islets, leading to implant oxygenation and neoangiogenesis advancement.

2.3.1 Cell Source

Numerous allogeneic cell types have been employed in cell encapsulation-based therapies. The suitable cells for encapsulation will be non-immunogenic, non-tumorigenic, devoid of ethical controversies, simple to obtain, abundant, well-characterized, and reproducible. The most crucial feature in cell choice, immunogenicity, should be taken into account first. Cells' potential to express a particular therapeutic molecule can occasionally restrict their choice. Due to the refined regulatory oversight of insulin expression in pancreatic cells to respond to glucose, the application of encapsulated cells to treat diabetes is a great example [121]. Due to the high immunogenicity of these cells and the fact that patients with diabetes already have an autoimmune reaction against pancreatic islets, overcoming this challenge will be extremely difficult [122]. The survival of the encapsulated cells is reduced when non-autologous encapsulated cells secrete cytokines that activate the host's immune system and induce an inflammatory process around the microcapsules. Numerous metabolic byproducts are released by living cells, some of which, like advanced glycation end (AGE) products and uric acid, can be identified by the host as damage-associated molecular patterns (DAMPs) [123]. Various DAMPs like nucleic acids, chromatin fragments, and ATP are released when encapsulated cells go through apo- or pyroptosis [124]. Numerous immune cells like natural killer (NK) cells, CD4+ T-cells, and B-cells are drawn to transplanted microcapsules, granulocytes, and myofibroblasts that stick to the capsule surface (Figure 1).

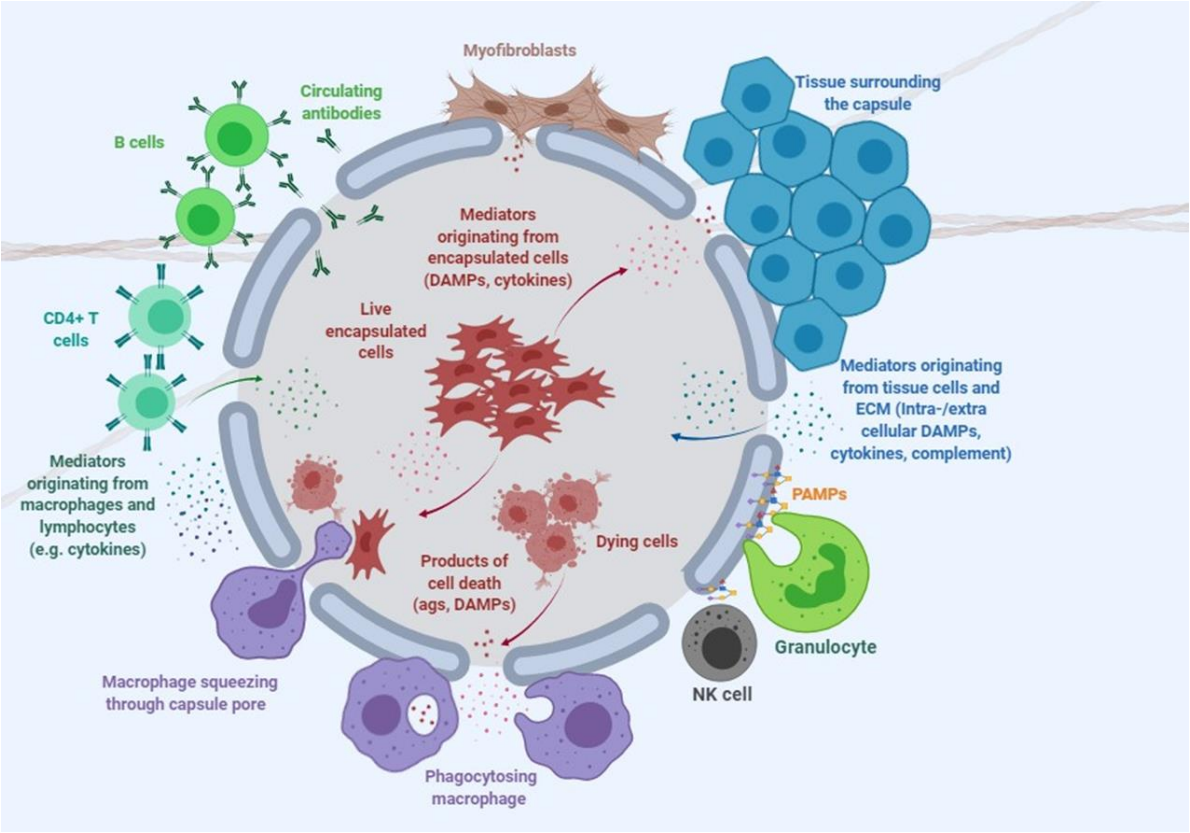

Figure 1. Host immune response to microencapsulated cells. This animation illustrates the complex connection between microcapsules, and immune system, and the surrounding tissue environment. DAMPs: damage-associated molecular patterns, PAMPs: pathogen-associated molecular patterns. Adapted from: **[125]**

For instance, Toll-like receptor 9 (TLR9) identifies double-stranded DNA used in cell genetic engineering as a DAMP. The production of pro-inflammatory cytokines like IL-6, IL-8, and TNF, as well as IFN and IFN-inducible genes, occurs as a consequence of this identification, which initiates a signaling cascade mediated by MyD88. It was possible to reduce this activation of the innate immune system by removing the unmethylated CpG sequences found in the vector DNA, which led to a major decrease in the titer of antibodies to the transgene [126]. Therefore, care should be taken when genetically modifying encapsulated cells with vectors that lower DAMP generation. Cell growth in the polymeric matrix should be taken into account as well. To avoid uncontrolled proliferation, cells should preferably be proliferative but with contact inhibition. Cell viability is decreased by increasing cell density and proliferation, decreasing nutrient permeability. Myoblasts can proliferate shortly in alginate capsules before going quiescent, but fibroblasts continue to proliferate for a very long time after encapsulation [127,128]. The islet cells of the pancreas are an

exception because once encapsulated, they do not proliferate [129]. Cell growth and the therapeutic effectiveness of the microcapsules are eventually decreased by this lack of proliferation [130]. Choosing suitable encapsulated cells will significantly minimize capsule immunogenicity and increase cell viability.

2.3.2 Biomaterials for Cell Encapsulation

Choosing a suitable biomaterial for stability and biocompatibility is undoubtedly one of the most crucial steps in designing the cell microencapsulation technique. A biomaterial's ability to function with a suitable host response in a particular application is referred to as biocompatibility [131]. It's essential to look into how the biomaterial and the enclosed cells interact in the case of cell microencapsulation. If keeping the encapsulated cells viable and functioning is to be accomplished, both aspects must be taken into account. Every material has a set of benefits and drawbacks that must first be taken into account.

Hydrogels are advantageous for cell encapsulation due to a number of characteristics [132]. Compared to other biomaterials, they have the highest levels of biocompatibility because of their hydrophilic characteristics. They have a physical structure and morphology that are similar to extracellular matrices and offer several benefits for microencapsulation [133,134,135].

Alginate has been the most frequently used polymer, either alone or in combination with other polymers **[136,137]**, despite the fact that a wide range of polymers has been mentioned to protect encapsulated allo- or xenogeneic cells [133]. This is due to its great *in vivo* gel-forming properties and high *in vivo* biocompatibility. Alginate is a naturally occurring polysaccharide purified from brown algae like *Laminaria hyperborea* and *lessonia*, with excellent biocompatibility and biodegradability and a spotless safety record [138–141]. It is a block copolymer made of combinations of the subunits of mannuronic acid (M) and guluronic acid (G) [136]. Based on the source of the alginate, different block types have different proportions. Today, alginate is offered in a range of commercial forms. For instance, it has been demonstrated that alginates with a high G content have better compatibility and are thus ideal for cell encapsulation applications [142,143]. Alginate can be produced with molecular weights ranging from 50 to 100 000 KDa, and as the shear rate increases, the viscosity of the alginate decreases [144].

When microcapsule beads are implanted, they experience osmotic swelling, which increases permeability, causes destabilization, and may cause bead breakage. This is because chelating substances like phosphate and citrate have a strong affinity for Ca^{+2} ions. The microcapsules are usually strengthened, and coating beads adjust their permeability with an extra polycation layer in a solution [131(p. 200)]. The polycation layer's toxic nature necessitates using a second coating layer.

The most popular and extensively researched polycation for cell encapsulation is poly-L-lysine (PLL), which was used to create the traditional alginate-poly-L-lysine-alginate microcapsules (APA). The pore size of the microcapsules can be more precisely controlled by crosslinking cationic substances like PLL with anionic alginate [145–148]. Tumor necrosis factor (TNF) was found in the supernatant of monocytes cultured with PLL, indicating that unbound PLL has an impact on capsule biocompatibility [149,150]. Barium [150,151] and strontium [152] have both been mentioned as alternatives to PLL as crosslinking agents. Numerous polycations have been suggested for capsule design, including photopolymerized biomaterials, chitosan, oligochitosan, poly-L-ornithine (PLO) [153,154]. In addition to the polycations listed here, several others have been suggested for use in microcapsule construction. However, to evaluate them to commonly used polycations and to investigate their impact on cell viability and functionality, comparative *in vivo* studies are required.

When the encapsulation procedure is carried out at physiological pH, at room temperature (RT), and with isotonic solutions, it is easier to control the process and increases cell viability during capsule development. Alginate microcapsules can be retrieved with a simple spatula after being implanted intraperitoneally in mice. These microcapsules can survive for months without being attached to the host tissues [113]. However, even though it is biocompatible, any impurities and endotoxins that are left over after the purification process will act as active ingredients to start and/or boost immune responses, leading to post-implantation pericapsular fibrotic uncontrolled cell growth [155–157].

Other Polymers and Biomaterials

Research on cell encapsulation has also been conducted with other polymers and biomaterials. While none of them have the same level of characterization as alginate, the potential benefits of the various other biomaterials can be applied in particular situations. An element of the ECM called HA takes part in vital biological procedures necessary for wound healing. These characteristics make HA an excellent choice for cell encapsulation. It has been demonstrated that MSCs enclosed in hydrogels based on HA shown to proliferate and behave normally [158,159]. To decrease immunogenicity while boosting cell viability, cross-linked polyethylene glycol (PEG) hydrogel microcapsules have also been used in cell encapsulation. However, PEG hydrogels' mechanical properties and cell viability are inferior to those of alginate microcapsules [131].

Photopolymerization has become very common in cell encapsulation techniques due to its capacity to form gels in a favorable physiological environment. However, there are some drawbacks to HA and PEG-based microcapsules crosslinked by photopolymerization in comparison to APA microcapsules [131]. To begin with, these processes necessitate highly reactive photoinitiator agents

like 4-Benzoylbenzyltrimethylammonium, which may cause chain transfer to molecules and proteins on the cell membrane. Second, a temporal spherical mold must be made because calcium alginate beads are used in fabrication. In light of this, photopolymerized hydrogel beads are more challenging to produce than APA microcapsules. Third, high molecular weight degradation products lessen the biocompatibility of the scaffold.

2.3.3 Immune response to encapsulated cells

Despite being appealing, no clinically approved therapeutic products based on cell encapsulation technology exist. While there are many factors why the technique has not met expectations, one of the critical issues is undoubtedly the host immune response that both the implanted capsule and the encapsulated cells trigger [160]. The polymer layer coated the cells in the capsule makes the first interaction with the host (Figure 1). Furthermore, by secreting soluble immune mediators and shedding antigens, the encapsulated cells themselves are crucial in triggering immune responses [137] (Figure 1). It's important to note that the total value of these impacts might be significantly efficient than the simple additive effect of the individual parts.

Contrarily, every transgene used to create encapsulated cells has a distinct immunogenicity, making it impossible to generalize findings from one transgene to others. Instead of producing antibodies to factor IX (FIX), microencapsulated G8 myoblasts produced antibodies to factor VIII (FVIII), a more immunogenic protein [161,162]. On the other hand, mice treated with encapsulated C2C12 experienced an efficient long-term release of erythropoietin, which raised their hematocrit level for more than 3 months [115]. As a result, it is not always possible to separate the immunogenicity of the cells from that of the transgene, making it difficult to predict or generalize the production of antibodies against the transgene. After xenotransplanted human stem cells that had differentiated into pancreatic cells (SC-cells) in immunocompetent mice for more than 150 days without the need for immunosuppression, Alagpulinsa et al. [122] discovered that adding chemokine (C-X-C motif) ligand (CXCL12) to alginate prevented pericapsular fibrotic overgrowth. The transmembrane chemokine receptor CXCR4, which plays a role in several biological processes, including tumor metastasis, cell angiogenesis, survival, and migration, is liganded by CXCL12 [163–165]. CXCL12 can inhibit immune surveillance and repel effector immune cells from capsules, which can modulate immune responses. It also attracts regulatory T-cells (Tregs) [166,167]. By using this innovative approach, encapsulated cells might find new uses in therapeutics. The immune reaction triggered against the microcapsules and their contents is a significant obstacle to the clinical application of cell encapsulation technology.

CHAPTER 3

Aim I: DELIVERY OF MONOCLONAL ANTI-EGFR AND ANTI-CD20 ANTIBODIES FROM MICROENCAPSULATED CELLS

We hypothesize that implanting encapsulated cells genetically engineered with expression vectors containing a DNA sequence coding for anti-EGFR (Cetuximab) and anti-CD20 (Rituximab) mabs of proven clinical efficacy would lead to sustained circulating levels of mabs, and potentially become cost-effective and safe treatment for cancer.

This study aimed to show the delivery of mab from encapsulated cells as a proof-of-concept, not to design novel mabs against cancer target antigens. Therefore, the DNA sequences coding for the variable regions of Cetuximab and Rituximab used in this study were obtained directly from the published patents of the above-mentioned mab and fused to human constant IgG sequences to design vectors to secrete mabs.

As mentioned earlier, many epithelial cancers overexpress the tyrosine kinase receptor known as the EGFR, which is an ErbB family member [78]. Anti-EGFR mabs are approved for cancer treatment by many medical agencies and are among the most effective in patients with solid malignancies [82].

B-lymphocytes express CD20 on the cell surface, an activated-glycosylated phosphoprotein. Due to its high and specific expression level in most B-cell malignancies, it is the most suitable target for mabs. Indeed, mabs targeting CD20 have been used in clinical practice for decades. Rituximab is a CD20-specific humanized antibody [35].

Several of the mab approved by the US FDA for clinical use target specifically EGFR and CD20. The available DNA sequences of these clinical mabs were used to design expression vectors, genetically engineer mammalian cells, and secrete mabs against EGFR and CD20 as described in this thesis.

3.1MATERIALS AND METHODS

pFUSE plasmids

pFUSE plasmids pFUSE-CLIg (Figure 2) and pFUSE-CHIg (Figure 3) plasmids (Invitrogen, Burlington, Canada) are designed to express the constant region of the heavy and light chains of human IgG, respectively. Upstream of these constant regions, both plasmids contain a multiple cloning site, enabling the cloning of the variable heavy and light regions of an antibody of interest. These plasmids can secrete entire IgG antibodies [168] from Fab or scFv fragments.

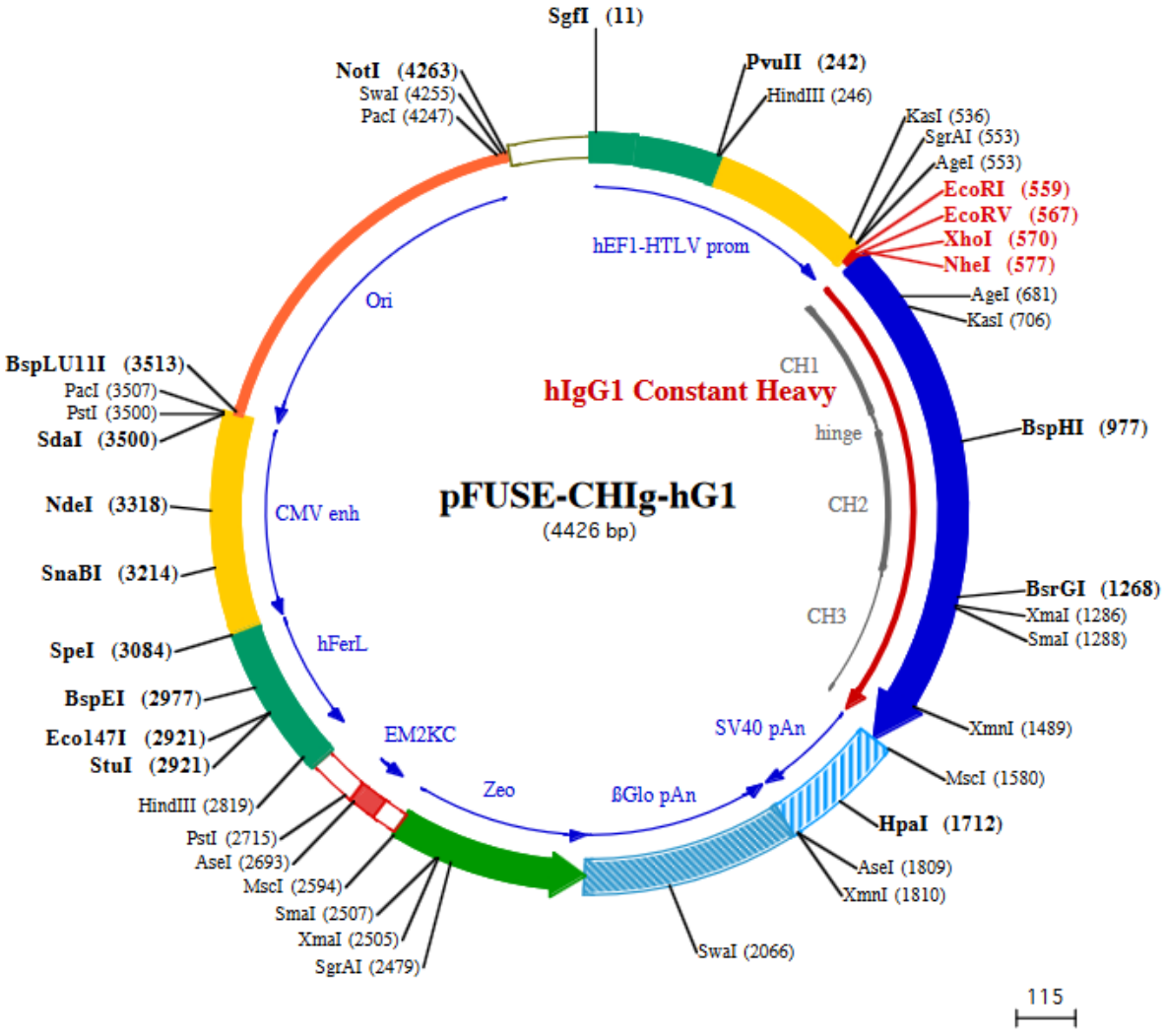

Figure 2. pFUSE plasmids (hIgGHc constant region).

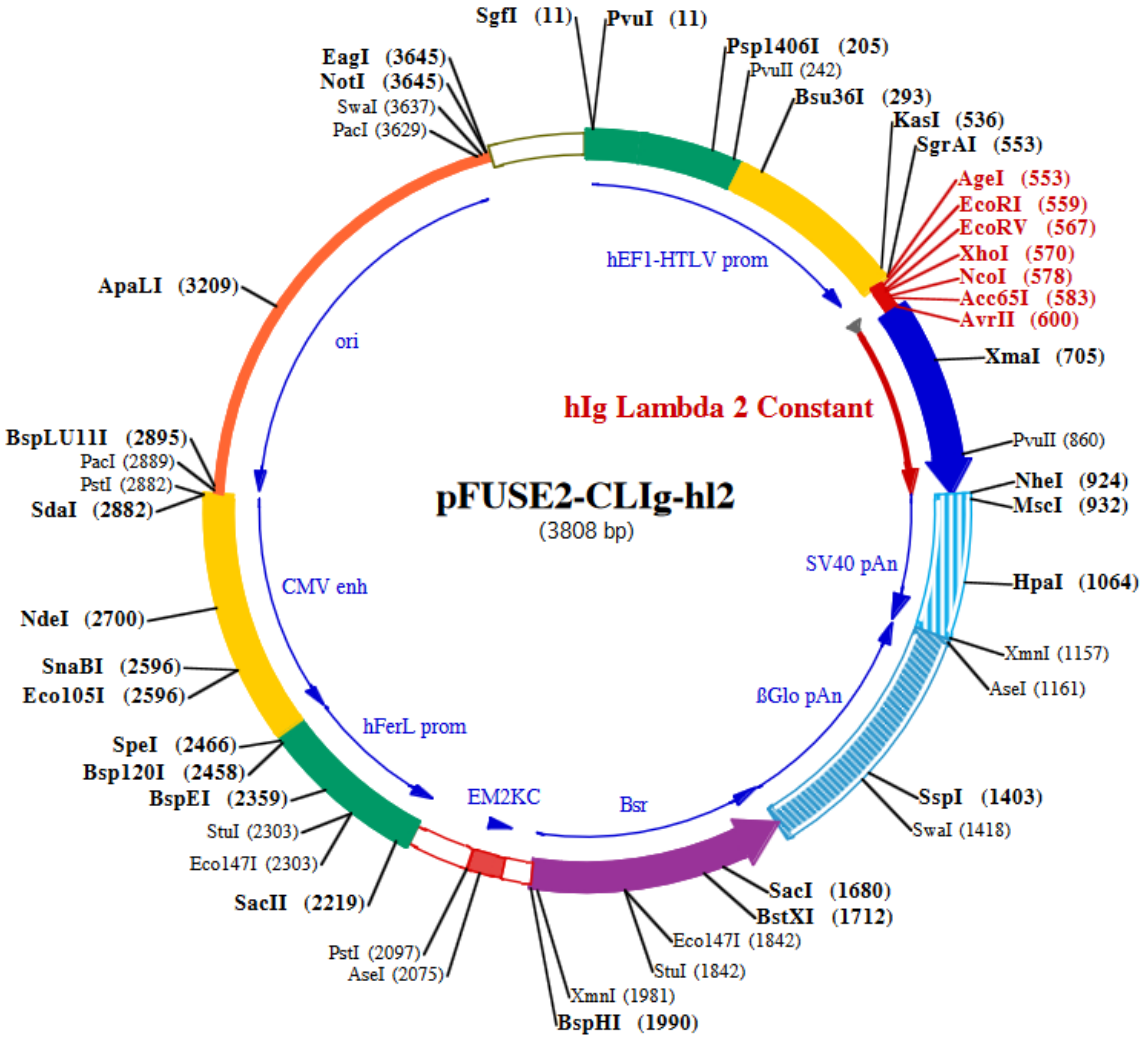

Figure 3. pFUSE plasmids (hIgGLc constant region).

After cloning the sequence coding for the variable region of the heavy chain of the antibody of interest into pFUSE-CHIg-hG1 and the sequence coding for the variable part of the light chain into pFUSE2-CLIghl2, respectively, co-transfection of mammalian cells with both plasmids leads to the generation and secretion of the complete and functional IgG antibody.

Design of mab DNA plasmid

The two non-viral vectors used to engineer cells for the secretion of mabs, pFUSE plasmids, use the strong and ubiquitous Elongation factor-1 (EF-1) promoter; this allows mab expression from a wide variety of mammalian cells. The co-transfection of both plasmids into cells results in the secretion of complete human IgG molecules. The DNA coding for the variable sequence of anti-CD20 and anti-EGFR (heavy and light chains) was synthesized (approximately 300 bp) and cloned into these vectors. The sequences for the variable fragment (H & L) of an anti-EGFR and anti-CD20

mabs is available from Drugbank.com (Figure 4).

>Cetuximab heavy chain
QVQLKQSGPGLVQPSQSLSITCTVSGFSLTNYGVHWVRQSPGKGLEWLGVIWSGGNT
DYN
TPFTSRLSINKDNSKSQVFFKMNSLQSNDTAIYYCARALTYYDYEFAYWGQGTLVTVSA
A
STKGPSVFPLAPSSKSTSGGTAALGCLVKDYFPEPVTVSWNSGALTSGVHTFPAVLQS
SG
LYSLSSVVTVPSSSLGTQTYICNVNHKPSNTKVDKKVEPKSCDKTHTCPPCPAPELLGG
P
SVFLFPPKPKDTLMISRTPEVTCVVVDVSHEDPEVKFNWYVDGVEVHNAKTKPREEQY
NS
TYRVVSVLTVLHQDWLNGKEYKCKVSNKALPAPIEKTISKAKGQPREPQVYTLPPSRDE
L
TKNQVSLTCLVKGFYPSDIAVEWESNGQPENNYKTTPPVLDSDGSFFLYSKLTVDKSR
WQ
QGNVFSCSVMHEALHNHYTQKSLSLSPGK

>Cetuximab light chain
DILLTQSPVILSVSPGERVSFSCRASQSIGTNIHWYQQRTNGSPRLLIKYASESISGIPS
RFSGSGSGTDFTLSINSVESEDIADYYCQQNNNWPTTFGAGTKLELKRTVAAPSVFIFP
P
SDEQLKSGTASVVCLLNNFYPREAKVQWKVDNALQSGNSQESVTEQDSKDSTYSLSS
TLT
LSKADYEKHKVYACEVTHQGLSSPVTKSFNRGEC

>Rituximab heavy chain chimeric
QVQLQQPGAELVKPGASVKMSCKASGYTFTSYNMHWVKQTPGRGLEWIGAIYPGNGD
TSY
NQKFKGKATLTADKSSSTAYMQLSSLTSEDSAVYYCARSTYYGGDWYFNVWGAGTTV
TVS
AASTKGPSVFPLAPSSKSTSGGTAALGCLVKDYFPEPVTVSWNSGALTSGVHTFPAVL
QS
SGLYSLSSVVTVPSSSLGTQTYICNVNHKPSNTKVDKKAEPKSCDKTHTCPPCPAPELL
G
GPSVFLFPPKPKDTLMISRTPEVTCVVVDVSHEDPEVKFNWYVDGVEVHNAKTKPREE
QY
NSTYRVVSVLTVLHQDWLNGKEYKCKVSNKALPAPIEKTISKAKGQPREPQVYTLPPSR
D

ELTKNQVSLTCLVKGFYPSDIAVEWESNGQPENNYKTTPPVLDSDGSFFLYSKLTVDKS
R
WQQGNVFSCSVMHEALHNHYTQKSLSLSPGK

>Rituximab light chain chimeric
QIVLSQSPAILSASPGEKVTMTCRASSSVSYIHWFQQKPGSSPKPWIYATSNLASGVPV
R
FSGSGSGTSYSLTISRVEAEDAATYYCQQWTSNPPTFGGGTKLEIKRTVAAPSVFIFPP
S
DEQLKSGTASVVCLLNNFYPREAKVQWKVDNALQSGNSQESVTEQDSKDSTYSLSSTL
TL
SKADYEKHKVYACEVTHQGLSSPVTKSFNRGEC

Figure 4. Amino acid sequences of Cetuximab and Rituximab in the patent.

Cell culture

HEK293 (human embryonic kidney cells) cells were cultured in DMEM medium supplied with 10,000 units /mL of penicillin and 10,000 μg/mL of streptomycin, and 10% Fetal Bovine Serum at 37°C in a CO_2 incubator with 5% CO_2. Cells were sub-cultured 2 times per week to avoid overgrowth in the cell culture flasks. For cell detachment flasks with 0.5%, Trypsin/EDTA was incubated for 2 minutes at 37°C.

Expression of mab

HEK293 cells were co-transfected with the heavy and light chains of anti-EGFR (Cetuximab) or anti-CD20 (Rituximab) plasmids at 60% confluency in 100 mm cell culture dishes using transfection reagent Escort-III (Figure 5). Briefly, cells were treated for 6 hours at 37°C with a pre-incubated combination of 5 μg of each plasmid and 5 μl of Escort-III in 990 μL of Redused-Serum Medium (Opti-MEM). Then, after two weeks of cell culture, stably expressing cells were selected by adding 400 μg/ml of zeocin and 10 μg/ml of blasticidin to the growth medium. ELISA and Western blotting were used to characterize the produced mabs.

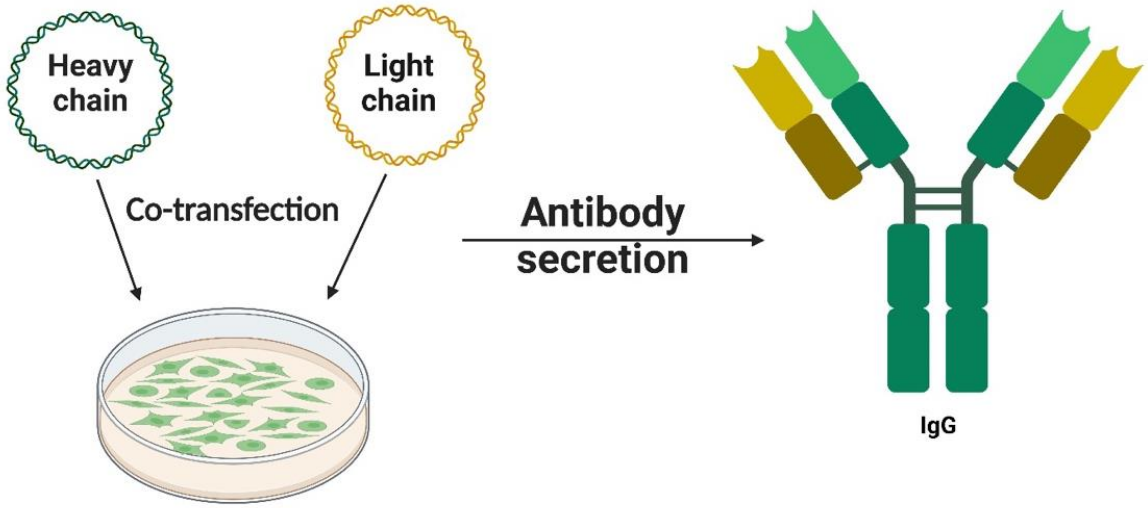

Figure 5. Co-transfection of cells with both plasmids coding for heavy and light chains leads to the secretion of entire IgG molecules.

Design of an ELISA test to quantify EGFR and CD20 mab secretion

A 96-well immunoplate (Thermo Fisher Scientific, Waltham, MA, USA) was coated with 2 ng/µl per well recombinant human EGFR (ab155639, Abcam, Cambridge, USA) or CD20 (ab158047) proteins diluted in coating buffer (100mM) and incubated overnight at 4°C. After being washed with PBST, the plates were blocked with 5% non-fat dry milk in PBST for 1 hour at RT and washed with PBST. 2 µg/ml per well of commercial human EGFR (MAB9577, R&D Systems Europe Ltd.) or CD20 (MSQC17, Sigma, USA) antibodies were used as a standard and positive control. At the same time, supernatants of untransfected HEK293 cells were added for negative control. Supernatants purified by protein G column chromatography and non-purified samples were added to detect antibody secretion. After 2 hours of incubation, the plate was washed three times in 1x PBST. Bound antibody was detected by incubating the plate with a 1:130000 dilution of rabbit anti-human IgG (H&L) HRP conjugate (ab6759, Abcam, Cambridge, USA) for 1 hour at 37°C. The TMB substrate solution was applied to the 96-well plates after being cleaned with PBST, and it was left there for 10 minutes at RT. The color reaction was stopped by using 2 M H_2SO_4. Using a spectrophotometer, the absorbance value was discovered at 450 nm (Thermo Electron Corporation).

Western Blotting

The specificity and size of the produced mab were confirmed by Western blotting. On a 10% SDS-PAGE gel, EGFR (ab155639) or CD20 (ab158047) proteins were separated. Then they were transferred for 1 hour at 350 mA onto a PVDF (Polyvinylidene fluoride) membrane. After blocking the membrane with 5% (w/v) dried milk powder in PBST (1 x PBS, 0.05% Tween 20), it was rinsed three times in TBST before being blotted with cell culture supernatant at 4°C overnight. HRP-conjugated anti-human antibodies specific to either whole human IgG (rabbit ab6759, Abcam) or the IgG Fc region (goat ab97225, Abcam) were used for mab detection. These antibodies were diluted to 1:10,000 and incubated on the membrane for 1 hour at RT. Before SDS-PAGE separation, purified (on Protein G HP Spin Trap, #28903134) cell supernatant was heated for 5 min at 95°C under reducing conditions to determine the mab's denatured form. The PageRuler Prestained Protein Ladder (#26616, #26619, Thermo Fisher Scientific) was used to determine the molecular weight by using human EGFR (MAB9577, 500 ng/well, 20 ng/μl) or CD20 (MAB9577, 500 ng/well, 20 ng/μl) mab as a control. ChemiDoc MP Imaging System (Bio-Rad) was used for image analysis.

Cell Encapsulation

Low-viscosity alginate powder was dissolved in 0.9% sodium chloride overnight at 37 °C and then filtered through a 0.22 μm filter to create an alginate solution (1.5%). An alginate solution containing 5×10^6 cells/mL was used as the suspension medium. Alginate microbeads were produced with a few slight modifications using the Var1 electrostatic encapsulator (Nisco Engineering Inc., Zurich, Switzerland) as previously described. In a nutshell, the cell suspension was pumped into a vial containing a cold 100 mM $CaCl_2$ solution using a NISCO Var-1 encapsulator (Nisco Engineering Inc., Zurich, Switzerland) at a voltage of 7.10 kV and a flow rate of 20 mL/h, generating microcapsules that were 300–500 μm in diameter. The cell-loaded microcapsules were subsequently rinsed with saline solution, and cross-linked with poly-L-lysine (PLL, 29 kDa, P7890, Sigma) for 6 minutes. Then, coated with an outer layer of alginate for 4 minutes. Following the addition of DMEM, the solution containing the microcapsules was transferred to an incubator. The viability of microencapsulated cells was evaluated using the trypan blue exclusion assay, in which 20 μL of microcapsules and 20 μL of trypan blue (Invitrogen, USA) were installed on a microscope slide and crushed by a glass coverslip to release the encapsulated cells. Then, the released cells were visualized and manually quantified using an inverted light microscope (Ceti, Medline Scientific, Chalgrove, UK) or by using an automated cell counter Countess 3 (Thermo Fisher). Microcapsules that had been air-dried for one hour at RT were imaged

using an electron microscope with the use of a JSM-IT200LA (JEOL, Akishima, Japan) scanning electron microscope.

Statistical analysis

GraphPad Prism V.9.3.1 was used for all analyses. The unpaired t-test was used to compare differences between groups, and the binomial "exact" method was used to calculate 95% confidence intervals (CI).

3.2 RESULTS

A. Design and synthesis of DNA sequences coding for the constant and variable regions of the heavy and light chains of monoclonal antibodies against EGFR and CD20 antigens.

The first step was to design the DNA sequence and synthesize the plasmids coding for the heavy and light chains of human IgG specific for EGFR and similar plasmids coding for a human IgG specific for CD20. The DNA sequences coding for the antibody's variable light and heavy chains were derived from the amino acid sequence obtained from Drugbank.com. The DNA sequence was compared to that found in free access through nucleotide search on National Center for Biotechnology Information (NCBI) website and patent applications for the two commercially available mabs. Nucleotide sequences are shown in Figure 6 for Cetuximab and Figure 7 for Rituximab mabs, respectively. Variable regions of chosen antibodies have signal peptides included in the DNA sequence cloned into pFUSE plasmids.

Cetuximab VH:
ATGGCCGT GCTGGGCCTG CTGTTCTGCC TGGTGACCTT CCCCAGCTGC
GTGCTGTCCC AGGTGCAGCT GAAGCAGAGC GGCCCTGGCC TGGTGCAGCC CTCTCAGTCC
CTCTCCATTA CCTGTACCGT GTCCGGCTTC TCTCTCACAA ATTATGGAGT CCATTGGGTG
CGCCAGAGCC CCGGCAAGGG CCTGGAGTGG CTGGGCGTGA TCTGGTCCGG CGGCAACACC
GACTACAACA CCCCCTTCAC CAGCAGACTG AGCATCAACA AGGACAACAG CAAGAGCCAG
GTGTTCTTCA AGATGAACAG CCTGCAGAGC AACGACACCG CCATCTACTA CTGCGCTCGC
GCTCTCACCT ACTACGACTA CGAGTTCGCC TACTGGGGCC AGGGCACCCT GGTGACCGTG
TCCGCC
Cetuximab VL:
CTCGAGACCG CCATGGTGTC CACCCCCCAG TTCCTCGTGT TCCTGCTGTT CTGGATCCCC
GCCAGCAGGG GCGACATCCT GCTGACCCAG AGCCCCGTGA TCCTGAGCGT GTCTCCCGGC
GAGAGGGTGT CCTTCAGCTG CAGAGCCAGC CAGAGCATCG GCACCAACAT CCACTGGTAT
CAGCAGAGGA CCAACGGCAG CCCCAGGCTG CTGATCAAGT ACGCCAGCGA GTCCATCAGC
GGCATCCCCA GCAGGTTCAG CGGCAGCGGC TCCGGCACCG ACTTCACCCT GAGCATCAAC
AGCGTGGAGA GCGAGGATAT CGCCGACTAC TACTGCCAGC AGAACAACAA CTGGCCCACC
ACCTTCGGCG CTGGCACCAA GCTGGAGCTG AAG

Figure 6. Sequences coding for variable heavy and variable light regions of Cetuximab. Yellow – signal sequence, green – variable region.

Rituximab VH:
ATGTATCTGG GATTGAATTG CGTCATTATC GTGTTTCTGC TCAAGGGTGT GCAAAGTCAG
GTCCAGCTGC AGCAGCCAGG CGCAGAGCTG GTTAAGCCAG GAGCCTCAGT GAAAATGAGC
TGCAAAGCCT CTGGCTACAC CTTTACCAGC TATAACATGC ATTGGGTGAA ACAGACACCC
GGCAGAGGGC TGGAATGGAT CGGAGCCATA TACCCCGGGA ACGGGGACAC CTCCTATAAC
CAGAAGTTCA AGGGAAAGGC CACACTCACT GCTGACAAGT CCAGTAGCAC CGCTTACATG
CAACTTTCAA GCTTGACATC AGAGGATTCT GCAGTTTACT ACTGTGCCCG GTCTACTTAC
TATGGCGGCG ATTGGTATTT CAATGTATGG GGTGCTGGCA CAACAGTCAC TGTGAGCGCA
Rituximab VL:
ATGGATATGA GGGTACCAGC ACAACTTCTC GGATTACTAT TGTTATGGCT GCGAGGTGCG
CGCTGTCAGA TTGTCTTGAG CCAGTCTCCC GCCATTTTGT CTGCCTCCCC TGGGGAGAAA
GTAACCATGA CTTGTCGCGC ATCCTCAAGC GTGAGTTACA TCCACTGGTT TCAGCAGAAG
CCTGGCAGCT CACCCAAGCC CTGGATCTAT GCTACCTCCA ACCTCGCTTC CGGAGTGCCT
GTGCGGTTTT CTGGGTCCGG TAGTGGTACC AGCTACTCAC TGACTATTTC AAGAGTTGAG
GCTGAAGATG CCGCAACCTA TTACTGCCAA CAGTGGACAA GTAATCCACC AACATTCGGT
GGCGGCACTA AACTGGAGAT CAAG

Figure 7. Sequences coding for variable heavy and variable light regions of Cetuximab. Yellow – signal sequence, green – variable region.

All nucleotide sequences were checked to have an integer number of codons regarding amino acids these codons encode. Synthesis of these sequences and cloning them into pFUSE plasmids were done by Eurofins Genomics company. The DNA of the cloned plasmids was sequenced to confirm its integrity (Eurofins Genomics). Figures 8 and 9 show the plasmid maps coding for the heavy and

light chain of 2 antibodies: -pCHIg-hG1-CetuximabVH/pCLIg-hk-CetuximabVL and -pCHIg-hG1-RituximabVH/pCLIg-hk-RituximabVL.

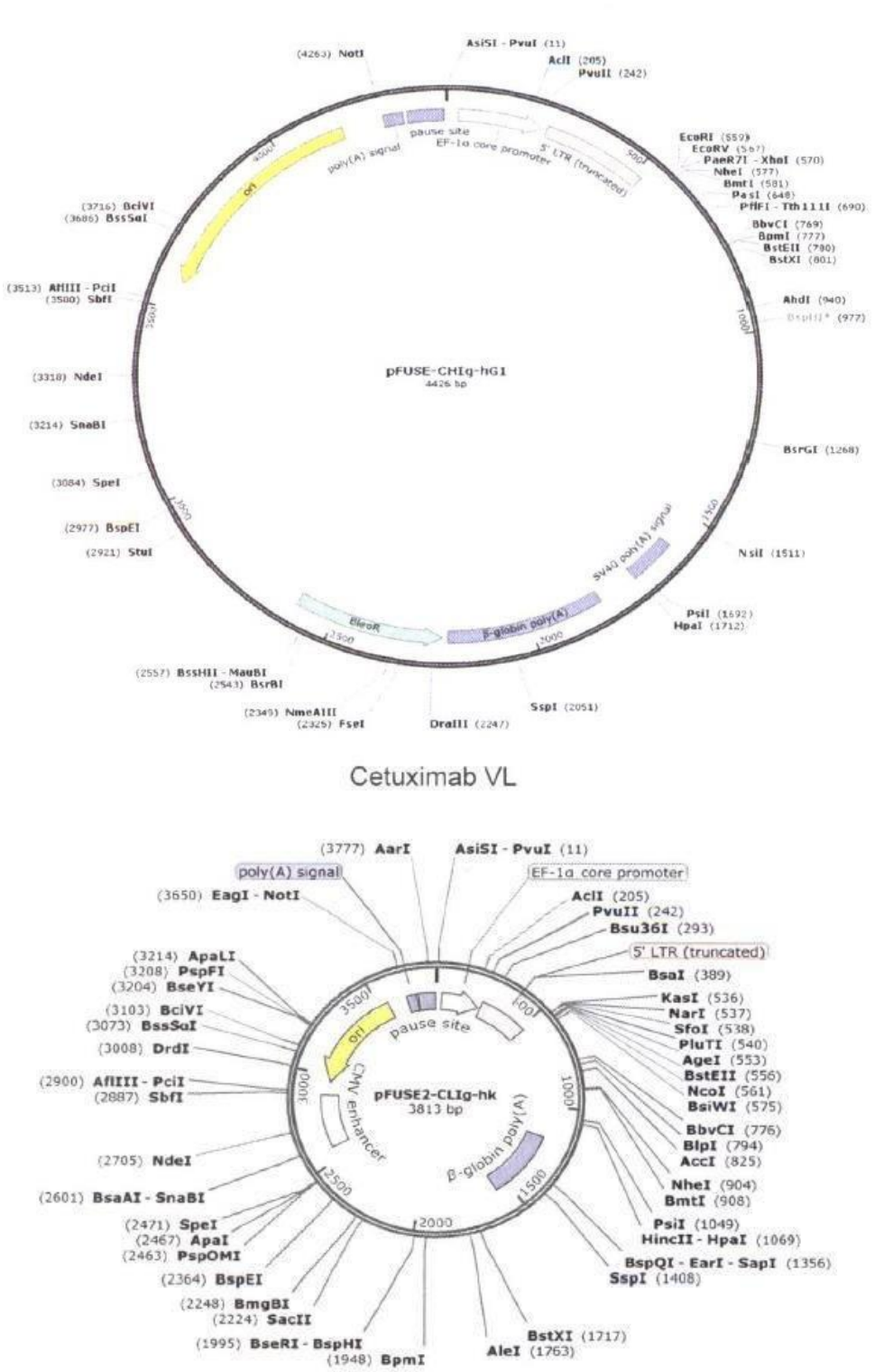

Cetuximab VL

Figure 8. Plasmid maps coding for Cetuximab's heavy (top panel) and light chain (bottom panel): pCHIg-hG1-CetuximabVH/pCLIg-hk-CetuximabVL.

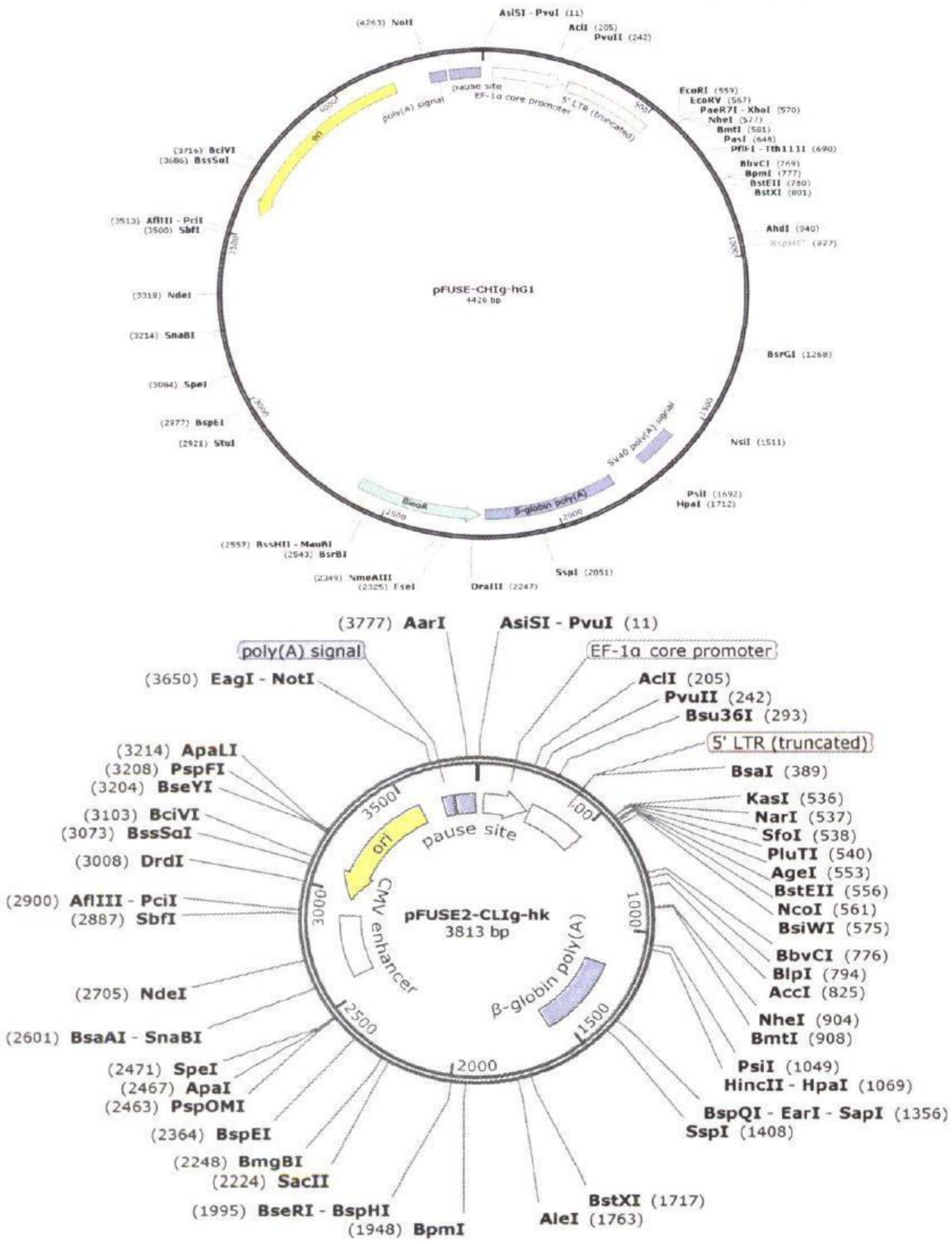

Figure 9. Plasmid maps coding for Rituximab's heavy (top panel) and light chain (bottom panel): pCHIg-hG1-RituximabVH/pCLIg-hk-RituximabVL.

B. HEK293 cells are capable of sustained mab expression.

Once the plasmids were generated, their ability to induce secretion of anti-EGFR and anti-CD20 mabs upon transfection of HEK293 cells was assessed. The expression of anti-EGFR and anti-CD20 antibodies in HEK293 cells was evaluated by ELISA tests designed in our laboratory. ELISA measurements of mab in the supernatant of transfected HEK293 cells showed a steady increase of human IgG after co-transfection. They were maintained at ~3.5 OD values per day for EGFR (Figure 10) and ~3.2 for CD20 (Figure 10). In contrast, cells transfected with only one of the plasmids -coding for either heavy or light chains- resulted in baseline similar levels of human IgG, comparable to that of non-transfected cells.

Since the object of this study is the delivery of mab from microencapsulated cells, assessing the permeability of mabs through alginate microcapsules is critical to this thesis and was evaluated. HEK293 cells genetically engineered with the plasmids encoding both chains for EGFR mab were encapsulated and cultured *in vitro*. ELISA quantified the level of mab specific to EGFR in the cell supernatant. The results (Figures 10 and 11) showed a high secretion of mab through microcapsules, supporting the feasibility of this thesis. A similar experiment was conducted for the quantification of mab specific to CD20. In agreement with the results obtained for EGFR mab, CD20 mab was secreted from encapsulated HEK293 cells at high levels.

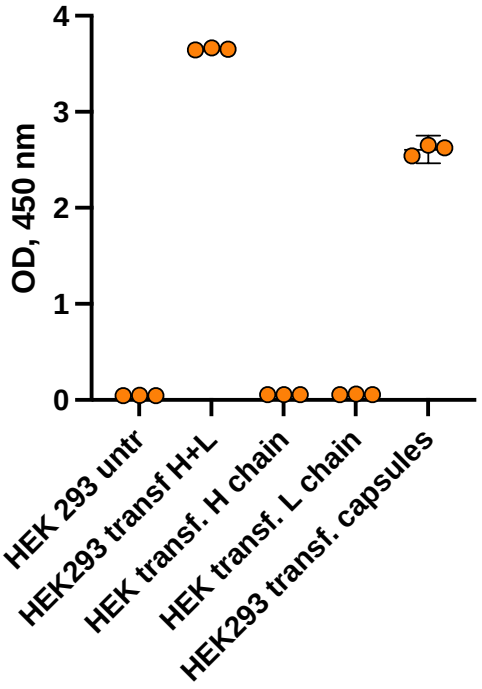

Figure 10. Representative ELISA plot of EGFR-IgG binding for HEK293 cell supernatants. Cell supernatants were incubated on plates coated with EGFR proteins. Supernatants were collected at 48h post-encapsulation. Experiments were conducted in triplicate, and error bars indicate standard

deviation.

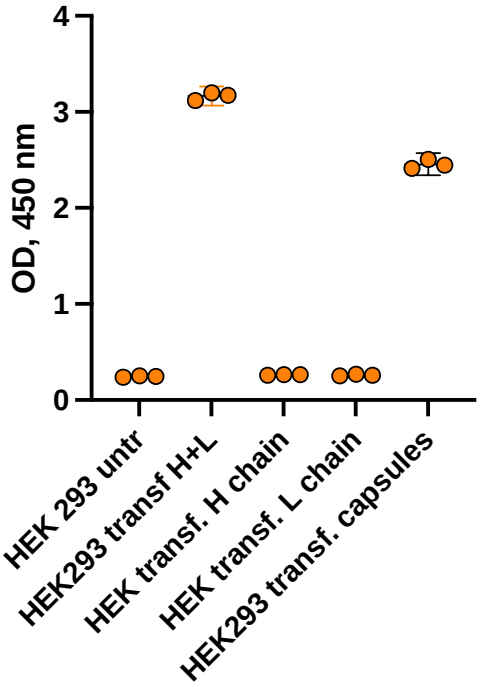

Figure 11. Representative ELISA plot of CD20-IgG binding for HEK293 cell supernatants. Cell supernatants were incubated on plates coated with CD20 proteins. Supernatants were collected at 48h post-encapsulation. Experiments were conducted in triplicate, and error bars indicate standard deviation.

C. Secreted mabs bind specifically to their target antigens.

The secreted mab to EFGR and CD20 were then characterized. First, they were evaluated by Western blotting experiments to determine the specificity of the mab to its intended antigens. Increasing concentrations of purified commercial EFGR (ab155639) and CD20 (158047) proteins were run by PAGE and blotted with supernatant from cultured cells. Western blotting demonstrated specificity, as the produced mabs bind to EGFR and CD20 proteins (Figures 12-16, respectively).

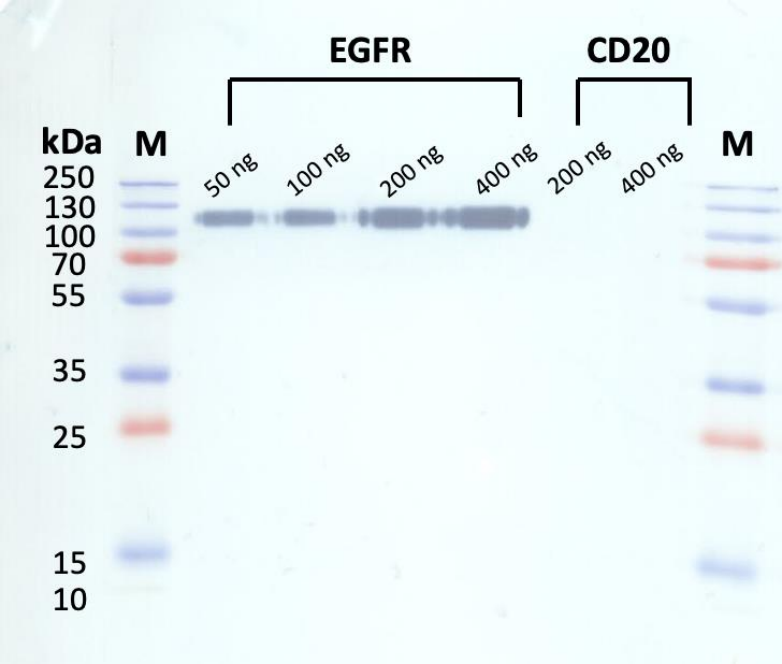

Figure 12. anti-EGFR monoclonal antibody (Cetuximab) secretion in HEK293 cells co-transfected with the EGFR heavy and light chains. Various concentrations of EGFR and CD20 proteins were run on a 10% SDS–PAGE gel. It was then transferred onto a PVDF membrane and blotted with HEK293 cell culture supernatant. An HRP-conjugated rabbit IgG specific to both the heavy and light chains of human IgG was used for the probing.

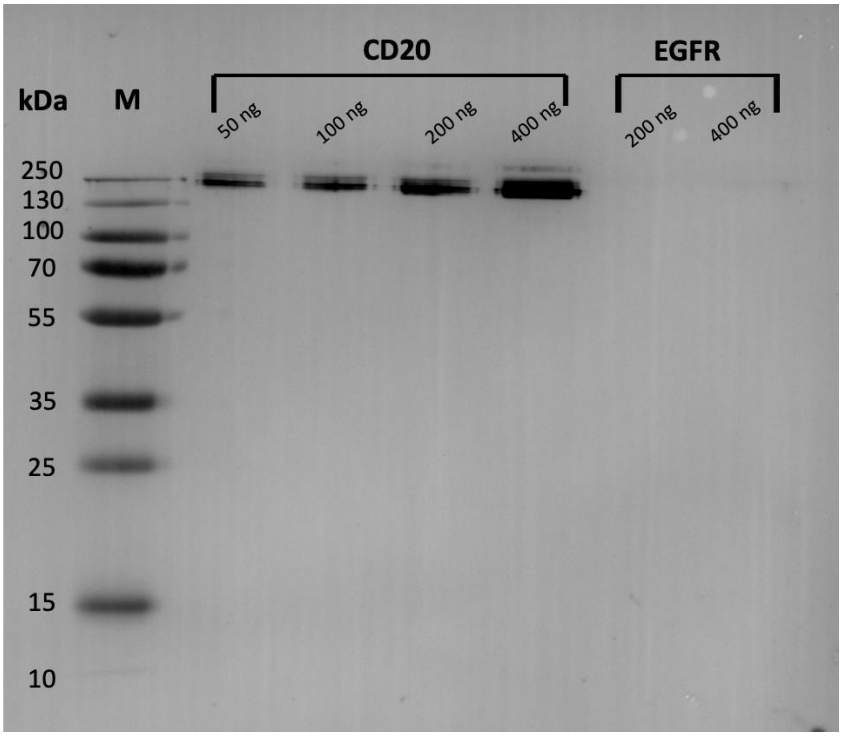

Figure 13. anti-CD20 (Rituximab) monoclonal antibody secretion in HEK293 cells co-transfected with the EGFR heavy and light chains. Various concentrations of CD20 and EGFR proteins were run on a 10% SDS–PAGE gel. It was then transferred onto a PVDF membrane and blotted with HEK293 cell culture supernatant. An HRP-conjugated rabbit IgG specific to both the heavy and light chains of human IgG was used for the probing.

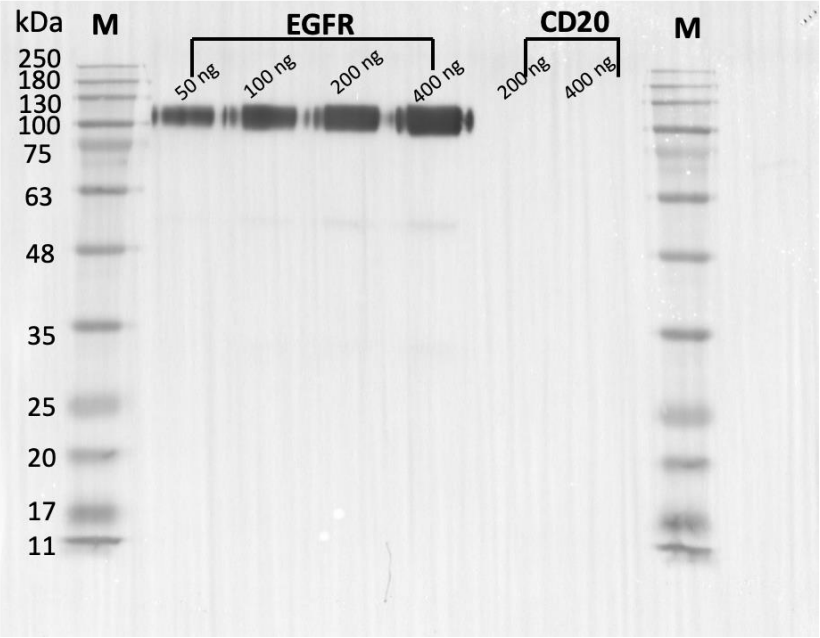

Figure 14. Western blotting with diluted anti-EGFR commercial mab (MAB9577). Various concentrations of EGFR and CD20 proteins were run on a 10% SDS–PAGE gel. It was then transferred onto a PVDF membrane and blotted with anti-EGFR mab. An HRP-conjugated rabbit IgG specific to both the heavy and light chains of human IgG was used for the probing.

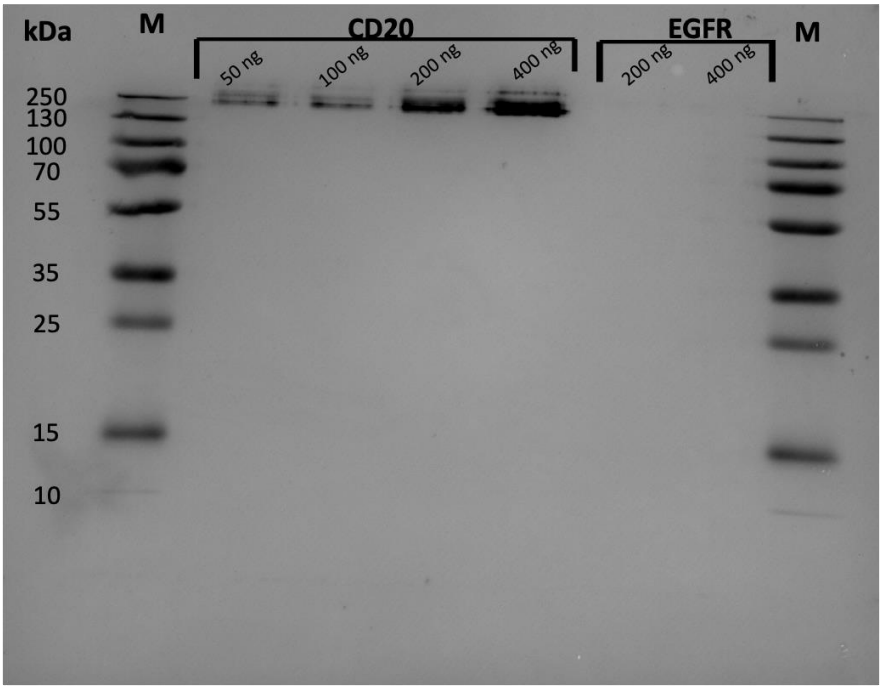

Figure 15. Western blotting with diluted anti-CD20 commercial mab (Rituximab). Various concentrations of CD20 and EGFR proteins were run on a 10% SDS–PAGE gel. It was then transferred onto a PVDF membrane and blotted with anti-CD20 mab (Rituximab). An HRP-conjugated rabbit IgG specific to both the heavy and light chains of human IgG was used for the probing. kDa-kilodaltons.

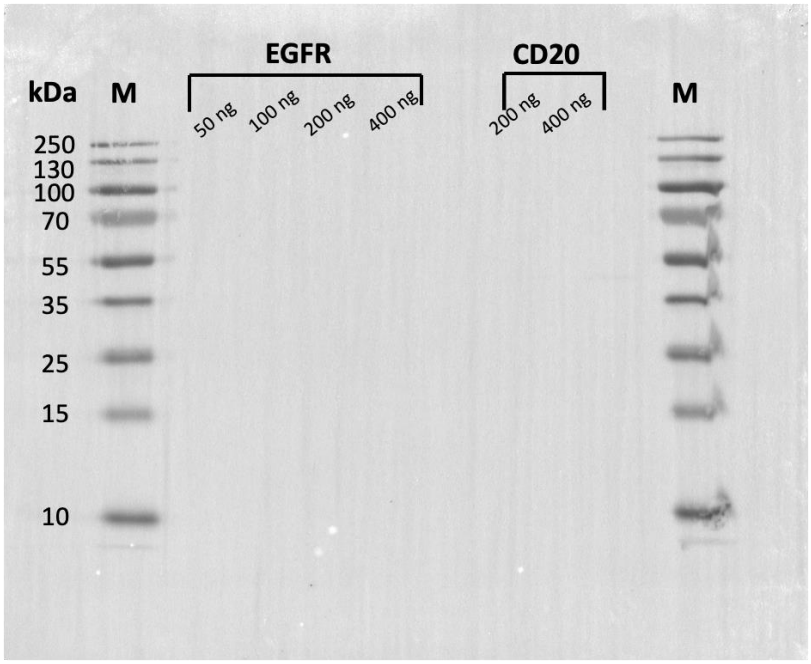

Figure 16. Western blotting with supernatant from control (non-transfected) HEK293 cells. Various concentrations of EGFR and CD20 proteins were run on a 10% SDS–PAGE gel. It was then transferred onto a PVDF membrane and blotted with supernatant from control (non-transfected) HEK 293 cells. An HRP-conjugated rabbit IgG specific to both the heavy and light chains of human IgG was used for the probing. kDa-kilodaltons.

D. Size of the secreted mabs.

As part of the characterization process, the size of the secreted mabs was also determined by PAGE. Supernatant from cultured HEK293 cells secreting mab specific to EGFR were separated by PAGE, transferred to a membrane, and blotted with an anti-human IgG antibody. As controls, commercial purified antibodies specific to EGFR and supernatant of untransfected HEK293 cells were tested alongside. The bands identified correspond to the expected size of denatured human IgG (Figure 17).

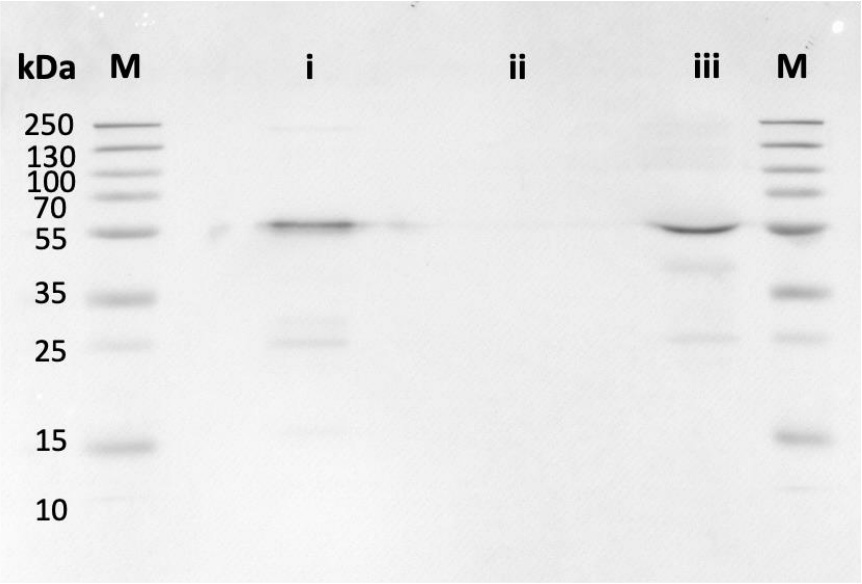

Figure 17. Western blotting for anti-EGFR monoclonal antibody size.

I: anti-EGFR mab (MAB9577); ii: Untransfected HEK293 supernatant; iii: Transfected HEK293 supernatant. Purified cell culture supernatants and the anti-EGFR mab (MAB9577) were denatured before Western blotting. An HRP-conjugated goat IgG specific to both the heavy and light chains of human IgG (H+L) was used for the probing. The size of proteins is shown in kDa (kilodaltons).

A similar experiment was conducted to determine the size of the secreted mab to CD20. Supernatant from cultured HEK293 cells secreting mab specific to CD20 were separated by PAGE, transferred to a membrane, and blotted with an anti-human IgG antibody. As controls, commercial purified

antibodies specific to CD20 and supernatant of untransfected HEK293 cells were tested alongside. The bands identified correspond to the expected size of denatured human IgG (Figure 18).

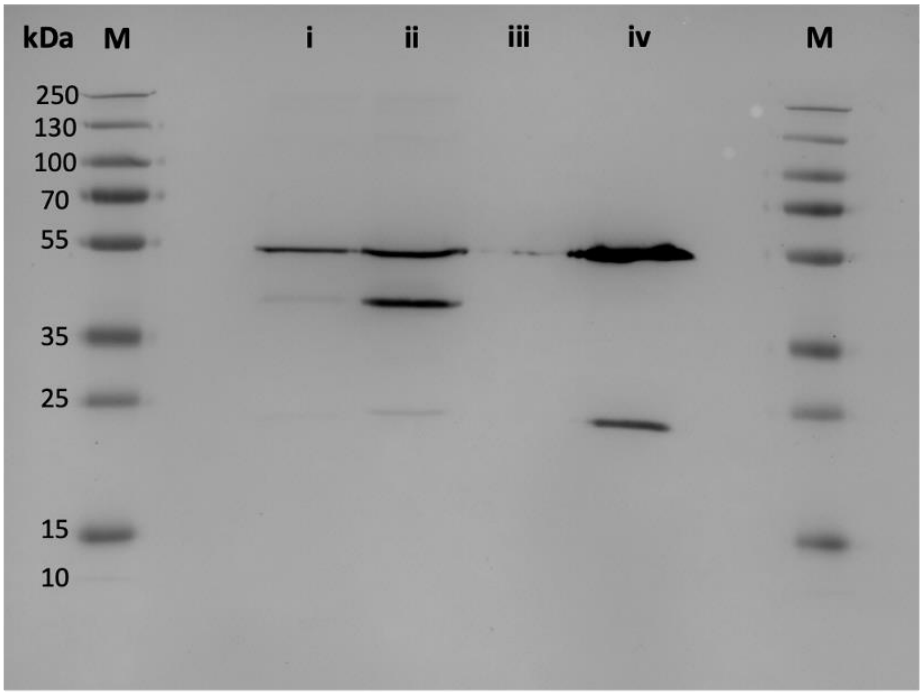

Figure 18. Western blotting for anti-CD20 monoclonal antibody (Rituximab) size. I: Transfected HEK293 secreting Rituximab; ii: Transfected HEK293 secreting Rituximab II; iii: Untransfected HEK293 supernatant, iv: anti-CD20 mab (MSQC17, Rituximab). Purified cell culture supernatants and the anti-CD20 mab were denatured before Western blotting. An HRP-conjugated goat IgG specific to both the heavy and light chains of human IgG (H+L) (ab6759) was used for the probing. The size of proteins is shown in kDa (kilodaltons).

Moreover, the commercial antibody to CD20 yielded a band of the same size. In contrast, the supernatant of untransfected cells did not reveal any bands. Therefore, the secreted mabs were specific to their antigens and had the expected size of functional human IgG (Figures 17, 18).

3.3 DISCUSSION

Using mammalian cell lines to produce mabs is a common practice. CHO and HEK293 cells are most frequently used for the ease of transfection and comparably high mab yields. There are different strategies for the production of entire IgG antibodies: (1) co-transfection of cells with two plasmids, one coding for the heavy chain of the antibody and the other plasmid for the light chain (this study), (2) selection of transfected cells with antibiotics after transfection with one of the plasmids, transfecting them later with the second plasmid [169] or (3) transfection of cells with only one plasmid coding for both heavy and light chains [170]. Mab production output depends on the ratio of heavy: light gene copies and, consequently, the ratio of heavy: light polypeptide expression. Transfection of the cells with two plasmids allows better control of the ratio of either chain.

On the other hand, mammalian expression systems express and secrete both chains concurrently. Hence, detecting antibody secretion and distinguishing between heavy and light chains is necessary. In this study, secreted mabs were seen using Fc-specific anti-human antibodies and found detectable mab levels in the supernatant of the cells co-transfected with both plasmids coding for heavy and light chains of antibodies, as well as in supernatants of cells transfected with just one of the plasmids (heavy or light chain). Schlatter and colleagues used secondary antibodies specific to γ-chain and κ-chain to specifically detect heavy or light chains in immunoblot analysis and Fab-specific antibodies to detect antibody production using ELISA [171]. Further, whether produced antibodies were specific to their targets (EGFR or CD20) was determined. Different conditions should be tested to obtain higher yields of antibodies.

Zhang with colleagues' described how different factors may affect production efficacy [172]. HEK293 cells are most commonly used for transient transfection, whereas CHO and NS0 cells are the most commonly used for generating stable cell lines. The dose of serum in DMEM culture media influences transfection efficacy and antibodies' expression after the transfection. Carton and colleagues demonstrated different ways to increase mab expression level [173]. The authors demonstrated the effects of coding sequence variation on the expression of mabs specific to human MCP-1. The effects of codon engineering on both transient and stable transfection were analyzed. NS0 cells showed more than an 8-fold increase of viable clones and more than a 2-fold increase of antibody titers. Transiently transfected HEK293 cells had 30% higher expression when a codon-engineered vector was used than the phage display library variant. However, another codon variant decreased the expression level 10-fold compared to the phage display library variant [173]. Sequences encoding the heavy and light chain of given antibodies in viral vectors may lead to even higher productivity.

In conclusion, the design, synthesis, and cloning of plasmid vectors containing DNA coding for the two IgG chains (heavy and light) for Cetuximab and Rituximab antibodies were accomplished. Further, human HEK293 cells co-transfected with vectors encoding a heavy and a light chain showed detectable levels of secreted human IgG. Characterization by Western blot showed that the expressed mab were of the expected size and confirmed specificity to their target antigens. A further study to assess the functionality of the secreted mabs will reveal whether the created vectors are suitable for delivering mabs using this proposed strategy and, thus, the potential applications in cancer treatment.

CHAPTER 4

Aim II: DELIVERY OF FUNCTIONAL MONOCLONAL ANTI-SPIKE ANTIBODIES FROM MICROENCAPSULATED CELLS

Even though coronavirus disease (COVID-19) remains a significant threat to global health, the rapid advancement of preventive and therapeutic antiviral modalities boosted by the international effort to end the pandemic has led to a decline in COVID-19 infection and mortality worldwide [174]. Anti-inflammatory corticosteroids, IL-6 receptor blockers (tocilizumab or sarilumab), the Janus kinase inhibitor baricitinib, and SARS-CoV-2-neutralizing mabs (sotrovimab, casirivimab, and imdevimab) are now on the list of therapeutics that are clinically approved [175]. SARS-CoV-2-targeting mabs stand out from the others due to their particular mode of action, neutralizing SARS-CoV-2[176]. Furthermore, growing clinical trial data suggests that mabs can lower SARS-CoV-2 viral loads and improve clinical outcomes in specific patient sub-categories [177]. Additionally, some research has indicated that COVID-19-exposed individuals might benefit from prophylactic use of SARS-CoV-2 mabs [177].

However, the complicated and expensive nature of mab manufacturing, where mab production and purification are costly and difficult product development, is a significant obstacle to implementing mab therapy in clinical trial practice. In addition, parenteral mab delivery poses additional clinical difficulties. Despite the fact that mab therapy generally has low reactogenicity, patients can still experience mild-to-moderate injection site and infusion-related side effects [178].

This thesis proposes that mabs specific to SARS-CoV-2 might be efficiently delivered by allogeneic cells expressing the encapsulated mab to increase cell viability and protect them against host immune rejection. Multiple diseases, including diabetes mellitus, anemia, cancer, and neurodegenerative disease, have been successfully treated in relevant animal models, and there have been clinical trials using the delivery of therapeutic agents from microencapsulated cells [179]. Therefore, SARS-CoV-2 mab delivery by encapsulated cells might be a successful substitute for bolus mab injection-based COVID-19 treatment. This hypothesis was tested in a pre-clinical murine model and the results show that implanted microcapsules can deliver systemically detectable levels of a SARS-CoV-2 mab sustained for up to 40 days after implantation.

4.1 MATERIALS AND METHODS

Cells

HEK293 human embryonic kidney cells (CRL-1573) and G8 murine fetal myoblasts (CRL-1456) were procured from American Type Culture Collection (ATCC, Manassas, VA, USA) and cultured in Dulbecco's Modified Eagle Medium (#61965-026, Gibco, Waltham, MA, USA) with 10% fetal bovine serum (FBS) and 1% penicillin/streptomycin.

Plasmids

The vectors for expressing human immunoglobulin heavy and light chains anti-severe acute respiratory syndrome coronavirus (SARS-CoV) were obtained from BEI (NIH, USA). These plasmids (NR-52399 and NR-52400) contain DNA sequences coding for vH and vL as per GenBank DQ168569 and DQ168570, respectively (Figure 19). This dual plasmid system codes for neutralizing mab CR3022 (BEI, NIH) that targets a highly conserved epitope of the *Spike* protein of SARS-CoV-2; the *spike* protein of the virus binds to the ACE2 receptor in human cells and initiates its cellular uptake. This dual plasmid vector (pFUSE) is the same one used for the secretion of mab to cancer antigens EGFR and CD20 in Chapter 3 of this thesis.

The vH and vL sequences were subcloned into mammalian expression vectors (pFUSEss-CHIg-hG1 and pFUSEss-CLIg-hk, respectively) and fused to the N-terminal interleukin 2 (IL-2) signal sequence and the C-terminal constant portions of human IgG1 (hIgG1) heavy or human Ig kappa (hIg) light chain. These plasmids end up being 4830 base pairs and 4190 base pairs in size, respectively (BEI, NIH). The CR3022 mab was expressed by co-transfecting plasmids NR-52399 and NR-52400.

>DQ168569.1 **Homo sapiens anti-SARS-CoV immunoglobulin heavy chain variable region mRNA, partial cds**
CAGATGCAGCTGGTGCAATCTGGAACAGAGGTGAAAAAGCCGGGGGAGTCTCTGAAGATCTCCTGTAAGG
GTTCTGGATACGGCTTTATCACCTACTGGATCGGCTGGGTGCGCCAGATGCCCGGGAAAGGCCTGGAGTG
GATGGGGATCATCTATCCTGGTGACTCTGAAACCAGATACAGCCCGTCCTTCCAAGGCCAGGTCACCATC
TCAGCCGACAAGTCCATCAACACCGCCTACCTGCAGTGGAGCAGCCTGAAGGCCTCGGACACCGCCATAT
ATTACTGTGCGGGGGGTTCGGGGATTTCTACCCCTATGGACGTCTGGGGCCAAGGGACCACGGTCACCGT
C
>DQ168570.1 **Homo sapiens anti-SARS-CoV immunoglobulin light chain variable region mRNA, partial cds**
GACATCCAGTTGACCCAGTCTCCAGACTCCCTGGCTGTGTCTCTGGGCGAGAGGGCCACCATCAACTGCA
AGTCCAGCCAGAGTGTTTTATACAGCTCCATCAATAAGAACTACTTAGCTTGGTACCAGCAGAAACCAGG
ACAGCCTCCTAAGCTGCTCATTTACTGGGCATCTACCCGGGAATCCGGGGTCCCTGACCGATTCAGTGGC
AGCGGGTCTGGGACAGATTTCACTCTCACCATCAGCAGCCTGCAGGCTGAAGATGTGGCAGTTTATTACT
GTCAGCAATATTATAGTACTCCGTACACTTTTGGCCAGGGGACCAAGGTGGAAATCAAA

Figure 19. DNA sequences coding for vH and vL regions of mab CR3022 against *Spike* protein.

Cell transfection

BEI Resources provided the CR3022 plasmid set (NR-53260), which encodes the vH and vL sequences fused to the C-terminal constant sections of human IgG1 (hIgG1) heavy or human Ig kappa (hIgκ) light chains, respectively (NIAID, NIH). Following the manufacturer's instructions, G8 and HEK293 cells were co-transfected with the CR3022 plasmids at 60% confluence in 100 mm cell culture dishes using liposome forming transfection reagent Escort-III (L3037, Sigma). Briefly, cells were treated for 6 hours at 37°C with a pre-incubated combination of 5 μg of each plasmid and 5 μl of Escort-III in 990 μL of Opti-MEM. Then, after two weeks of cell culture, stable expressing cells were chosen by adding 400 μg/ml of zeocin and 10 μg/ml of blasticidin to the growth medium. Western blotting and ELISA were used to measure the secretion of mabs.

Western Blotting

The specificity and size of the produced mab were confirmed by Western blotting. On a 10% SDS-PAGE gel, *spike* (NR-722, BEI Resources, NIAID, NIH, Bethesda, MD, USA) and nucleocapsid (NR-48761, BEI Resources) proteins were separated. Then they were transferred for 1 hour at 350 mA onto a PVDF (Polyvinylidene fluoride) membrane. After blocking the membrane with 5% (w/v) dried milk powder in PBST (1 x PBS, 0.05% Tween 20), it was rinsed three times in TBST before being blotted with cell culture supernatant at 4°C overnight. HRP-conjugated anti-human antibodies specific to either full human IgG (rabbit ab6759, Abcam) or the IgG Fc region (goat ab97225, Abcam) were used for mab detection. These antibodies were diluted to 1:10,000 and incubated on the membrane for 1 hour at RT. Before SDS-PAGE separation, purified (on Protein G HP Spin Trap) cell supernatant was heated for 5 min at 95°C under reducing conditions to determine the mab's denatured form. The PageRuler Prestained Protein Ladder (#26616, Thermo Fisher Scientific) was used to determine the molecular weight by using human mab CR3022 from BEI Resources (NR-52481, 500 ng/well, 20 ng/μl) as a control. ChemiDoc MP Imaging System (Bio-Rad) was used for image analysis.

Designed ELISA test to detect SARS-CoV-2 antibodies

Thermo Fisher Scientific's #460984 Flat-Bottom Immuno Nonsterile 96-well plates were coated with *Spike* protein at a concentration of 2 ng/μL for overnight incubation at 4°C (NR-722, BEI Resources). The wells were rinsed three times with PBST the next day, after which they were blocked for an hour at RT with 5% milk in PBST. Plasma or Cell culture supernatant (at a dilution

of 1:100, 100 μL) was added to every well and incubated for 2 hours at RT. After washing, a 1:100,000 diluted horseradish peroxidase (HRP)-conjugated goat anti-human IgG (Fc-specific, ab97225, Abcam) solution was added to the plate for 1 hour. A final wash was followed by adding TMB (3,3′,5,5′-tetramethylbenzidine) chromogenic substrate (#34029, Thermo Fisher Scientific) and a 15-minute incubation period in the dark. 50 μL of stop solution (#SS04, Thermo Fisher Scientific) was used to stop the process. Total human IgG measurement was performed using the above-described *Spike* detection methodology, with the following modifications: plates were coated with primary goat anti-human IgG (Fc specific, Sigma-Aldrich, I2136) at 1:10,000 dilution, and secondary rabbit anti-human IgG H+L (ab6957) mab at 1:100,000 dilution.

The Varioscan Flash microplate reader (Thermo Fisher Scientific) was used to detect absorbance at 450 nm. The CR3022 (NR-52481, BEI Resources) mab was diluted in PBS starting at a maximum concentration of 4 μg/mL in order to build a calibration curve.

For the RBD ELISA, the plates were coated with RBD protein (BEI, NIH) at a concentration of 2ng/μL for overnight incubation at 4°C (NR-72946, BEI Resources). The mab concentrations were determined using standard curves and experimental optical density (OD) readouts normalized to average baseline values obtained for respective controls, i.e., untransfected supernatant or blood plasma from CR3022-naive G8 capsule implanted animals. The respective control OD values were subtracted from the experimental OD readings to determine the mab concentrations. Human plasma from COVID-19 seroprevalence and vaccination research findings was used to validate the in-house ELISA, compared to a commercially available S-IgG assay (Euroimmun Medizinische Labordiagnostika AG, Lübeck, Germany). The Research Ethics Board of Karaganda Medical University approved these studies. The 20 human samples included 10 subjects who had received the vaccine (SARS-CoV-2 Ab+) and 10 pre-pandemic (SARS-CoV-2 Ab-negative) samples randomly selected according to availability.

For the detection of mouse antibodies against the delivered monoclonal CR3022, plates were coated with CR3022. Following incubation with mice plasma samples. Bound antibodies were detected with goat anti-mouse IgG secondary antibody.

Cell Encapsulation

Low viscosity alginate powder (Keltone LV, 50-80 kD MW#9005-38-3, San Diego, CA, USA) was dissolved in 0.9% sodium chloride overnight at 37°C and then filtered through a 0.22 μm filter to create an alginate solution (1.5%). An alginate solution containing 5×10^6 cells/mL was used as the suspension medium. As previously described, alginate microbeads were produced with slight

modifications using the Var1 electrostatic encapsulator (Nisco Engineering Inc., Zurich, Switzerland). In a nutshell, the cell suspension was pumped into a vial containing a cold 100 mM $CaCl_2$ solution using a NISCO Var-1 encapsulator (Nisco Engineering Inc., Zurich, Switzerland) at a voltage of 7.10 kV and a flow rate of 20 mL/h, generating microcapsules that were 300–500 μm in diameter (Figure 20). The cell-loaded microcapsules were subsequently rinsed with saline solution, cross-linked with PLL for 6 minutes, and then coated with an outer layer of alginate for 4 minutes. Following the addition of DMEM, the solution containing the microcapsules was transferred to an incubator. The viability of microencapsulated cells was evaluated using the trypan blue exclusion assay, in which 20 μL of microcapsules and 20 μL of trypan blue (Invitrogen, USA) were installed on a microscope slide and crushed by a glass coverslip to release the encapsulated cells. Then, the released cells were visualized and manually quantified using an inverted light microscope (Ceti, Medline Scientific, Chalgrove, UK) or by using an automated cell counter Countess 3 (Thermo Fisher). Microcapsules that had been air-dried for one hour at RT were imaged using an electron microscope with a JSM-IT200LA scanning electron microscope.

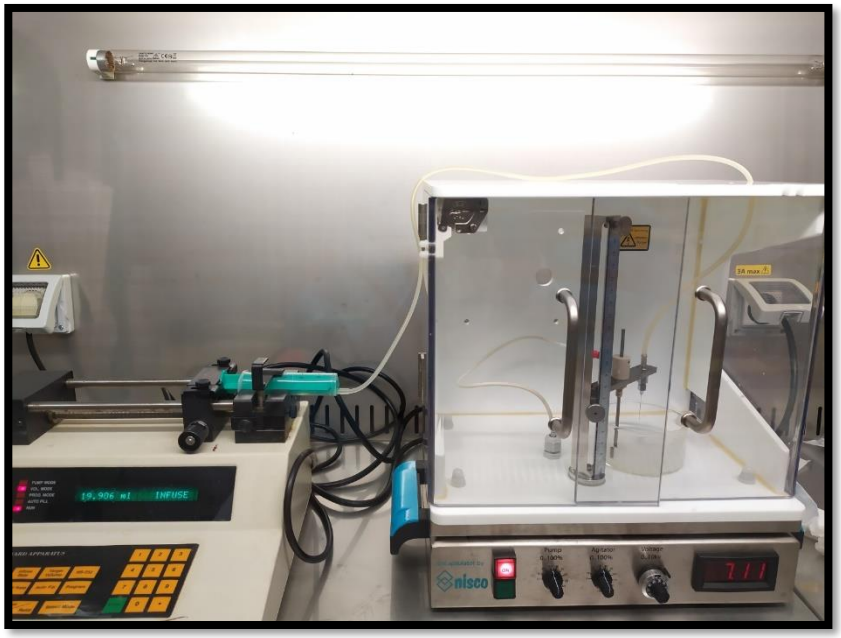

Figure 20. Nisco Var1 electrostatic encapsulator machine.

Animal studies

All animal treatments were carried out following the National Center for Biotechnology and Nazarbayev University's Animal Ethics Guidelines (Nur-Sultan, Kazakhstan). Eight-week-old

C57BL/6J female mice were obtained from the National Center for Biotechnology's animal facility. The animals (initially obtained from Charles River, Germany) were kept in a pathogen-free setting. There were three experimental groups: group #1 received microcapsules containing non-transfected cells (n=4), group #2 received microcapsules containing transfected cells (n=6), and group #3 received an intraperitoneal injection of 1 ml of 5 mg/ml polyclonal human IgG (#A50170H, Meridian Life Sciences, Memphis, TN, USA) in PBS solution using an 18G cannula (n=2). Animals were given isoflurane anesthesia before the capsules were implanted (Harvard Apparatus, UK). Microcapsules were injected intraperitoneally with a G18 catheter that included 3 ml of microcapsule solution at an average rate of 5000 microcapsules per 1 ml (Figure 21).

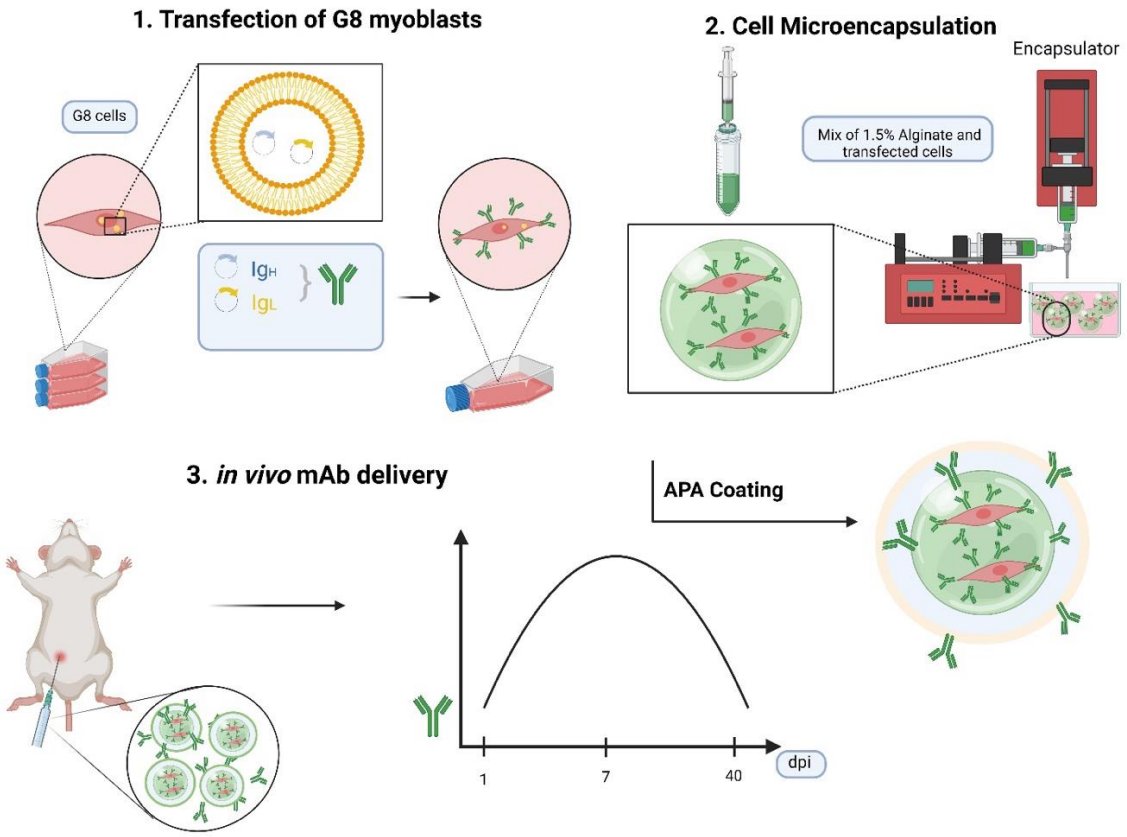

Figure 21. Schematic representation of mab secretion from microencapsulated cells. Partially adapted from[125].

Plasma was extracted from tail vein blood by centrifuging at 2000g for 10 minutes and stored at 20°C before use. Mice were sacrificed by anesthesia overdose 40 days after implantation and microcapsules (available volume 2.5 ml) were collected and examined using inverted light

microscopy (EVOS FL Auto, Thermo Fisher Scientific). The microcapsules were washed in PBS before cell viability, and mab secretion was tested.

Statistical analysis

GraphPad Prism V.9.3.1 was used for all analyses. The unpaired t-test was used to compare differences between groups, and the binomial "exact" method was used to calculate 95% confidence intervals (CI).

4.2 RESULTS

Genetic engineering of mammalian cells with plasmids coding for the heavy and light chains of a monoclonal antibody against SARS-CoV-2.

Plasmids (pFUSE) encoding the heavy and the light chains of CR3022 specific to the *spike* protein of SARS-CoV-2 were obtained through the research repository of BEI (NIH, USA) and used to co-transfect HEK293 and G8 cells. This plasmid backbone is the same described in Chapter 3 for the secretion of mab for cancer treatment (against EGFR and CD20).

A. G8 myoblasts are capable of sustained CR3022 expression.

The production of CR3022 mab by murine G8 myoblasts was assessed after being co-transfected with pFUSE plasmids encoding heavy and light chains. The expression of CR3022 by G8 myoblasts in tissue culture was determined by an in-house ELISA test and found to be comparable to that of HEK293 cells in ELISA experiments (Figure 22). In addition to transient transfection, stable clones secreting *Spike* were obtained from G8 and HEK293 cells. Stable clones secreted higher levels of mab to *Spike* than transiently transfected cells (Figure 22).

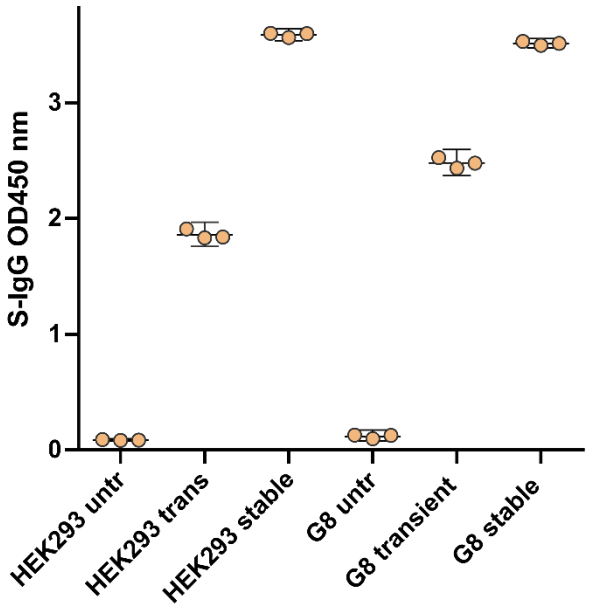

Figure 22. Representative ELISA plot of S-IgG binding for HEK293 and G8 cell supernatants. Cell supernatants were incubated on plates coated with S-proteins. Supernatants were collected at 48h post-encapsulation. Experiments were conducted in triplicate, and error bars indicate standard deviation.

In addition to the binding of CR3022 mab to the *spike* protein, the specificity of the mab to the RBD of the *spike* was also investigated. An ELISA specific to the RBD was designed in our laboratory and used to quantify the mab in the supernatant of transfected G8 cells. The ELISA results suggest the specificity of CR3022 mab to RBD (Figure 23). The secretion of mab by cultured G8 cells showed good level that steadily rose after transfection and was maintained at a level of ~310 ng/10^6 cells per day (Figure 23), again suggesting the potential of the transfected cells to deliver sustained levels of mab.

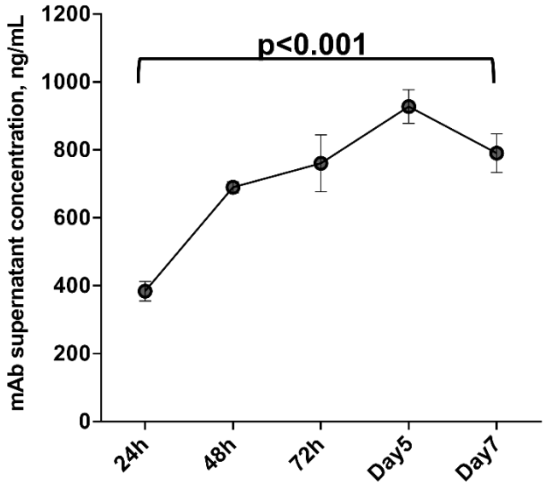

Figure 23. Secretion levels of CR3022 in cultured G8 cells were measured using receptor binding domain (RBD) ELISA and standardized to the non-transfected supernatant readout. Cell media were replaced every 24 h. Experiments were conducted in triplicate, and error bars indicate standard deviation.

B. Characterization of secreted monoclonal antibodies in transfected cells.

The specificity of the secreted mab was determined by Western blotting. Purified proteins from the SARS-CoV-2 *spike* and nucleocapsid (BEI, NIH) were separated by PAGE and blotted with supernatant from cultured G8 cells secreting CR3022 mab. The results showed that labeled anti-human IgG revealed bands consistent with the *spike* protein in a dose-dependent manner (Figure 24), indicating the presence of human IgG in the supernatant of co-transfected G8 cells. In contrast, nucleocapsid protein did not react with the supernatant, indicating that the secreted mab is specific to *spike* and not nucleocapsid. As a negative control, supernatant from untransfected G8 cells did not yield any signal for either *spike* or nucleocapsid (Figure 25, a). As a positive control, blotting with purified CR3022 IgG obtained from BEI (NIH, USA) reacted with *spike* protein but not nucleocapsid (Figure 25, b). The separated proteins were shown to be specific to *spike* but not to the SARS-CoV-2 nucleocapsid protein.

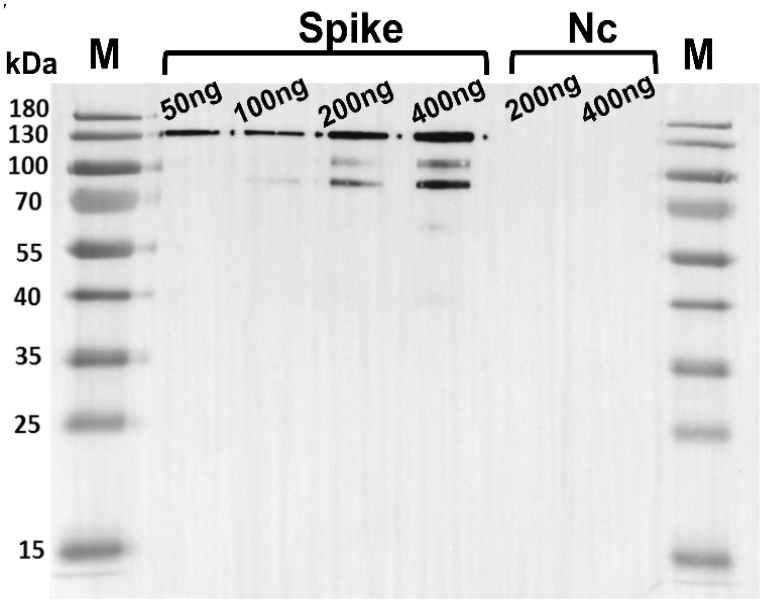

Figure 24. SARS-CoV-2 monoclonal antibody secretion in G8 cells co-transfected with the CR3022 heavy and light chains. Various concentrations of *Spike* and Nucleocapsid proteins were run on a 10% SDS–PAGE gel. It was then transferred onto a PVDF membrane and blotted with G8 cell culture supernatant. An HRP-conjugated rabbit IgG specific to both the heavy and light chains of human IgG was used for the probing.

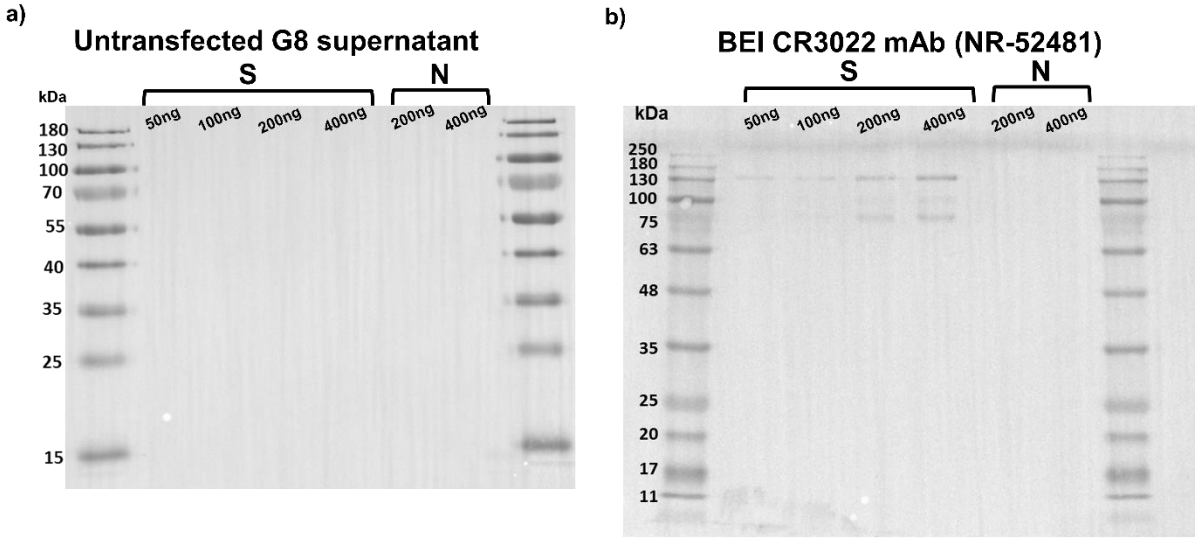

Figure 25. Western blotting of supernatants from control (non-transfected) G8 cells (a) and commercial BEI CR3022 mab (b). Various concentrations of *Spike* and Nucleocapsid proteins were run on a 10% SDS–PAGE gel. It was then transferred onto a PVDF membrane and blotted with G8 cell culture supernatant. An HRP-conjugated rabbit IgG specific to both the heavy and light chains of human IgG was used for the probing.

A similar characterization was performed for the mab against *spike* secreted from human HEK293 cells genetically engineered with the two pFUSE plasmids encoding for the heavy and light chains of mab CR 3022. As described earlier, purified *spike* and nucleocapsid proteins from SAR-CoV-2 were run by PAGE, and the resulting pattern was blotted against supernatant from HEK293 cells. As described for G8 cells, the results showed that labeled anti-human IgG revealed bands consistent with the *spike* protein in a dose-dependent manner (Figure 26, a), indicating the presence of human IgG in the supernatant of co-transfected HEK293 cells. In contrast, nucleocapsid protein did not react with the supernatant, indicating that the secreted mab is specific to *spike* and not nucleocapsid. As a negative control, supernatant from untransfected HEK293 cells did not yield any signal for either spike or nucleocapsid (Figure 26, b).

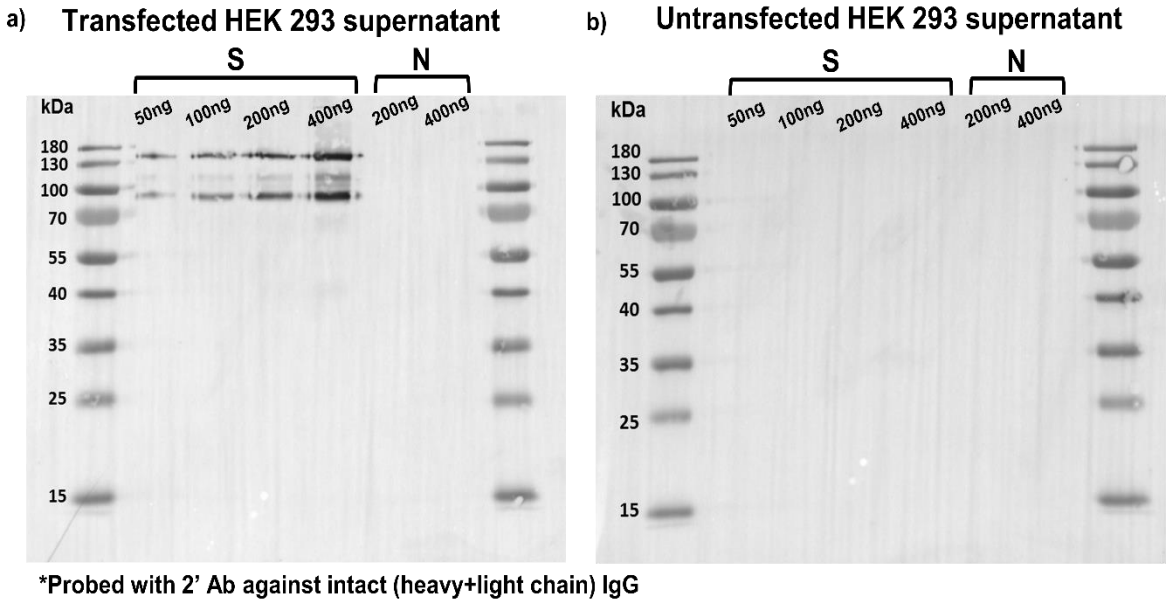

Figure 26. SARS-CoV-2 monoclonal antibody secretion in HEK293 cells co-transfected with the CR3022 heavy and light chains. Various concentrations of *Spike* and Nucleocapsid proteins were run on a 10% SDS–PAGE gel. It was then transferred onto a PVDF membrane and blotted with HEK293 cell culture supernatant a) co-transfected; b) non-transfected. An HRP-conjugated rabbit IgG specific to both the heavy and light chains of human IgG was used for the probing.

Furthermore, the positive bands identified by western blotting have an apparent molecular weight of approximately 140-160 kDa, which is consistent with the reported size of the *spike* protein [180] (Figure 27).

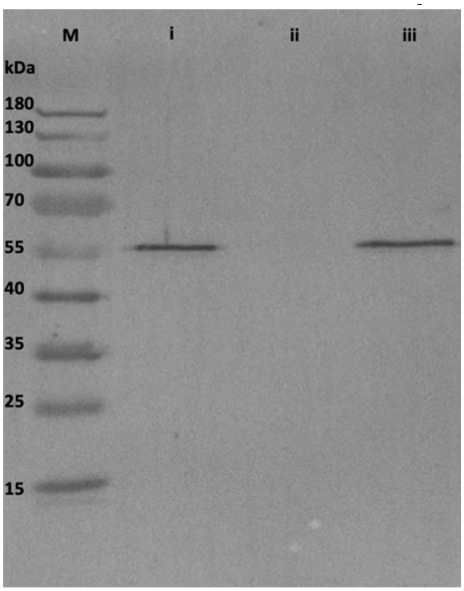

Figure 27. Purified cell culture supernatants and the BEI CR3022 mab were denatured prior to Western blotting. I: Transfected HEK293 supernatant; ii: Untransfected HEK293 supernatant; iii: BEI CR3022 mab (NR-52481). An HRP-conjugated goat IgG specific to both the heavy chain Fc region of human IgG was used for the probing. kDa-kilodaltons.

Taken together, these experiments suggest the specificity for the *spike* of the secreted mab from both human HEK293 and murine G8 myoblast cells, as well as the secretion of a functional mab to *spike* from murine G8 and human HEK293 cells.

G8 microcapsules secrete detectable levels of CR3022.

As per the previous chapter, the delivery of mab from microencapsulated cells was evaluated to confirm the permeability of mabs to the *spike* protein through alginate microcapsules. G8 cells genetically engineered with the plasmids encoding both chains of *spike* mab were encapsulated and cultured *in vitro*. ELISA quantified the level of mab specific to *spike* in the cell supernatant. The results (Figure 28) showed a high secretion of mab through microcapsules, supporting the feasibility of this thesis. Interestingly, the OD obtained from encapsulated and free cells alike was higher than in a control plasma sample of a volunteer after receiving a COVID vaccine.

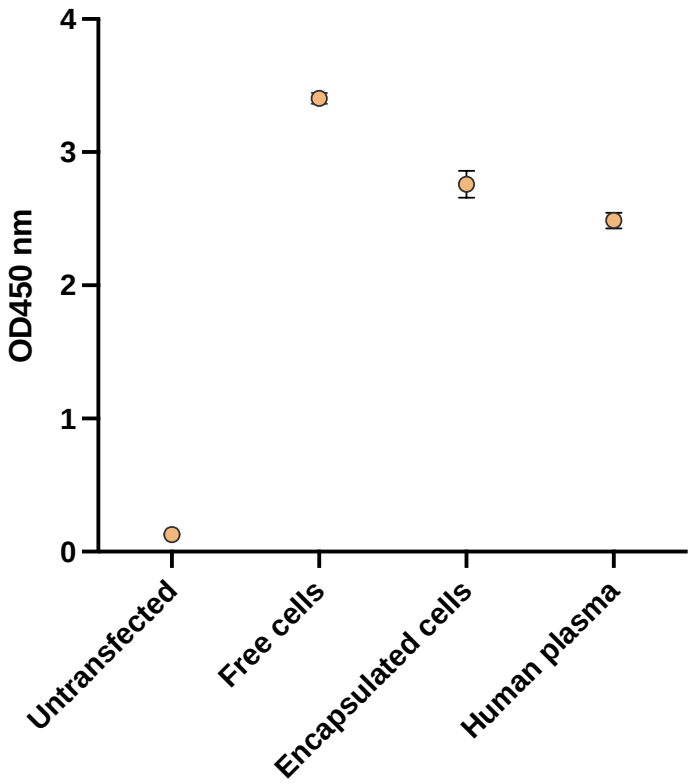

Figure 28. Representative ELISA plot of S-IgG binding for G8 cell supernatants untransfected, transfected, encapsulated cells to compare with the human plasma of a patient with COVID-19. Cell supernatants were incubated on plates coated with S-protein. Supernatants were collected at 48h post-encapsulation. Experiments were conducted in triplicate, and error bars indicate standard deviation.

G8 cells have been used more frequently than other cell types for prolonged cell encapsulation and microcapsule implantation because of their low immunogenicity features [114,181]. Therefore, using our previously validated method, which resulted in microcapsules containing highly viable cells[182], to encapsulate G8 cells that were consistently producing CR3022 through alginate microcapsules at a concentration of about 1000 cells/capsule [114,181]. This method produced round microcapsules with an average diameter of 106 [range= 79-110] μm, pores with an average diameter of 595 [range= 306-920] nm (Figure 27), and cell viability of approximately 95% (Figure 29).

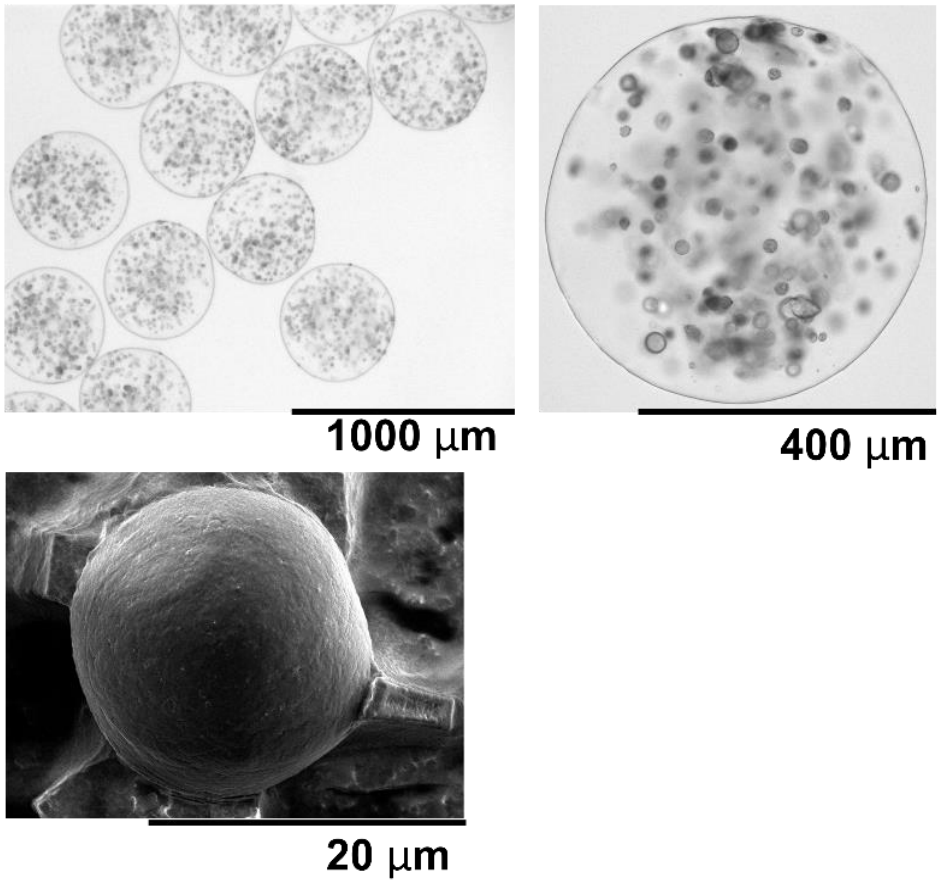

Figure 29. Alginate microcapsules containing G8 cells. Images were taken using light (at ×4 and ×10 magnification) and scanning electron microscopy (at ×800 magnification).

Figure 30. Representative output from the automated cell counter shows the cells' count and viability from retrieved microcapsules.

Compared to free (unencapsulated) cells, encapsulated G8 cells produced CR3022 mab at quantities similar to those of encapsulated human HEK293 cells (Figures 22, 30), though at lower levels. The medium supernatant was consistently enriched with measurable levels of CR3022 mab from cultivated G8 microcapsules.

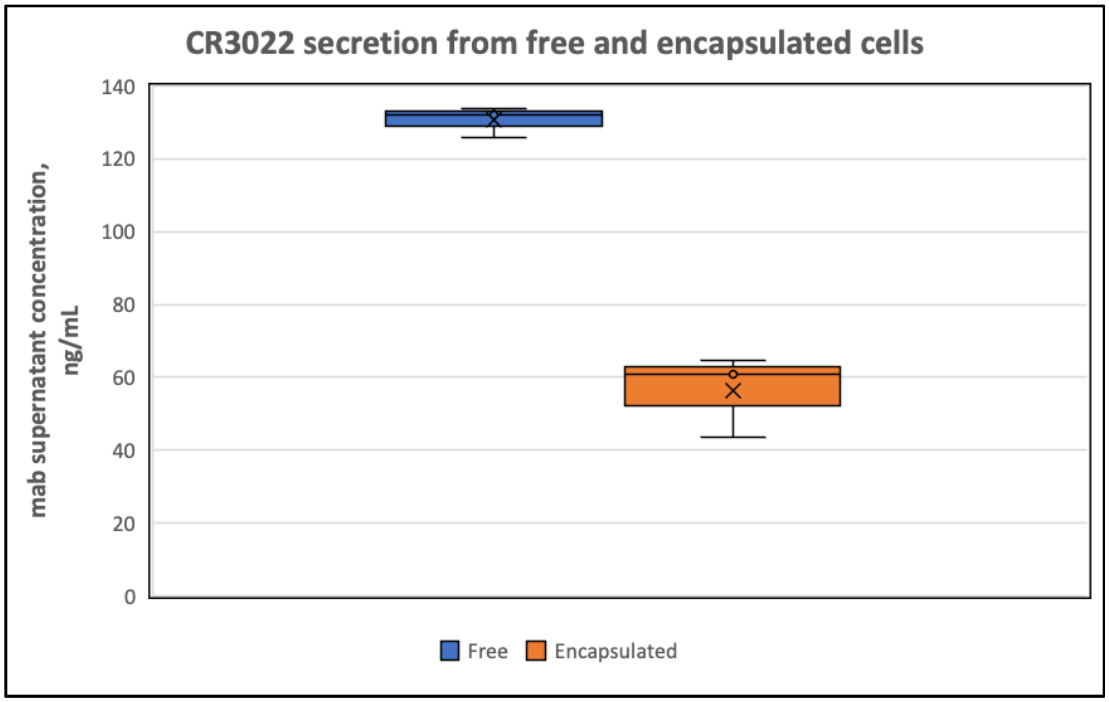

Figure 31. Supernatants obtained from non-encapsulated and encapsulated G8 cells consistently secreting CR3022 48 hours after the last culture media change. On RBD-coated ELISA plates, supernatants (diluted to 1/100) were incubated. Standard curves were created using CR3022 mab (NR-52481, BEI Resources) dilutions on experimental readouts adjusted to the equivalent baseline control (untransfected supernatant) OD readouts (see Methods). Experiments were conducted in triplicate, and error bars indicate standard deviation.

In conclusion, it was confirmed that encapsulated G8 and HEK293 cells secrete sustainable CR3022 mab into the supernatant at levels lower than free cells.

C. Delivery of monoclonal antibodies in mice implanted with microencapsulated cells.

In vivo microcapsule implantation results in systemically detectable CR3022 mab

Once the secretion of mab from encapsulated cells was confirmed, this therapeutic strategy's feasibility in delivering mab *in vivo* was investigated. Microencapsulated G8 cells expressing CR3022 mab were implanted intraperitoneally in immunocompetent C57BL/6J mice (n=6). Mice were bled before implantation and at various time points after implantation. The concentration of CR3022 mab in treated mice was monitored CR3022 levels in blood post-implantation (HPI), quantifying the concentration of mab using the designed RBD-specific ELISA (Figure 32, A, B). At 24 hours post-injection, CR3022 was detected in the blood plasma of treated mice. Its concentration grew steadily until 7 days later when it peaked at 1923 ng/ml [95% CI, 1656.1-2189.9

ng/ml] (Figure 32, B). After then, CR3022 titers gradually decreased, even though they were still detectable 40 days later at a concentration of 522.0 ng/ml [95% CI, 400.8 - 642.7] (Figure 32, B). In contrast, no circulating mab was found in the control group of mice (n=4), which were treated with encapsulated but untransfected cells.

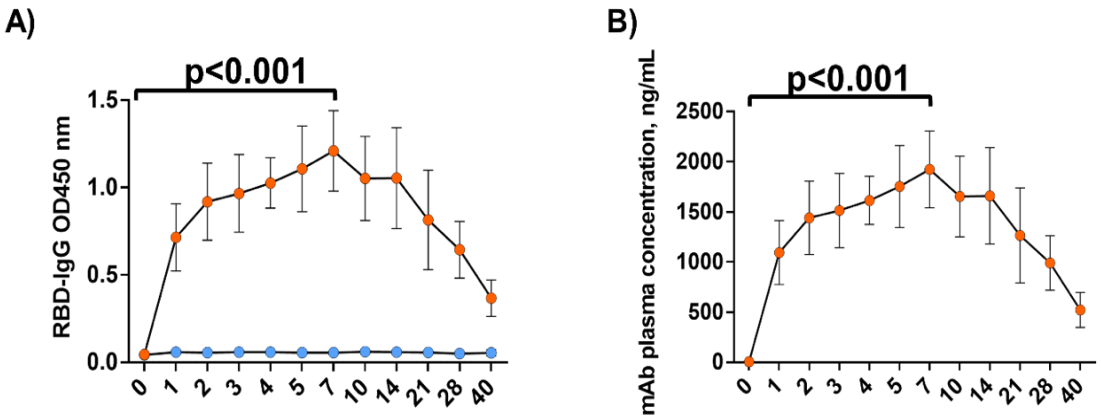

Figure 32. A, B) Changes in the levels of circulating SARS-CoV-2 mab following the administration of microcapsules. Blood from mice was obtained pre-implantation (day 0) and following days up to day 40 post-implantation to get plasma for the ELISA tests. Results from the RBD-IgG ELISA were shown as OD450 readings (A) and mab concentration adjusted to mouse plasma implanted with the CR3022-naïve G8 microcapsules (B). Concentrations were measured based on experimental readouts adjusted to the relevant baseline control (blood plasma from CR3022-naive G8 capsule implants) using a standard curve created using a CR3022 mab (NR-52481) from BEI (see Methods). Experiments were conducted in triplicate, and error bars indicate standard deviation.

Yet another group of mice (n=4) received a clinical dose (1 mg/kg) of polyclonal human IgG (IVIG). This control group of mice did not test positive for RBD, indirectly indicating the specificity of the secreted mab to RBD (Figure 32, C).

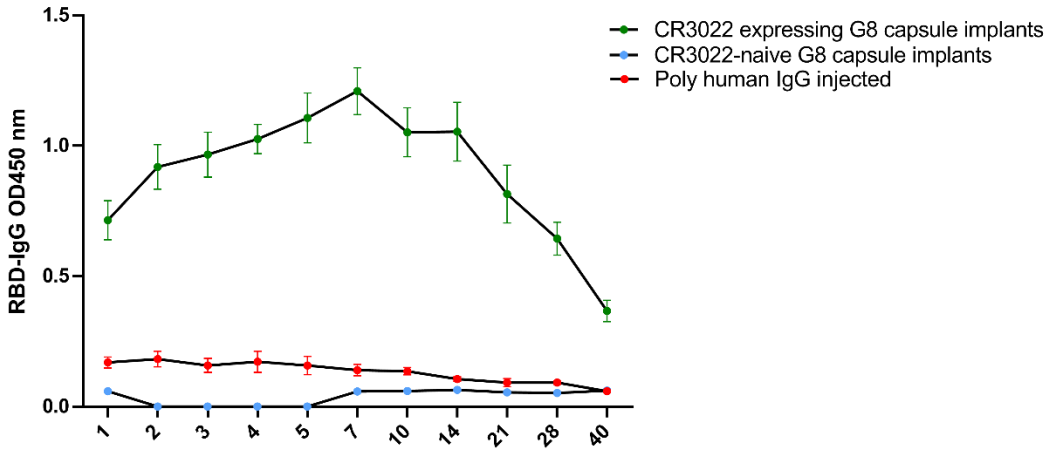

Figure 32. C) SARS-CoV-2 monoclonal antibody (CR3022) identification in mice after implantation for more than 40 days. Experiments were conducted in triplicate, and error bars indicate standard deviation.

D. Functional characterization of secreted monoclonal antibodies

In cases involving a slow, prolonged release of the mab over an extended period, cell encapsulation-aided mab delivery is preferable to bolus mab administration. This proposed strategy is an example of a prophylactic mab administration that could be recommended for immunocompromised patients. The goal is to deliver neutralizing mab titers at a level required to inhibit or reduce SARS-CoV-2 infections. Because microcapsules can deliver mab gradually, reactogenicity -typically linked to bolus mab infusions- may also be reduced. In addition, microencapsulation of cells expressing various mabs would enable consistent release of combined mabs with a potentially more substantial prophylactic or therapeutic effect given the known drawbacks of monotherapy and the higher likelihood of SARS-CoV-2 resistance development associated with monotherapy.

A large-scale library screen initially identified CR3022 mab as a SARS-CoV-1 neutralizing mab, but later tests revealed that it also neutralized SARS-CoV-2 *[183,184]*. The ability of CR3022 to neutralize different strains of the virus has been shown to vary across assays, and a recent study found that CR3022 can neutralize SARS-CoV-2 without interfering with the interaction between the ACE2 and RBD *[185]*.

In our laboratory, CR3022 mab had a modest neutralizing activity (Figure 33). The experiment was conducted using a GenScript neutralizing assay for human plasma, with slight modifications.

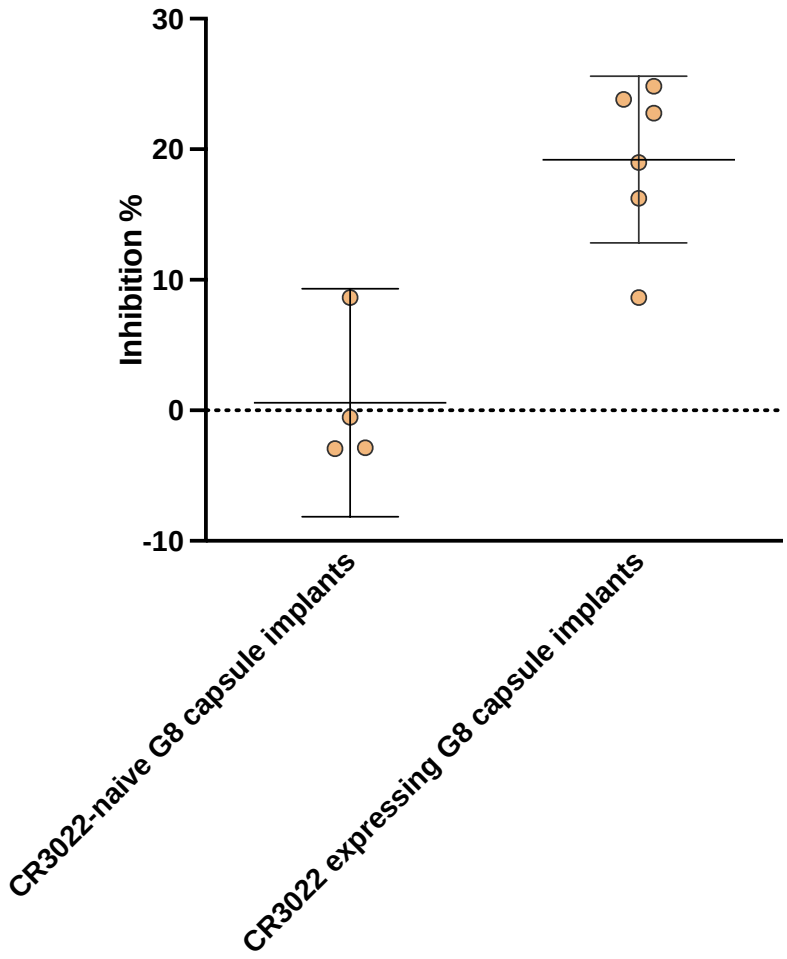

Figure 33. Neutralization assay showing partial neutralization. The manufacturer's instructions were followed, except the incubation time of plasma samples was extended to 1 hour instead of 30 minutes. Experiments were conducted in triplicate, and error bars indicate standard deviation.

The data presented here indicate that CR3022 has partial neutralization activity (~30%). This partial neutralization activity may explain the controversial neutralization activity found for this mab in current literature reports.

Host anti-CR3022 response and per-capsule mab expression changes.

The detection of mab *in vivo* strongly supports the feasibility of this strategy to deliver mabs. However, the levels of mab peaked on day 7 and gradually decreased after that. Thus, the next goal was to determine whether the observed reduction in CR3022 titers 7 days post implantation (dpi) was caused by reduced secretion of mab per capsule or by developing a host immune response. The presence of antibodies to human IgG would explain the gradual loss of mab in the circulation of treated mice. An ELISA test determined the antibodies to CR3022 in mouse plasma over 40 days

of the experiment (Figure 34). The titers of mouse anti-CR3022 IgG steadily rose, culminating at about days 10 to 14, which would explain the observed decrease in mab. At 40 days post-implantation, we removed a sample of the implanted microcapsules from the peritoneal cavity and tested their ability to produce CR3022 in culture.

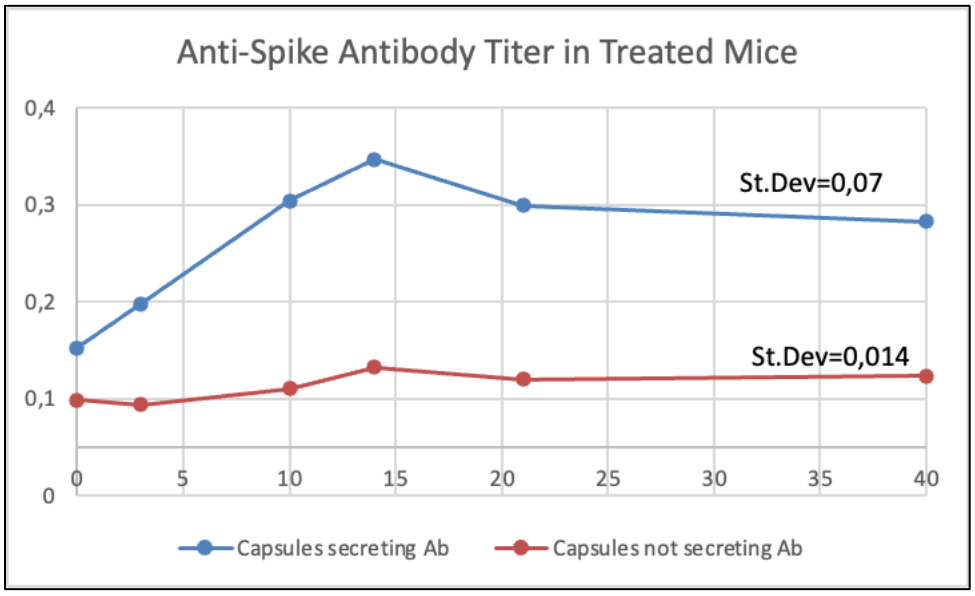

Figure 34. ELISA measurement of the mouse anti-CR3022 antibody response. Experiments were conducted in triplicate, and error bars indicate standard deviation.

The cell viability of the retrieved microcapsules was also determined. At 40 dpi, the microcapsules retrieved from the peritoneal cavity showed no prominent cellular infiltration, indicating good biocompatibility (Figure 35).

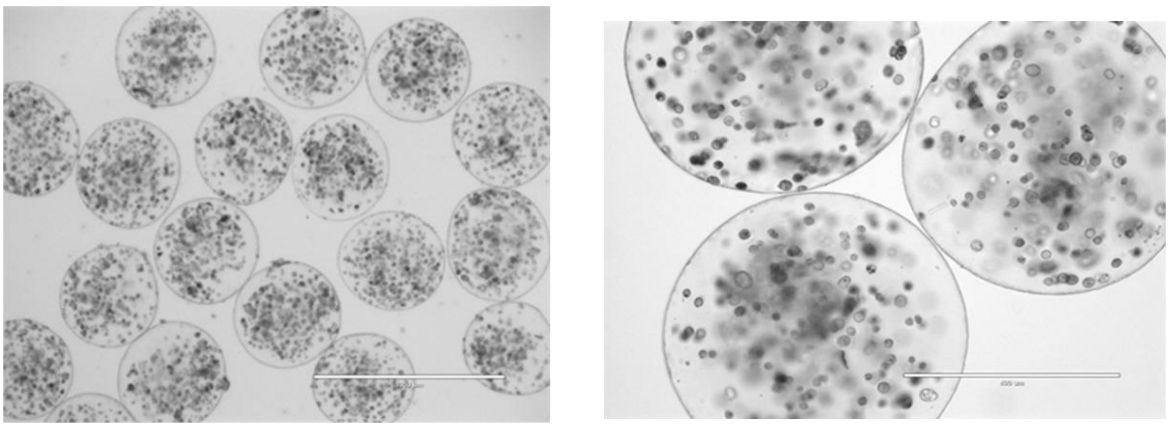

Figure 35. G8 cell-containing alginate microcapsules were removed from the peritoneal cavity after 40 dpi. Images were obtained using light microscopy at ×4 (left panel) and ×10 (right panel) magnifications.

At that same time, post-implantation, an RBD ELISA revealed that the secretion of CR3022 decreased from 45 ng per 10^4 microcapsules per day before implantation to 30 ng per 10^4 microcapsules per day, which is statistically significant (Figure 36).

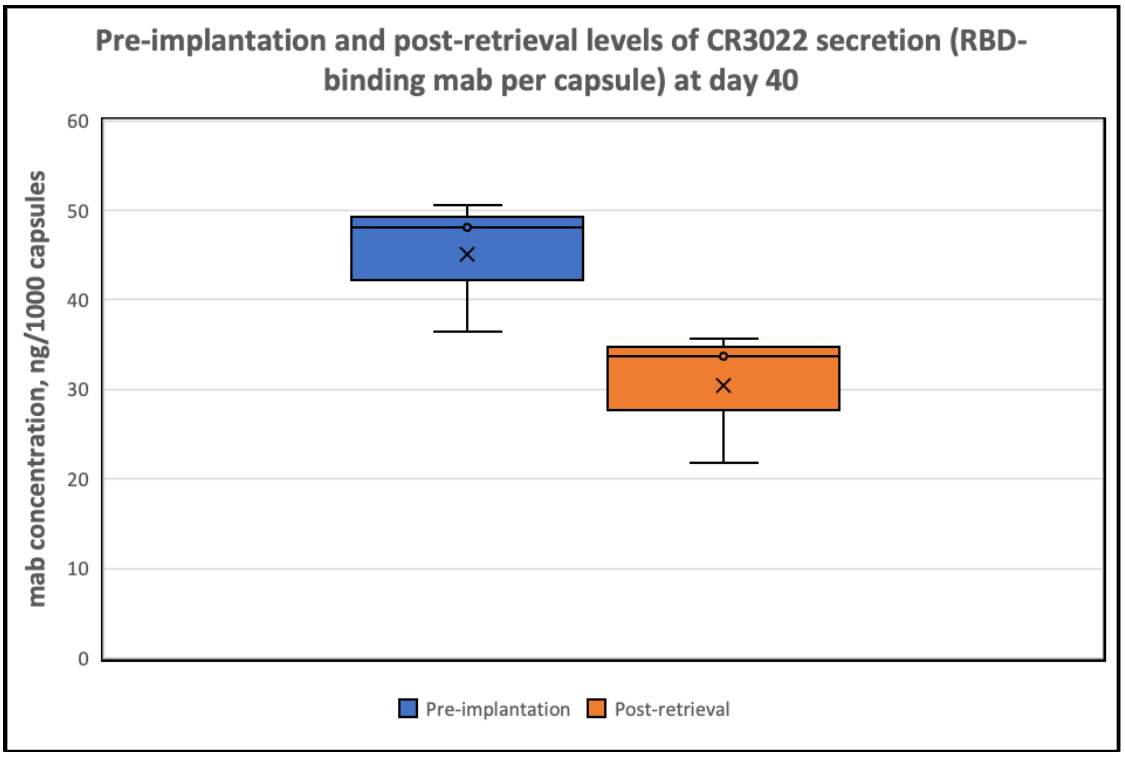

Figure 36. Pre-implantation and post-retrieval levels of CR3022 secretion (RBD-binding mab per capsule) at day 40. A standard curve was created using a CR3022 mab (NR-52481) from BEI (not shown). Experiments were conducted in triplicate, and error bars indicate standard deviation.

Additionally, the viability of cells from retrieved capsules was slightly lower than pre-implantation (85% vs. 95%). Overall, CR3022 levels were still detectable at 40 dpi, although at decreased levels. This is consistent with a host immune response against the human mab and a potential decrease in CR3022 production per microcapsule by day 40 post-implantation.

4.3 DISCUSSION

Different methods for treating and preventing disease have advanced quickly due to the COVID-19 pandemic's pressure to create effective therapies. One such strategy relies on the use of mabs and, although it is very promising, has been limited by the difficulties in mab delivery and production[186]. Consequently, in this proof-of-concept research, we investigated the application of cell microencapsulation [103,187] for sustained release of CR3022, a well-characterized human SARS-CoV-2 mab, in a pre-clinical animal model. We show that after implantation, alginate microcapsules with G8 myoblasts secreting CR3022 have detectable levels of CR3022 in blood. Furthermore, CR3022 remained detectable in circulation for up to 40 days, the entire length of this experiment.

FDA has approved the use of mab for the treatment -and prophylaxis- of COVID-19 [97]. Such development supports the feasibility of a sustained delivery strategy for mab, such as the one proposed in this thesis. It is also essential to recognize that the levels of mab achieved in this proof-of-concept were about 100 times lower than in the latest clinical studies of bolus casirivimab and imdevimab infusion [98,188,189]. Our laboratory has comprehensive research experience with cell encapsulation technology [113,114,181,187,190–192]. Encapsulated cell-aided mab delivery can be tailored for various indications, such as COVID-19, as treatment and prophylaxis if the mab expression per implant can be increased. Therefore, achieving clinically significant systemic mab titers would be possible by increasing the implanted microcapsules and/or improving per-cell mab expression. In this proof-of-concept study, plasmids were used to engineer cells. Furthermore, co-transfection with a two-plasmid system is not the most efficient. A single vector expressing both heavy and light chains would increase expression. The use of two plasmid systems was chosen to determine weather the expression of both antibody chains is necessary for the secretion of functional mabs from engineered cells. Non-viral vectors such as plasmids induce transgene expression levels that are notoriously lower -at least one or two orders of magnitude- than those achieved with viral vectors such as adenovirus or lentivirus.

Nevertheless, the mab titers observed in our research are comparable to similar published findings [193]. Mice that received microencapsulated hybridoma cells had an average of 0.9 μg/ml IgG in plasma [193], similar to levels reported in this thesis. However, the anti-*Spike* mabs levels in patients who received FDA-approved mabs and were protective against SARS-CoV-2 infection were approximately 10 times higher [194]. Therefore, a higher level of efficiency from encapsulated cells must be achieved. Optimizing the vector use could lead to higher mab expression. The use of a viral vector such as lentivirus could increase the expression at least 10 times [195,196]. Of course, the highly

secreted mabs must remain functional, as the mabs shown in this thesis. Additional studies will have to assess this.

As more information about mab efficacy in various populations and drug-resistant virus strains becomes available, microencapsulation may combine microencapsulated cells that secrete different mab sub-types or target multiple epitopes. In addition to COVID-19, the microencapsulation platform might supply additional therapeutic mabs, such as IL-6 receptor blockers (tocilizumab or sarilumab). An example of the potential application of this technology to cancer is presented in Chapter 3.

An unprecedented possibility to apply these mabs in different combinations for COVID-19 treatment and prophylaxis has been made possible by the recent influx of data on clinically significant SARS-CoV-2 mabs currently available. Therefore, mabs other than CR3022 could be used-and even preferred-in subsequent stages of microencapsulation-assisted mab delivery, as neutralizing antibodies are considered vital to reducing the infection ability of cells by SARS-CoV-2.

The mab concentration peaked on day 7 and then steadily dropped until day 40 when the study ended. The continued detection of CR3022 mab in blood indicates that the mab is continuously being delivered from the microcapsules *in vivo*. It is tempting to speculate that the demonstrated decrease in blood CR3022 was partly caused by the host's immune response to CR3022 because the microcapsules were still intact and free of overgrowth when retrieved on day 40. The viability of the retrieved encapsulated cells was still high (85%). It has been reported that human IgG has a shorter half-life in mice than in humans. Based on this information, one would be tempted to hypothesize that if the CR3022 human mab were expressed in humans, it would result in a significantly longer half-life over time, thus achieving a higher concentration.

Reduced per-capsule CR3022 production, which might have happened as a result of one or more of the following events, including encapsulated cells losing one or both of their plasmids, hypoxia, waste buildup, and a declining nutrient supply progressively accumulating around the microcapsules in the peritoneal cavity [192], which may also have contributed to the decreasing trend of CR3022 titers. No cell growth was seen around the microcapsules upon retrieval on day 40 post-implantation, in agreement with previous studies in our laboratory that showed effective microcapsule implantation for more than 120 days [162(p. 20)], emphasizing the weak immunogenicity of microcapsules. The immunogenicity of the microcapsules would be further diminished in a prospective clinical setting by using GMP-grade alginate that has had the majority of its endotoxins

cleared. Studies described that commercial alginates contain PAMPs peptidoglycan, lipoteichoic acid, and flagellin [145,150,156].

A related finding is that secretion from encapsulated cells was found to be lower than from free cells (Figure 31). This was consistently the case whether the cells secreted anti-*Spike* (Figure 31), anti-EGFR (Figure 10), or anti-CD20 (Figure 11). Furthermore, this is an agreement with a multitude of previously published studies [192,197]. The reason for this might be due to the lack of ideal attachment of the cells in the capsule alginate matrix as compared to cells attached to a plastic substrate *in vitro* [198]. However, additional explanations are also possible. The microcapsules may also affect the free diffusion of nutrients and chemicals across the alginate matrix [116,150].

This research aimed to provide proof-of-concept data on the viability of using genetically engineered encapsulated cells for the sustained delivery of functional mab to SARS-CoV-2 in a pre-clinical mouse model in the absence of concurrent SARS-CoV-2 exposure or active infection. Here, we demonstrate that the mab generated by engineered myoblasts has the predicted size and exhibits the appropriate specificity when targeting and binding to the desired RBD of the *Spike* protein. Additionally, the mab has a modest neutralizing activity (~30%), consistent with the mab CR3022's published literature [199]. More recent studies questioned the broad neutralizing nature of CR3022 [186], and today its neutralizing nature is considered equivocal. The results presented in this part indicate a partial neutralization activity for CR3022, which would be consistent with this equivocal consideration. Delivery of mab was demonstrated in earlier studies using hybridoma cell lines [112]. Hybridoma cells, on the other hand, are murine cells produced when a B lymphocyte is fused to a cancer myeloma cell and, thus, are unsuitable for human implantation.

The objective of this study was not to determine whether encapsulated murine myoblasts have preventative or therapeutic clinical benefits. Although myoblasts are appealing as encapsulated cells, murine myoblasts wouldn't be used for human implantations. Furthermore, the efficacy of the produced mab binding and blocking cell entry to SARS-CoV-2 is directly related to the therapeutic potential of the microcapsule strategy against COVID-19. This, in turn, depends on the sequence of the selected mab (s) to be secreted. The main objective of this study was to determine whether genetically modified cells could secrete and deliver sustained human mab to SARS-CoV-2. This study also demonstrated that functional mab could be produced by genetically modified muscle cells (G8) and human cells (HEK293). This proof-of-concept study evaluated neither the long-term fate of the implanted microcapsule dosing regimens nor the exploration of various microcapsule dosing regimens to study dose-dependent pharmacodynamics. Additionally, although the biocompatibility of alginate microcapsules has been thoroughly investigated [145,200], we did not

directly assess the longevity of microcapsules after 40 dpi. Depending on how much crosslinking agent is present, alginate degrades at a different rate *in vivo* [201]. This study used a well-established method for delivering microcapsules in the field intraperitoneally. The methodology should be optimized further for its potential use in clinical trials, including exploring alternative implantation routes. A wide variety of implantation rotes have been described in literature reports, such as the intraperitoneal [117], intratumoral [118], intrathecal [108], and intraocular [119]. However, it is very important to note that the levels of transgenes expressed from microcapsules implanted intraperitoneally are already very high and would be difficult to improve.

The possibility of genetically engineered cells escaping from microcapsules *in vivo*, proliferating, and migrating is also a legitimate concern. Genetically altering cells to make them susceptible to an antibiotic or other drug, in case there is a need to undo the treatment, would be another safety measure to control the continuing survival of encapsulated cells.

Our findings suggest that cell microencapsulation is a feasible strategy for systemic drug delivery of an intact SARS-CoV-2 mab in a pre-clinical model, justifying further research into its potential for use in clinical practice. The primary goal of future research will be to improve the pharmacodynamics and pharmacokinetics of this strategy for particular indications involving COVID-19 prophylaxis and treatment.

CHAPTER 5

Aim III: MODULATION OF IMMUNE RESPONSE

5.1 INTRODUCTION

The implantation of cells enclosed in biocompatible, semi-permeable microcapsules allows the continuous delivery of therapeutic peptides. In contrast, the cells are protected from the host immune response, which makes allogeneic transplantation feasible [113,141,162,182,202–204]. Should it become essential to stop the therapy, peritoneal lavage could remove the majority of the implanted microcapsules. Additionally, encapsulated cells could be genetically engineered to render them sensitive to an exogenously administered drug. An advantage of this strategy over many viral vectors used today in gene therapy applications is that it doesn't alter the host genome. Prior to encapsulation, recombinant cells could be carefully characterized, and individual clones of genetically engineered cells could be selected for unintended genomic rearrangements as an extra safety step. By genetically engineering a universal cell line that can be transplanted in a wide range of patients, it is possible to avoid the laborious and costly engineering of autologous cells for each patient. The delivery of hFIX in mice from implanted engineered cells was previously reported using alginate microcapsules containing recombinant fibroblasts, C2C12, or G8 myoblasts [127,162,182,204]. A critical finding from those studies is that the implanted encapsulated cells are crucial to the host's immunological response against the transgene [204]. The same research revealed that G8 fetal murine myoblasts are less immunogenic than C2C12 transformed murine myoblasts and thus better suited for applications to chronic diseases such as hemophilia because they do not induce the robust immune response to FIX that transformed myoblasts do [204].

The immune responses generated by gene therapy protocols are well described [205] and pose a challenge for any application of gene therapy for chronic diseases. Therefore, the immune responses to encapsulated cells need to be considered. This chapter is devoted to efforts undertaken to modulate the immune response induced by implanted microencapsulated cells.

HYPOTHESIS

Following previous research on the immunomodulatory properties of human IgG Fc fragment and the anti-inflammatory function of IL-10, we hypothesize that co-secretion of coagulation FIX and IgG-Fc or mouse IL-10 from microencapsulated engineered G8 and C2C12 myoblast cells will modulate the production of antibodies to FIX in mice. FIX was chosen as an antigen model because

it is not considered a strong immunogen, and subtle immune modulations can be observed. Additionally, our laboratory has extensive experience delivering FIX from encapsulated cells.
The hypothesis was supported by prior research that demonstrated the anti-inflammatory effects of the cytokine mIL-10 and the capacity of Fc to activate Treg-based immunological tolerance [206].

SPECIFIC AIMS

The specific aims of this chapter are:

A. To genetically engineer G8 and C2C12 cells secreting FIX and either human IgG-Fc or mIL-10.

B. To encapsulate the engineered cells and evaluate the release of recombinant proteins from the microencapsulated cells.

C. Implant encapsulated recombinant cells in mice and quantify the concentration of mouse IgG to FIX in the blood of treated mice over time.

FIX protein: structure, function, and immunogenicity

A 56 kDa protein called FIX is mainly produced and released by hepatocytes. This plasma serine protease that depends on vitamin K is necessary for FIX to be activated in the coagulation cascade. Plasma serine proteases FVIIa or FXIa cleave the activation peptide, which then causes FIX to become active. A disulfide link connects the 145aa light chain and 236aa heavy chain, which are the resultant FIXa serine protease. The FIX gene, which spans 8 exons over 34 kb and is found on the X chromosome (Xq27), consists of 92% of introns. This gene is prone to point, insertional, and deletional mutations. Missense mutations, which account for 60% of instances of severe hemophilia B, are the most common disease-associated FIX changes. High-expression FIX variants could be applied in hemophilia B gene delivery techniques. The effectiveness of gene delivery systems can be improved using these modified versions.
FIX is not considered a highly immunogenic protein, as shown by the fact that only around 2-3% of patients suffering from severe hemophilia B develop antibodies to the regular intravenous infusions of FIX protein [207]. Regarding encapsulated cells, when transformed C2C12, a murine myoblast cell line was genetically modified to produce FIX and implanted into hemophilia B KO mice; the expression was transient due to the development of antibodies to FIX [162]. Implanted cells also induced cellular immunity, resulting in the development of cytotoxic T lymphocytes that were particular to released FIX [208]. In addition, this transformed cells line caused the development of

tumors in immunocompromised mice, showing the potential risks of the use of transformed cells [182].

The G8 fetal murine myoblast cell line has been used in the past to encapsulate cells that produce the FVIII [203] and FIX [162] proteins. It has been demonstrated that encapsulating this myoblast cell line delivers functional FIX to groups of C57BL/6J and Hemophilia B mice effectively and safely for up to 4 months in immunocompromised animals [204]. Additionally, in contrast, to FIX delivery from C2C12 cells, FIX produced by encapsulated G8 cells did trigger a negligible response in mice. These results support the use of G8 cells to deliver sustained levels of FIX while inducing a modest level of anti-FIX antibodies.

Tregitopes-Fc

There is ample evidence that the Fc portion of the human IgG molecule has immunomodulatory activity [12]. Although the precise method of modulation is still unclear, intravenous immunoglobulin G (IVIG) infusion treatment is effectively utilized to treat autoimmune and inflammatory illnesses [209]. In order to reduce inflammation, autoimmune illnesses are treated with IVIG therapy, which has been found to promote the growth of Tregs and to increase the concentration of anti-inflammatory cytokines like IL-10 [206]. Two epitopes (Tregitope 289 and 167) in the Fc portion that may bind to and activate Tregs to promote immune tolerance were discovered by De Groot and colleagues in 2008 by computational scanning in the Fc region of human IgG [210]. Additionally, their team demonstrated the proliferation of CD4+/CD25hi/FoxP3 Tregs in mice and put forth a theory for the induction of immune tolerance by activating Tregs and squelching CD4, CD8, or Th17 T-cells [206]. These authors demonstrated that tregitopes could reduce the immunological response specific to B- and T-cells and can modulate the immune system in a way that is antigen-specific [206].

IL-10 as an anti-inflammatory cytokine

IL-10 is a crucial anti-inflammatory cytokine released by various immune cells [211]. It is believed that IL-10 has a wide range of effects since it is expressed by multiple cell types and under different circumstances [212]. It is hypothesized that IL-10 suppresses the generation of cytokines that promote inflammation in macrophages and dendritic cells, where it predominantly acts on its immunosuppressive effects [213]. Additionally, it inhibits T-cell production of the pro-inflammatory cytokine IFN- γ, which lowers T-cell-mediated immunity [214]. Furthermore, regulatory B-cells (Bregs), a subgroup of B-cells that produce IL-10, can inhibit the immune system and promote

tolerance [215]. Numerous preclinical and clinical investigations have been conducted on using IL-10 as an immunomodulator in treating autoimmune and inflammatory illnesses. Additionally, IL-10 was employed as an immune modulator in clinical trials to treat psoriasis and Crohn's disease, with some degree of effectiveness [216].

Modulating immunogenicity

Myoblast cell lines from C2C12 mice that were genetically modified to produce FIX at therapeutic doses in naked animals were encapsulated by Hortelano and colleagues [127]. However, the expression was only brief due to the formation of the antibody. The implanted animals also induced cellular immunity, resulting in the development of cytotoxic T lymphocytes that were particular to released FIX. In addition, the therapy caused tumors to develop later in naked mice, showing that the line was not safe [182]. The G8 mice myoblast cell line has been used to encapsulate cells that produce the FVIII protein [203]. It has been demonstrated that encapsulating this myoblast line delivers functional FIX to groups of C57BL/6J and Hemophilia B mice effectively and safely for up to 4 months in immunocompromised animals. Additionally, despite FIX secreted by C2C12 cells, FIX produced by encapsulated G8 cells did not trigger an immunological response, and anti-FIX antibody titers *in vivo* were negligible [204]. As a result, it is hypothesized that using G8 cell lines to administer FIX is reasonably safe and less immunogenic. Thus, the objective of this chapter was to deliver FIX from immunogenic C2C12 while delivering immune modulators from G8.

5.2 MATERIALS AND METHODS

Cell culture

The G8 mice myoblast and C2C12 fibroblast cell lines were obtained from ATCC (CRL-1456 and CRL-1772, respectively). As previously described, cells were cultured in Dulbecco's modified eagle's medium (DMEM), supplemented with 10% FBS and 1% Penicillin-Streptomycin.

Cell transfection

For transfections, the plasmid DNAs listed below were used: PCMV6KN for mouse IL-10 expression (Origene, MD, USA); pFUSE-Lucia-cHIg-IgGI for Fc and Lucia protein expression (Invivogen, CA, USA); pcDNA-IVS- hFIX for human FIX expression (Queen's University, Kingston, Canada). EscortIII transfection reagent was used to transfect cells following the manufacturer's recommendations. Cells were allowed to reach 60% confluency in a 10 cm cell culture dish, and 5 μg of plasmid with a 5 μl of transfection reagent formulation in OPTI-MEM was added. OPTI-MEM was changed to DMEM 8 hours post-transfection. To obtain stably transfected cell lines, cells were split 1:10 24 hours post-transfection, and an appropriate selective reagent was added to the cells. Every 2 days, new media containing a selective reagent was added. For Fc-transfected cells, Zeocin (Invivogen, USA) was employed as a selecting reagent, and G418 (Sigma-Aldrich, USA) was applied for the remaining cell lines. An antibiotic susceptibility experiment was conducted to identify the selected reagent's proper doses (400 ng/ml). Antibiotic selection continued for two weeks, after which 12 individual clones of stably transfected cells were obtained for each transfected cell using special cloning cylinders. Clones were cultured in 48- and 24-well plates before being tested for Quanti-Luc secretion by ELISA. No clones of the mIL-10 transfected cells were produced; instead, a pool of transfected cells was employed.

Quantification of Lucia's expression

The Quanti-Luc (Invivogen) luminescence test examined Lucia's expression. In Synergy H1 (Biotech), relative light units were measured at 465-493 nm (RLU) wavelength.

Alginate purification

Low-viscosity alginate powder (Keltone LV, San Diego, CA, USA) was dissolved in 0.9% sodium chloride overnight at 37°C and then filtered through a 0.22 μm filter to create an alginate solution (1.5%). After microencapsulation, prepared microcapsules were rinsed with saline solution, cross-linked with PLL for 6 minutes, and then coated with an outer layer of alginate for 4 minutes (Figure

37). Following the addition of DMEM, the solution containing the microcapsules was transferred to an incubator.

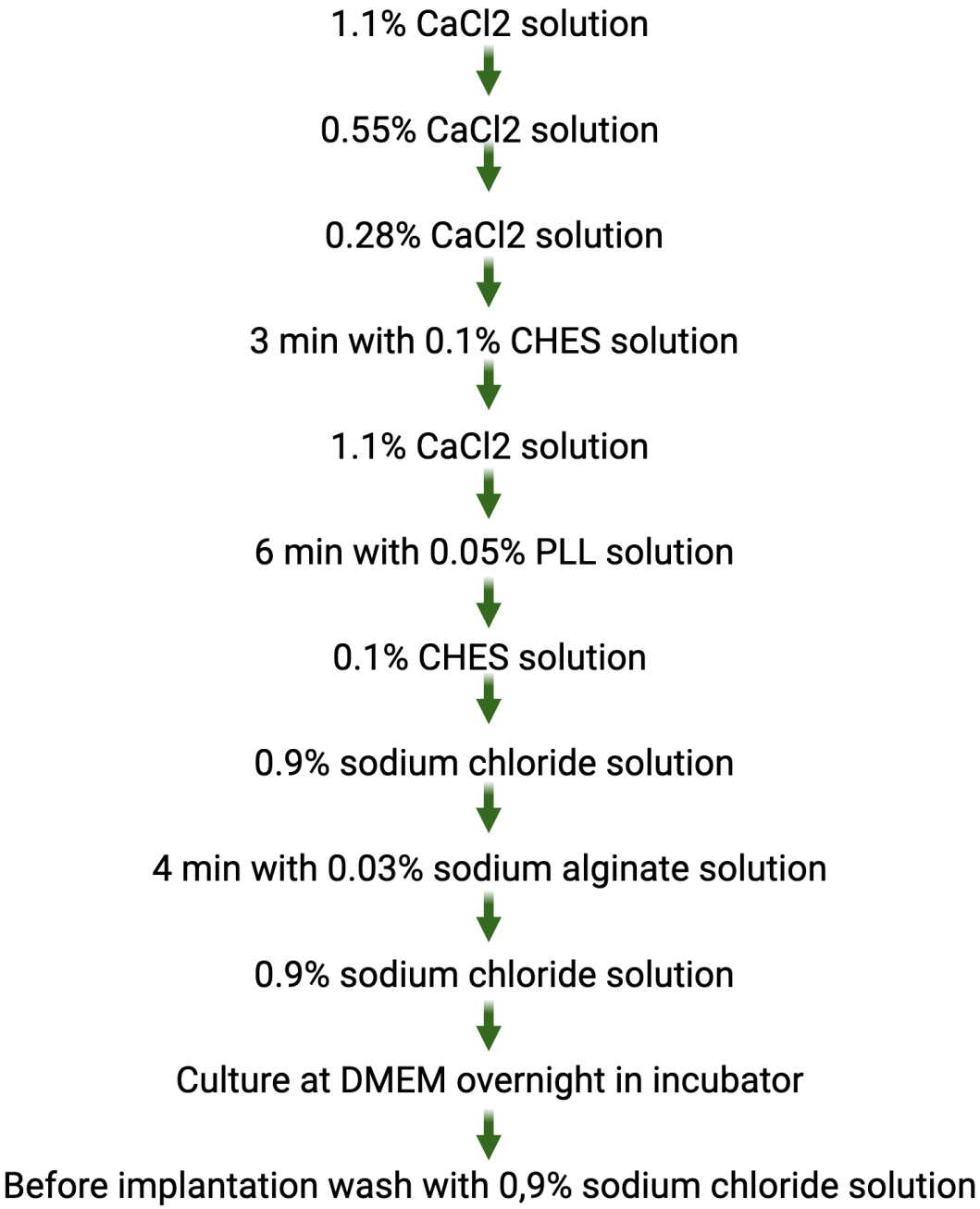

Figure 37. Alginate microcapsules washing steps. When time is not indicated, a brief wash period followed by suction of solution was used.

Animal studies

All animal procedures were conducted under the Animal Ethics Guidelines of Nazarbayev University. C57BL/6J mice were purchased from Charles River (Montreal, QC, Canada) and maintained at the National Center for Biotechnology, Astana. Mice were anesthetized with isofluorane in a small animal anesthetic machine. An intraperitoneal G18 catheter was used to administer 2 mL of microcapsules to each mouse. 4 groups of C57BL/6J (n=5) were implanted intraperitoneally with hFIX, hFIX+hFc, and hFIX+mIL-10 expressing cells (Tables 2,3). Blood samples were collected using the tail-clip assay in heparinized tubes. Plasma samples were collected on days 0, 14, and 28. All mice were sacrificed on day 28 post-treatment with CO_2, and implanted capsules were retrieved and analyzed by inverted light microscopy. Good biocompatibility was indicated by the absence of any apparent outgrowth surrounding the APA microcapsules.

Human FIX Ag detection ELISA

The ELISA assay was used to identify the human FIX antigen using the Affinity Biologicals Inc. (Ancaster, ON, Canada) reagents and procedure, as previously described [204]. The expression of hFIX was identified using matched pair antibody sets (Affinity Biologicals, Canada). Following overnight incubation with the primary antibody, the incubation was blocked for one hour at RT with 5% skim milk (blotto) in PBS. Recombinant Kogenate Fs Antihemophilic factor (Bayer HealthCare) was diluted appropriately to measure hFIX. Plasma from control mice (implanted with empty capsules) was a negative control. To detect hFIX in mice, plasma standard dilutions were prepared using the supplied diluent. For all ELISA studies, TMB was used as a substrate for visualizing, and OD was determined at 450 nm.

Statistical analysis

GraphPad Prism V.9.3.1 was used for all analyses. The unpaired t-test was used to compare differences between groups, and the binomial "exact" method was used to calculate 95% confidence intervals (CI).

5.3 RESULTS

The immune responses to administered recombinant products are a severe concern in the clinical management of medical conditions. Although it is risky to generalize, and as an example related to hemophilia A -not hemophilia B- the incidence of severe patients of hemophilia A (due to coagulation FVIII deficiency) that develop antibodies to the administered protein is in the order of 20-40% [207]. Indeed, developing inhibitors (neutralizing antibodies to FVIII) in response to the administration of FVIII protein is arguably the most significant challenge in the management of hemophilia A patients [208]. This concern can also be extended to gene therapy applications for diseases that require prolonged transgene delivery [217]. Therefore, the characterization of the immune responses elicited by encapsulated cells is highly relevant to evaluate the feasibility of this gene therapy strategy. Indeed, the possibility of modulating the immune responses generated by encapsulated cells was a focus of this chapter. Specifically, this chapter aimed to assess the effect of human IgG-Fc and murine IL-10 on developing antibodies in response to encapsulated cells secreting FIX.

Murine G8 myoblasts genetically engineered to secrete either murine IL-10 or human IgG-Fc fraction were used, together with C2C12 myoblasts secreting FIX. The experiment was designed to test whether co-secretion of FIX and immune modulators (hIgG-Fc or mIL-10) would reduce the host's humoral immune response to FIX.

Following transfection, the ability of G8 and C2C12 cells to secrete the transgenes was quantified by ELISA. The secretion levels of FIX by C2C12 and G8 myoblasts were comparable (Figure 38). Further, engineered cells were encapsulated in alginate-PLL microcapsules, and the secretion of recombinant proteins from the encapsulated cells was characterized. In agreement with previously published studies from our laboratory and in a previous chapter (Figure 31), secretion from free cells was higher than from microencapsulated cells (Figure 38).

However, prior research showed that the production of FIX inhibitors cleared the produced FIX protein after a few days of encapsulation [162].

In this chapter's initial *in vitro* part, C2C12 and G8 cells were engineered to express either FIX, and G8 cells were engineered to secrete Fc or mIL-10. Further, engineered cells were encapsulated in alginate-PLL microcapsules, and secretion of our recombinant proteins from the encapsulated cells was characterized by ELISA. The engineered G8 and C2C12 cells secreted relevant and comparable FIX amounts (Figure 38).

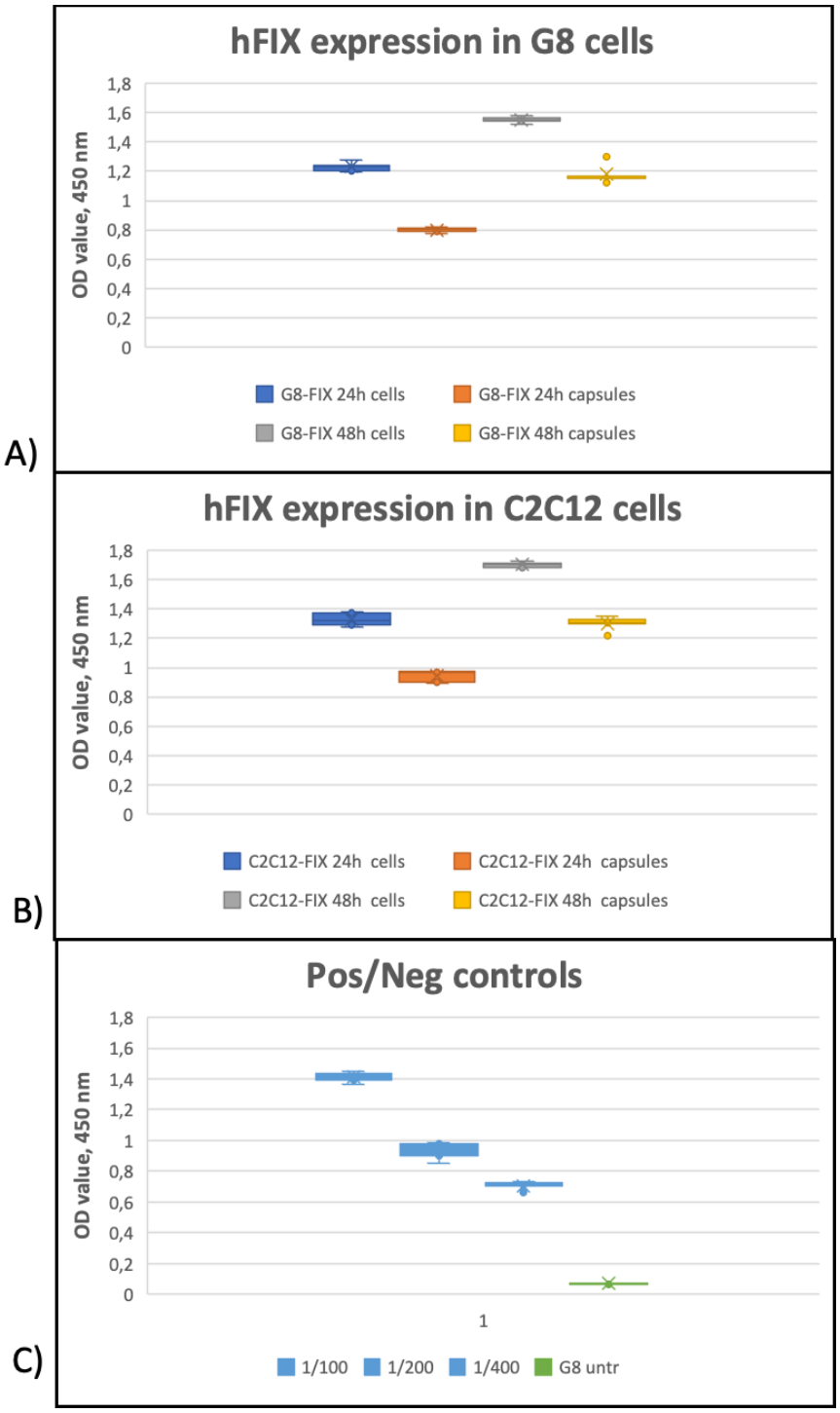

Figure 38. OD values of *in vitro* expression of human FIX from A) G8 , B) C2C12 cells. C) Pos/Neg controls. Experiments were conducted in triplicate, and error bars indicate standard deviation.

The encapsulated cells also demonstrated promising *in vitro* viability, consistently being >95% viable for both cell types (data not shown), consistent with our previous encapsulation experience.

The expression of mouse IL-10 from engineered G8 was quantified in our laboratory as 710 pg/10^6 cells, which was reduced to 565 pg/10^6 cells after encapsulation (Zhansaya Kanketayeva, MSc thesis, NU). The sustained secretion of ,IL-10 from encapsulated G8 cells was deemed unsafe in prolonged experiments (Zhansaya Kanketayeva, MSc thesis, NU). Therefore, it was decided to use transiently transfected G8 cells in this experiment that would deliver mIL-10 for a short period of time.

In this vector, the secreted Lucia is fused to Fc. Therefore, the expression of human IgG-Fc from a stably engineered G8 cell clone was quantified using Lucia as a surrogate marker. The expression level of human IgG-Fc from a stably engineered G8 cell clone is presented in Table 1 below.

Table 1. Secretion of human IgG-Fc from untransfected G8 vs a stably engineered G8 cell clone.

Untransfected G8, 24h	**G8 stably expressing hFc, 24h**
1,3 RLU ± 0,57	8,497,828 RLU ± 637,562

After the *in vitro* characterization of the encapsulated cells, an *in vivo* experiment was conducted (Tables 2, 3).

Table 2. A number of mice implanted per group

	Groups			
Days	**C2C12-FIX+IL-10**	**C2C12-FIX+hfc**	**C2C12-FIX+G8**	**Naïve**
Day 0	5	5	5	5
Day 14	5	5	5	5
Day 28	5	4	4	5

Table 3. A number of implanted cells per mouse

Groups	**Mice**	**Microcapsules, (mL/mouse)**	**Cells/ml microcapsules**
C2C12-FIX+G8-IL-10	5	3	$5x10^6$
C2C12-FIX+G8-hfc	5	3	$5x10^6$
C2C12-FIX+G8	5	3	$5x10^6$
Naïve	5	No microcapsules	None

The following groups of mice (n=5) were implanted intraperitoneally with 3 ml of microcapsules per mouse, except into the naïve mice:

- Group 1 – Received encapsulated **C2C12-FIX + G8-IL-10** cells
- Group 2 – Received encapsulated **C2C12-FIX + G8-Fc** cells
- Group 3 – Received encapsulated **C2C12-FIX + untransfected G8** cells
- Group 4 – Naïve untreated mice

Blood samples were collected using the tail-clip assay. Plasma samples were collected on days 0, 14, and 28. One of the mice from Group 2 and Group 3 died during the experiment from fighting wounds (Table 2).

All mice were sacrificed on day 28 post-treatment with CO_2, and implanted capsules were retrieved and analyzed by inverted light microscopy. High biocompatibility was indicated by the absence of any apparent outgrowth surrounding the APA microcapsules (Figure 39).

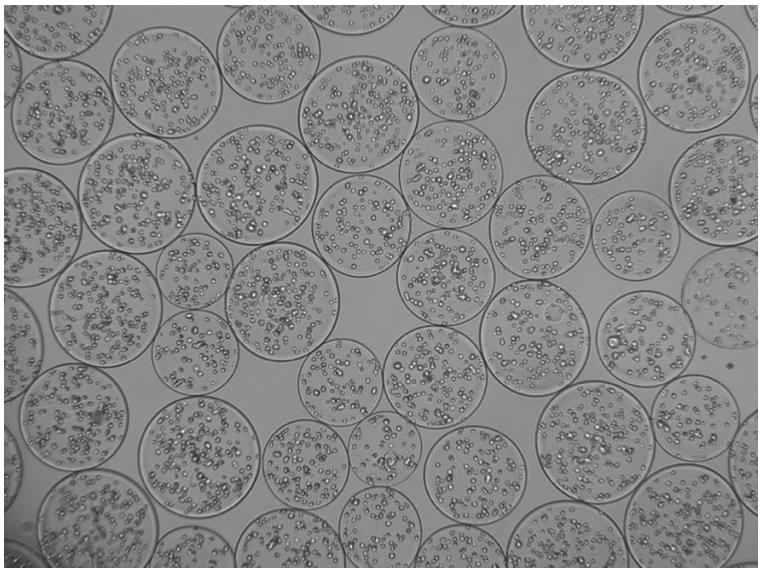

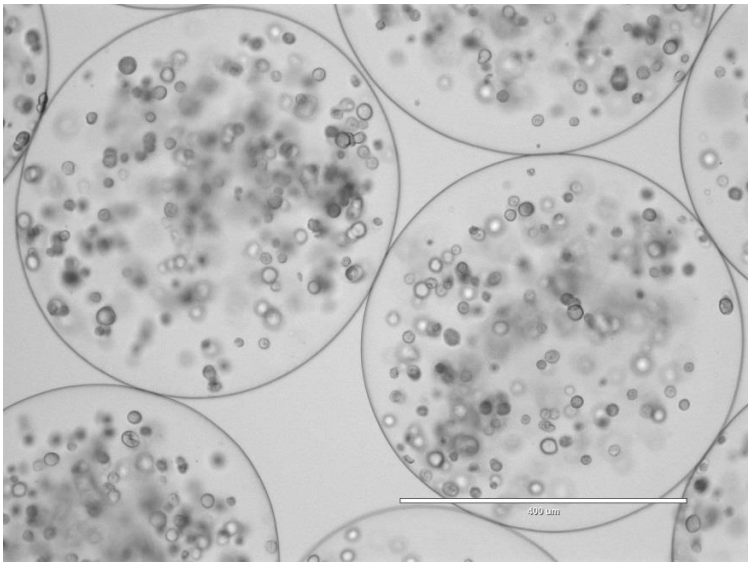

Figure 39. Images of alginate microcapsules containing cells after retrieval from mice. Images were taken using light microscopy (at ×4 (top panel) and ×10 (bottom panel) magnification, respectively).

ELISA was used to determine the presence of mouse antibodies to FIX in treated mice. According to the findings, all the treatment groups had detectable antibodies, although with important differences. The co-expression of mIL-10 did not cause immune modulation; it produced a similar or greater FIX-specific antibody response than the control group (cells expressing FIX alone), which was not statistically different ($p<0.30$) (Figure 40).

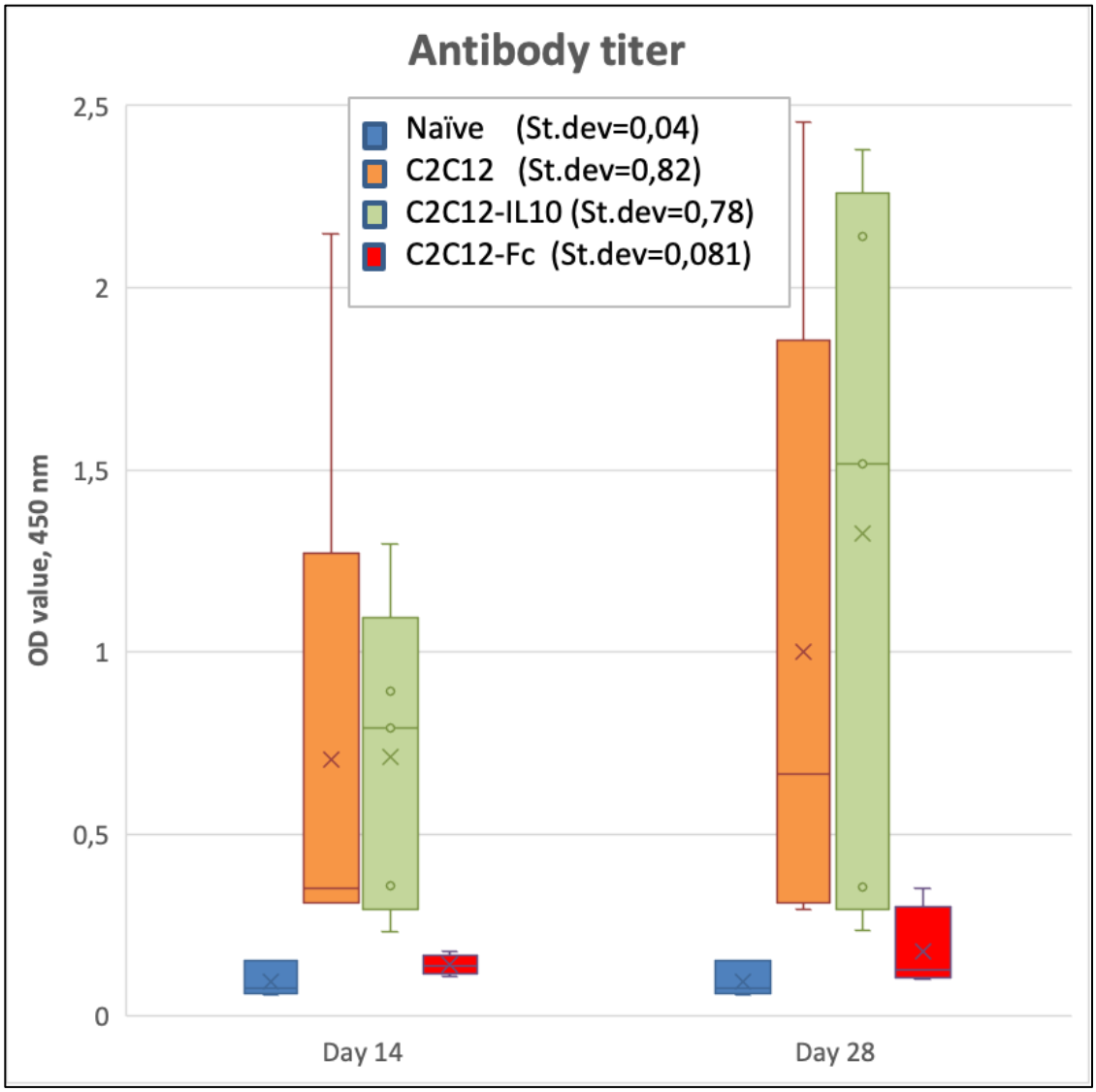

Figure 40. Mouse antibodies level to human FIX. Experiments were conducted in triplicate, and error bars indicate standard deviation.

Interestingly, the titer of antibodies to FIX in Group 2 (Fc) at 48 hours was not statistically significantly different from that of naïve mice ($p<0.17$), indicating a modulatory effect for Fc. Furthermore, Group 2 (Fc) had statistically significantly different titers from Group 1 (IL-10, $p<0.02$) and Group 3 (only FIX expression, $p<0.05$). Additionally, 3 out of 4 mice in the Group 2 (Fc) had baseline levels of antibodies with OD lower than 0.15 on day 28 (Figure 40).

5.4 DISCUSSION

In this study, mouse IL-10 and the Fc part of human IgG were co-delivered with FIX by encapsulating G8 and C2C12 cells in an immunocompetent mouse model, aiming to examine any potential immune modulatory effects. The hypothesis was supported by earlier research showing the role of Fc and IL-10 in immune modulation [218,219]. In this study, mouse IL-10 and the Fc part of human IgG were co-delivered with FIX by encapsulated G8 and C2C12 cells in a mouse model to examine their potential immune modulatory effects. The study was divided into two main sections: G8 and C2C12 cell lines that stably express Fc, IL-10, or human FIX are created *in vitro* and then enclosed in alginate microcapsules; 2) encapsulated cells are then implanted intraperitoneally into healthy mice to test the immune response of engineered (mIL-10+hFIX or Fc+hFIX) and control groups. As a result, a detectable immune response to FIX was observed in all groups following the implantation of the encapsulated cells into mice and subsequent plasma analysis. However, the co-delivery of Fc modulated the immune system noticeably. To optimize the Fc concentration required for immunological regulation, we hypothesize that different doses of Fc concentration and different ratios of Fc-expressing cells to FIX-expressing cells could be assessed. It is also possible that effective immunological modulation may require the physical fusion of the FIX antigen to the Fc, as is the case of the commercial FVIII-Fc protein (Eloctate, Sanofi). However, in this study, we co-delivered two separate proteins that were not fused.

Interestingly, as a separate protein, Fc modulated the antibody response to FIX, which was secreted from the same microcapsules but in different cells; FIX was secreted from C2C12 cells and Fc from G8 cells. Studies often use viral transduction rather than plasmid transfection to induce high FIX expression in cells. The use of viral vectors to engineer encapsulated cells would increase several folds the expression of FIX. However, the main objective of this chapter was to explore the possibility of modulating the immune system's response to a transgene such as FIX rather than achieving high expression of the protein.

The Quanti-Luc test could not detect any circulating LUCIA in mouse plasma on day 28 (data not shown), for which there could be several reasons. The development of antibodies to human IgG (mab) delivered from encapsulated cells shown in Chapter 4 could also explain the absence of LUCIA in plasma in this modulation experiment. There is published evidence that the co-administration of human IgG and FVIII proteins in mice modulates the development of antibodies to FVIII, which could be explained -among other hypotheses- by competitive antigen presentation [220]. Recombinant murine IL-10 was challenging to distinguish in the treated mice. Therefore, IL-10 plasma levels were not examined.

This study has demonstrated the ability of recombinant G8 and C2C12 myoblasts to co-deliver FIX and detectable quantities of hFc and mIL-10 through the capsules while maintaining good viability. The described proteins were co-administered to mice *in vivo*, and the Fc group showed an immunomodulatory effect. The suggested strategy using encapsulated FIX-secreting cells involves several crucial procedures, beginning with the engineering of numerous stable cell lines, controlling the concentration of all secreted proteins, and obtaining the proper composition and structure of microcapsules. In conclusion, the experiment could be optimized with different concentrations of FIX and Fc proteins, including more animal groups, before considering clinical studies.

CHAPTER 6

CONCLUSIONS AND FUTURE WORKS

This Ph.D. thesis explored the concept of using alginate microcapsules to deliver mabs. I have shown that recombinant G8 myoblasts, HEK293 cells encapsulated in alginate-PLL microcapsules can successfully secrete detectable levels of functional levels of mabs against cancer (Cetuximab and Rituximab) and against SARS-CoV-2 (CR3022), the virus causing COVID-19. The secreted mabs have the intended specificity and can be delivered through the microcapsules while sustaining the good viability of the enclosed cells.

This thesis also shows the potential of inducing immune modulation as a way to reduce the immune response to transgenes. In particular, the co-delivery of FIX by encapsulated cells and the immunomodulatory molecule human IgG-Fc could have potential practical applications that still need to be explored beyond this proof-of-concept stage. The microcapsules were synthesized using alginate and poly-lysine and produced by a standard encapsulation technique with slight modifications. Alginate was purified from various impurities before encapsulation as a key step for reducing the presence of endotoxins. This, in turn, would reduce the immunogenicity of the microcapsules upon implantation.

The novelty of this thesis is based on determining that encapsulated non-professional immune cells such as myoblasts produce and release clinically relevant levels of mabs (mabs) against SARS-CoV-2 *Spike* protein in mice for at least 40 days. Additionally, engineered cells also expressed and secreted through microcapsules mabs targeting CD20 and EGFR antigens.

In future directions, the application of microcapsules as a treatment for COVID-19 patients could be optimized by choosing mabs with proven neutralizing activity. Additionally, a judicious choice of encapsulated cells is also critical. This therapeutic strategy for COVID-19 could be beneficial for immunocompromised patients who are unable to develop an antibody response.

Similarly, there are potential applications of implantable microcapsules as a treatment for cancer. This strategy needs to be tested in suitable animal cancer models to assess the potential of this strategy to reduce or even eliminate preexisting tumors. Overall, new applications of cell encapsulation are promising, and this interdisciplinary area of research ought to be explored further.

REFERENCES

1. Strebhardt, K., & Ullrich, A. (2008). Paul Ehrlich's magic bullet concept: 100 years of progress. *Nature Reviews Cancer*, *8*(6), Article 6. https://doi.org/10.1038/nrc2394
2. Köhler, G., & Milstein, C. (1975). Continuous cultures of fused cells secreting antibody of predefined specificity. *Nature*, *256*(5517), Article 5517. https://doi.org/10.1038/256495a0
3. Jr, C. A. J., Travers, P., Walport, M., Shlomchik, M. J., Jr, C. A. J., Travers, P., Walport, M., & Shlomchik, M. J. (2001). *Immunobiology* (5th ed.). Garland Science.
4. Alberts, B., Johnson, A., Lewis, J., Raff, M., Roberts, K., & Walter, P. (2002). B Cells and Antibodies. *Molecular Biology of the Cell. 4th Edition*. https://www.ncbi.nlm.nih.gov/books/NBK26884/
5. Elmore, S. (2007). Apoptosis: A Review of Programmed Cell Death. *Toxicologic Pathology*, *35*(4), 495–516. https://doi.org/10.1080/01926230701320337
6. Charles A Janeway, J., Travers, P., Walport, M., & Shlomchik, M. J. (2001). The structure of a typical antibody molecule. *Immunobiology: The Immune System in Health and Disease. 5th Edition*. https://www.ncbi.nlm.nih.gov/books/NBK27144/
7. Elkabetz, Y., Ofir, A., Argon, Y., & Bar-Nun, S. (2008). Alternative pathways of disulfide bond formation yield secretion-competent, stable and functional immunoglobulins. *Molecular Immunology*, *46*(1), 97–105. https://doi.org/10.1016/j.molimm.2008.07.005
8. D'Angelo, S., Ferrara, F., Naranjo, L., Erasmus, M. F., Hraber, P., & Bradbury, A. R. M. (2018). Many Routes to an Antibody Heavy-Chain CDR3: Necessary, Yet Insufficient, for Specific Binding. *Frontiers in Immunology*, *9*. https://www.frontiersin.org/articles/10.3389/fimmu.2018.00395
9. Tsuchiya, Y., & Mizuguchi, K. (2016). The diversity of H3 loops determines the antigen-binding tendencies of antibody CDR loops. *Protein Science : A Publication of the Protein Society*, *25*(4), 815–825. https://doi.org/10.1002/pro.2874
10. Sela-Culang, I., Kunik, V., & Ofran, Y. (2013). The Structural Basis of Antibody-Antigen Recognition. *Frontiers in Immunology*, *4*, 302. https://doi.org/10.3389/fimmu.2013.00302
11. Strohl, W. R., & Strohl, L. M. (Eds.). (2012). 3—Antibody structure–function relationships. In *Therapeutic Antibody Engineering* (pp. 37–595). Woodhead Publishing. https://doi.org/10.1533/9781908818096.37
12. van Erp, E. A., Luytjes, W., Ferwerda, G., & van Kasteren, P. B. (2019). Fc-Mediated Antibody Effector Functions During Respiratory Syncytial Virus Infection and Disease. *Frontiers in Immunology*, *10*, 548. https://doi.org/10.3389/fimmu.2019.00548
13. Ferris, R. L., Jaffee, E. M., & Ferrone, S. (2010). Tumor Antigen–Targeted, Monoclonal Antibody–Based Immunotherapy: Clinical Response, Cellular Immunity, and Immunoescape. *Journal of Clinical Oncology*, *28*(28), 4390–4399. https://doi.org/10.1200/JCO.2009.27.6360
14. Schroeder, H. W., & Cavacini, L. (2010). Structure and Function of Immunoglobulins. *The Journal of Allergy and Clinical Immunology*, *125*(2 0 2), S41–S52. https://doi.org/10.1016/j.jaci.2009.09.046
15. Gong, S., & Ruprecht, R. M. (2020). Immunoglobulin M: An Ancient Antiviral Weapon – Rediscovered. *Frontiers in Immunology*, *11*. https://www.frontiersin.org/articles/10.3389/fimmu.2020.01943
16. Sathe, A., & Cusick, J. K. (2022). Biochemistry, Immunoglobulin M. In *StatPearls*. StatPearls Publishing. http://www.ncbi.nlm.nih.gov/books/NBK555995/
17. Keyt, B. A., Baliga, R., Sinclair, A. M., Carroll, S. F., & Peterson, M. S. (2020). Structure, Function, and Therapeutic Use of IgM Antibodies. *Antibodies*, *9*(4), 53. https://doi.org/10.3390/antib9040053
18. Charles A Janeway, J., Travers, P., Walport, M., & Shlomchik, M. J. (2001). The distribution and functions of immunoglobulin isotypes. *Immunobiology: The Immune System in Health and Disease. 5th Edition*. https://www.ncbi.nlm.nih.gov/books/NBK27162/
19. Johansen, F. E., Braathen, R., & Brandtzaeg, P. (2000). Role of J chain in secretory immunoglobulin formation. *Scandinavian Journal of Immunology*, *52*(3), 240–248. https://doi.org/10.1046/j.1365-3083.2000.00790.x
20. Rogentine, G. N., Rowe, D. S., Bradley, J., Waldmann, T. A., & Fahey, J. L. (1966). Metabolism of

human immunoglobulin D (IgD). *Journal of Clinical Investigation*, *45*(9), 1467–1478.
21. Chen, K., Xu, W., Wilson, M., He, B., Miller, N. W., Bengten, E., Edholm, E.-S., Santini, P. A., Rath, P., Chiu, A., Cattalini, M., Litzman, J., Bussel, J., Huang, B., Meini, A., Riesbeck, K., Cunningham-Rundles, C., Plebani, A., & Cerutti, A. (2009). Immunoglobulin D enhances immune surveillance by activating antimicrobial, pro-inflammatory and B cell-stimulating programs in basophils. *Nature Immunology*, *10*(8), 889–898. https://doi.org/10.1038/ni.1748
22. Geisberger, R., Lamers, M., & Achatz, G. (2006). The riddle of the dual expression of IgM and IgD. *Immunology*, *118*(4), 429–437. https://doi.org/10.1111/j.1365-2567.2006.02386.x
23. Steffen, U., Koeleman, C. A., Sokolova, M. V., Bang, H., Kleyer, A., Rech, J., Unterweger, H., Schicht, M., Garreis, F., Hahn, J., Andes, F. T., Hartmann, F., Hahn, M., Mahajan, A., Paulsen, F., Hoffmann, M., Lochnit, G., Muñoz, L. E., Wuhrer, M., … Schett, G. (2020). IgA subclasses have different effector functions associated with distinct glycosylation profiles. *Nature Communications*, *11*(1), Article 1. https://doi.org/10.1038/s41467-019-13992-8
24. Woof, J. M., & Kerr, M. A. (2004). IgA function – variations on a theme. *Immunology*, *113*(2), 175–177. https://doi.org/10.1111/j.1365-2567.2004.01958.x
25. Charles A Janeway, J., Travers, P., Walport, M., & Shlomchik, M. J. (2001). Structural variation in immunoglobulin constant regions. *Immunobiology: The Immune System in Health and Disease. 5th Edition*. https://www.ncbi.nlm.nih.gov/books/NBK27106/
26. Lombana, T. N., Rajan, S., Zorn, J. A., Mandikian, D., Chen, E. C., Estevez, A., Yip, V., Bravo, D. D., Phung, W., Farahi, F., Viajar, S., Lee, S., Gill, A., Sandoval, W., Wang, J., Ciferri, C., Boswell, C. A., Matsumoto, M. L., & Spiess, C. (2019). Production, characterization, and in vivo half-life extension of polymeric IgA molecules in mice. *MAbs*, *11*(6), 1122–1138. https://doi.org/10.1080/19420862.2019.1622940
27. Hu, J., Chen, J., Ye, L., Cai, Z., Sun, J., & Ji, K. (2018). Anti-IgE therapy for IgE-mediated allergic diseases: From neutralizing IgE antibodies to eliminating IgE+ B cells. *Clinical and Translational Allergy*, *8*(1), 27. https://doi.org/10.1186/s13601-018-0213-z
28. Vidarsson, G., Dekkers, G., & Rispens, T. (2014). IgG Subclasses and Allotypes: From Structure to Effector Functions. *Frontiers in Immunology*, *5*, 520. https://doi.org/10.3389/fimmu.2014.00520
29. Junker, F., Gordon, J., & Qureshi, O. (2020). Fc Gamma Receptors and Their Role in Antigen Uptake, Presentation, and T Cell Activation. *Frontiers in Immunology*, *11*. https://www.frontiersin.org/articles/10.3389/fimmu.2020.01393
30. Saylor, C. A., Dadachova, E., & Casadevall, A. (2010). Murine IgG1 and IgG3 isotype switch variants promote phagocytosis of Cryptococcus neoformans through different receptors. *Journal of Immunology (Baltimore, Md. : 1950)*, *184*(1), 336–343. https://doi.org/10.4049/jimmunol.0902752
31. Gondo, A., Saeki, N., & Tokuda, Y. (1987). IgG4 antibodies in patients with atopic dermatitis. *The British Journal of Dermatology*, *117*(3), 301–310. https://doi.org/10.1111/j.1365-2133.1987.tb04136.x
32. Lu, R.-M., Hwang, Y.-C., Liu, I.-J., Lee, C.-C., Tsai, H.-Z., Li, H.-J., & Wu, H.-C. (2020). Development of therapeutic antibodies for the treatment of diseases. *Journal of Biomedical Science*, *27*(1), 1. https://doi.org/10.1186/s12929-019-0592-z
33. Ecker, D. M., Jones, S. D., & Levine, H. L. (2015). The therapeutic monoclonal antibody market. *MAbs*, *7*(1), 9–14. https://doi.org/10.4161/19420862.2015.989042
34. Kaplon, H., Muralidharan, M., Schneider, Z., & Reichert, J. M. (2019). Antibodies to watch in 2020. *MAbs*, *12*(1), 1703531. https://doi.org/10.1080/19420862.2019.1703531
35. Maloney, D. G., Grillo-López, A. J., White, C. A., Bodkin, D., Schilder, R. J., Neidhart, J. A., Janakiraman, N., Foon, K. A., Liles, T.-M., Dallaire, B. K., Wey, K., Royston, I., Davis, T., & Levy, R. (1997). IDEC-C2B8 (Rituximab) Anti-CD20 Monoclonal Antibody Therapy in Patients With Relapsed Low-Grade Non-Hodgkin's Lymphoma. *Blood*, *90*(6), 2188–2195. https://doi.org/10.1182/blood.V90.6.2188
36. Grilo, A. L., & Mantalaris, A. (2019). The Increasingly Human and Profitable Monoclonal Antibody Market. *Trends in Biotechnology*, *37*(1), 9–16. https://doi.org/10.1016/j.tibtech.2018.05.014
37. Kaplon, H., & Reichert, J. M. (2019). Antibodies to watch in 2019. *MAbs*, *11*(2), 219–238. https://doi.org/10.1080/19420862.2018.1556465
38. Ménard, S., Canevari, S., & Colnaghi, M. I. (1991). Monoclonal antibodies as carriers for delivering cytotoxic agents. *Annali Dell'Istituto Superiore Di Sanita*, *27*(1), 87–89.

39. Molina, M. A., Codony-Servat, J., Albanell, J., Rojo, F., Arribas, J., & Baselga, J. (2001). Trastuzumab (herceptin), a humanized anti-Her2 receptor monoclonal antibody, inhibits basal and activated Her2 ectodomain cleavage in breast cancer cells. *Cancer Research*, *61*(12), 4744–4749.
40. Feldmann, M., & Maini, R. N. (2003). TNF defined as a therapeutic target for rheumatoid arthritis and other autoimmune diseases. *Nature Medicine*, *9*(10), 1245–1250. https://doi.org/10.1038/nm939
41. Burmester, G. R., Blanco, R., Charles-Schoeman, C., Wollenhaupt, J., Zerbini, C., Benda, B., Gruben, D., Wallenstein, G., Krishnaswami, S., Zwillich, S. H., Koncz, T., Soma, K., Bradley, J., Mebus, C., & ORAL Step investigators. (2013). Tofacitinib (CP-690,550) in combination with methotrexate in patients with active rheumatoid arthritis with an inadequate response to tumour necrosis factor inhibitors: A randomised phase 3 trial. *Lancet (London, England)*, *381*(9865), 451–460. https://doi.org/10.1016/S0140-6736(12)61424-X
42. Sator, P. (2018). Safety and tolerability of adalimumab for the treatment of psoriasis: A review summarizing 15 years of real-life experience. *Therapeutic Advances in Chronic Disease*, *9*(8), 147–158. https://doi.org/10.1177/2040622318772705
43. Monaco, C., Nanchahal, J., Taylor, P., & Feldmann, M. (2015). Anti-TNF therapy: Past, present and future. *International Immunology*, *27*(1), 55–62. https://doi.org/10.1093/intimm/dxu102
44. Cáceres, M. C., Guerrero-Martín, J., Pérez-Civantos, D., Palomo-López, P., Delgado-Mingorance, J. I., & Durán-Gómez, N. (2019). The importance of early identification of infusion-related reactions to monoclonal antibodies. *Therapeutics and Clinical Risk Management*, *15*, 965–977. https://doi.org/10.2147/TCRM.S204909
45. Doessegger, L., & Banholzer, M. L. (2015). Clinical development methodology for infusion-related reactions with monoclonal antibodies. *Clinical & Translational Immunology*, *4*(7), e39. https://doi.org/10.1038/cti.2015.14
46. Roselló, S., Blasco, I., García Fabregat, L., Cervantes, A., & Jordan, K. (2017). Management of infusion reactions to systemic anticancer therapy: ESMO Clinical Practice Guidelines. *Annals of Oncology*, *28*, iv100–iv118. https://doi.org/10.1093/annonc/mdx216
47. Gupta, A., Gonzalez-Rojas, Y., Juarez, E., Crespo Casal, M., Moya, J., Rodrigues Falci, D., Sarkis, E., Solis, J., Zheng, H., Scott, N., Cathcart, A. L., Parra, S., Sager, J. E., Austin, D., Peppercorn, A., Alexander, E., Yeh, W. W., Brinson, C., Aldinger, M., & Shapiro, A. E. (2022). Effect of Sotrovimab on Hospitalization or Death Among High-risk Patients With Mild to Moderate COVID-19. *JAMA*, *327*(13), 1236–1246. https://doi.org/10.1001/jama.2022.2832
48. Chames, P., Van Regenmortel, M., Weiss, E., & Baty, D. (2009). Therapeutic antibodies: Successes, limitations and hopes for the future. *British Journal of Pharmacology*, *157*(2), 220–233. https://doi.org/10.1111/j.1476-5381.2009.00190.x
49. Mayrhofer, P., & Kunert, R. (n.d.). Nomenclature of humanized mAbs: Early concepts, current challenges and future perspectives. *Human Antibodies*, *27*(1), 37–51. https://doi.org/10.3233/HAB-180347
50. Dillman, R. O., Shawler, D. L., McCallister, T. J., & Halpern, S. E. (1994). Human anti-mouse antibody response in cancer patients following single low-dose injections of radiolabeled murine monoclonal antibodies. *Cancer Biotherapy*, *9*(1), 17–28. https://doi.org/10.1089/cbr.1994.9.17
51. Tjandra, J. J., Ramadi, L., & McKenzie, I. F. (1990). Development of human anti-murine antibody (HAMA) response in patients. *Immunology and Cell Biology*, *68 (Pt 6)*, 367–376. https://doi.org/10.1038/icb.1990.50
52. Harding, F. A., Stickler, M. M., Razo, J., & DuBridge, R. B. (2010). The immunogenicity of humanized and fully human antibodies. *MAbs*, *2*(3), 256–265.
53. Morrison, S. L., Johnson, M. J., Herzenberg, L. A., & Oi, V. T. (1984). Chimeric Human Antibody Molecules: Mouse Antigen-Binding Domains with Human Constant Region Domains. *Proceedings of the National Academy of Sciences of the United States of America*, *81*(21), 6851–6855.
54. Duvall, M., Bradley, N., & Fiorini, R. N. (2011). A novel platform to produce human monoclonal antibodies. *MAbs*, *3*(2), 203–208. https://doi.org/10.4161/mabs.3.2.14774
55. Tamhane, U. U., & Gurm, H. S. (2008). The chimeric monoclonal antibody abciximab: A systematic review of its safety in contemporary practice. *Expert Opinion on Drug Safety*, *7*(6), 809–819. https://doi.org/10.1517/14740330802500353
56. Riechmann, L., Clark, M., Waldmann, H., & Winter, G. (1988). Reshaping human antibodies for therapy. *Nature*, *332*(6162), Article 6162. https://doi.org/10.1038/332323a0

57. Tsurushita, N., Hinton, P. R., & Kumar, S. (2005). Design of humanized antibodies: From anti-Tac to Zenapax. *Methods (San Diego, Calif.)*, *36*(1), 69–83. https://doi.org/10.1016/j.ymeth.2005.01.007
58. Better, M., Chang, C. P., Robinson, R. R., & Horwitz, A. H. (1988). Escherichia coli secretion of an active chimeric antibody fragment. *Science (New York, N.Y.)*, *240*(4855), 1041–1043. https://doi.org/10.1126/science.3285471
59. Skerra, A., & Plückthun, A. (1988). Assembly of a functional immunoglobulin Fv fragment in Escherichia coli. *Science (New York, N.Y.)*, *240*(4855), 1038–1041. https://doi.org/10.1126/science.3285470
60. Nelson, P., Reynolds, G., Waldron, E., E, W., K, G., & Murray, P. (2000). Monoclonal antibodies. *Molecular Pathology*, *53*, 111–117.
61. Rosano, G. L., & Ceccarelli, E. A. (2014). Recombinant protein expression in Escherichia coli: Advances and challenges. *Frontiers in Microbiology*, *5*. https://www.frontiersin.org/articles/10.3389/fmicb.2014.00172
62. Andersen, D. C., & Krummen, L. (2002). Recombinant protein expression for therapeutic applications. *Current Opinion in Biotechnology*, *13*(2), 117–123. https://doi.org/10.1016/s0958-1669(02)00300-2
63. Sarramegna, V., Talmont, F., Demange, P., & Milon, A. (2003). Heterologous expression of G-protein-coupled receptors: Comparison of expression systems from the standpointof large-scale production and purification. *Cellular and Molecular Life Sciences CMLS*, *60*(8), 1529–1546. https://doi.org/10.1007/s00018-003-3168-7
64. Walsh, C., Duffy, G., O'Mahony, R., Fanning, S., Blair, I. S., & McDowell, D. A. (2006). Antimicrobial resistance in Irish isolates of verocytotoxigenic Escherichia coli (E. coli)—VTEC. *International Journal of Food Microbiology*, *109*(3), 173–178. https://doi.org/10.1016/j.ijfoodmicro.2006.01.023
65. Moshitch-Moshkovitz, S., Heldman, Y., Yayon, A., & Katchalski-Katzir, E. (2000). Sorting polyclonal antibodies into functionally distinct fractions using peptide phage display: "a library on top of a library." *Journal of Immunological Methods*, *242*(1–2), 183–191. https://doi.org/10.1016/s0022-1759(00)00247-7
66. Li, S. J., & Hochstrasser, M. (2000). The yeast ULP2 (SMT4) gene encodes a novel protease specific for the ubiquitin-like Smt3 protein. *Molecular and Cellular Biology*, *20*(7), 2367–2377. https://doi.org/10.1128/MCB.20.7.2367-2377.2000
67. Hoogenboom, H. R. (2005). Selecting and screening recombinant antibody libraries. *Nature Biotechnology*, *23*(9), 1105–1116. https://doi.org/10.1038/nbt1126
68. Hoet, R. M., Cohen, E. H., Kent, R. B., Rookey, K., Schoonbroodt, S., Hogan, S., Rem, L., Frans, N., Daukandt, M., Pieters, H., van Hegelsom, R., Neer, N. C., Nastri, H. G., Rondon, I. J., Leeds, J. A., Hufton, S. E., Huang, L., Kashin, I., Devlin, M., … Ladner, R. C. (2005). Generation of high-affinity human antibodies by combining donor-derived and synthetic complementarity-determining-region diversity. *Nature Biotechnology*, *23*(3), 344–348. https://doi.org/10.1038/nbt1067
69. Karbalaei, M., Rezaee, S. A., & Farsiani, H. (2020). Pichia pastoris: A highly successful expression system for optimal synthesis of heterologous proteins. *Journal of Cellular Physiology*, *235*(9), 5867–5881. https://doi.org/10.1002/jcp.29583
70. Chiba, Y., & Jigami, Y. (2007). Production of humanized glycoproteins in bacteria and yeasts. *Current Opinion in Chemical Biology*, *11*(6), 670–676. https://doi.org/10.1016/j.cbpa.2007.08.037
71. Orlean, P. (2012). Architecture and Biosynthesis of the Saccharomyces cerevisiae Cell Wall. *Genetics*, *192*(3), 775–818. https://doi.org/10.1534/genetics.112.144485
72. Li, F., Vijayasankaran, N., Shen, A. (Yijuan), Kiss, R., & Amanullah, A. (2010). Cell culture processes for monoclonal antibody production. *MAbs*, *2*(5), 466–477. https://doi.org/10.4161/mabs.2.5.12720
73. Farid, S. S. (2006). Established bioprocesses for producing antibodies as a basis for future planning. *Advances in Biochemical Engineering/Biotechnology*, *101*, 1–42. https://doi.org/10.1007/10_014
74. Farid, S. (2009). Economic Drivers and Trade-Offs in Antibody Purification Processes. *BioPharm International*, *2009 Supplement*(2). https://www.biopharminternational.com/view/economic-drivers-and-trade-offs-antibody-purification-processes
75. Grodzki, A. C., & Berenstein, E. (2010). Antibody purification: Ion-exchange chromatography. *Methods in Molecular Biology (Clifton, N.J.)*, *588*, 27–32. https://doi.org/10.1007/978-1-59745-324-0_4
76. Hernandez, I., Bott, S. W., Patel, A. S., Wolf, C. G., Hospodar, A. R., Sampathkumar, S., & Shrank, W. H. (2018). Pricing of monoclonal antibody therapies: Higher if used for cancer? *The American Journal*

of Managed Care, *24*(2), 109–112.
77. Graumann, K., & Premstaller, A. (2006). Manufacturing of recombinant therapeutic proteins in microbial systems. *Biotechnology Journal*, *1*(2), 164–186. https://doi.org/10.1002/biot.200500051
78. Baselga, J., & Arteaga, C. L. (2005). Critical update and emerging trends in epidermal growth factor receptor targeting in cancer. *Journal of Clinical Oncology: Official Journal of the American Society of Clinical Oncology*, *23*(11), 2445–2459. https://doi.org/10.1200/JCO.2005.11.890
79. Yarden, Y., & Sliwkowski, M. X. (2001). Untangling the ErbB signalling network. *Nature Reviews. Molecular Cell Biology*, *2*(2), 127–137. https://doi.org/10.1038/35052073
80. Wieduwilt, M. J., & Moasser, M. M. (2008). The epidermal growth factor receptor family: Biology driving targeted therapeutics. *Cellular and Molecular Life Sciences: CMLS*, *65*(10), 1566–1584. https://doi.org/10.1007/s00018-008-7440-8
81. Scaltriti, M., & Baselga, J. (2006). The epidermal growth factor receptor pathway: A model for targeted therapy. *Clinical Cancer Research: An Official Journal of the American Association for Cancer Research*, *12*(18), 5268–5272. https://doi.org/10.1158/1078-0432.CCR-05-1554
82. Scott, A. M., Allison, J. P., & Wolchok, J. D. (2012). Monoclonal antibodies in cancer therapy. *Cancer Immunity*, *12*, 14.
83. Amado, R. G., Wolf, M., Peeters, M., Van Cutsem, E., Siena, S., Freeman, D. J., Juan, T., Sikorski, R., Suggs, S., Radinsky, R., Patterson, S. D., & Chang, D. D. (2008). Wild-type KRAS is required for panitumumab efficacy in patients with metastatic colorectal cancer. *Journal of Clinical Oncology: Official Journal of the American Society of Clinical Oncology*, *26*(10), 1626–1634. https://doi.org/10.1200/JCO.2007.14.7116
84. Siena, S., Sartore-Bianchi, A., Di Nicolantonio, F., Balfour, J., & Bardelli, A. (2009). Biomarkers Predicting Clinical Outcome of Epidermal Growth Factor Receptor–Targeted Therapy in Metastatic Colorectal Cancer. *JNCI Journal of the National Cancer Institute*, *101*(19), 1308–1324. https://doi.org/10.1093/jnci/djp280
85. Mehra, R., Cohen, R. B., & Burtness, B. A. (2008). The Role of Cetuximab for the Treatment of Squamous Cell Carcinoma of the Head and Neck. *Clinical Advances in Hematology & Oncology : H&O*, *6*(10), 742–750.
86. Obukhanych, T. V., & Nussenzweig, M. C. (2006). T-independent type II immune responses generate memory B cells. *The Journal of Experimental Medicine*, *203*(2), 305–310. https://doi.org/10.1084/jem.20052036
87. Glennie, M. J., French, R. R., Cragg, M. S., & Taylor, R. P. (2007). Mechanisms of killing by anti-CD20 monoclonal antibodies. *Molecular Immunology*, *44*(16), 3823–3837. https://doi.org/10.1016/j.molimm.2007.06.151
88. Casan, J. M. L., Wong, J., Northcott, M. J., & Opat, S. (2018). Anti-CD20 monoclonal antibodies: Reviewing a revolution. *Human Vaccines & Immunotherapeutics*, *14*(12), 2820–2841. https://doi.org/10.1080/21645515.2018.1508624
89. Saini, S., Rosen, K. E., Hsieh, H.-J., Wong, D. A., Conner, E., Kaplan, A., Spector, S., & Maurer, M. (2011). A randomized, placebo-controlled, dose-ranging study of single-dose omalizumab in patients with H1-antihistamine-refractory chronic idiopathic urticaria. *The Journal of Allergy and Clinical Immunology*, *128*(3), 567-573.e1. https://doi.org/10.1016/j.jaci.2011.06.010
90. Jaglowski, S. M., Alinari, L., Lapalombella, R., Muthusamy, N., & Byrd, J. C. (2010). The clinical application of monoclonal antibodies in chronic lymphocytic leukemia. *Blood*, *116*(19), 3705–3714. https://doi.org/10.1182/blood-2010-04-001230
91. The species Severe acute respiratory syndrome-related coronavirus: Classifying 2019-nCoV and naming it SARS-CoV-2. (2020). *Nature Microbiology*, *5*(4), 536–544. https://doi.org/10.1038/s41564-020-0695-z
92. *Weekly epidemiological update on COVID-19—27 July 2022*. (n.d.). Retrieved January 31, 2023, from https://www.who.int/publications/m/item/weekly-epidemiological-update-on-covid-19---27-july-2022
93. Huang, Y., Yang, C., Xu, X., Xu, W., & Liu, S. (2020). Structural and functional properties of SARS-CoV-2 spike protein: Potential antivirus drug development for COVID-19. *Acta Pharmacologica Sinica*, *41*(9), Article 9. https://doi.org/10.1038/s41401-020-0485-4
94. Harvey, W. T., Carabelli, A. M., Jackson, B., Gupta, R. K., Thomson, E. C., Harrison, E. M., Ludden, C., Reeve, R., Rambaut, A., Peacock, S. J., & Robertson, D. L. (2021). SARS-CoV-2 variants, spike

mutations and immune escape. *Nature Reviews Microbiology*, *19*(7), Article 7. https://doi.org/10.1038/s41579-021-00573-0
95. *WHO recommends against the use of remdesivir in COVID-19 patients*. (n.d.). Retrieved January 31, 2023, from https://www.who.int/news-room/feature-stories/detail/who-recommends-against-the-use-of-remdesivir-in-covid-19-patients
96. Beigel, J. H., Tomashek, K. M., Dodd, L. E., Mehta, A. K., Zingman, B. S., Kalil, A. C., Hohmann, E., Chu, H. Y., Luetkemeyer, A., Kline, S., Lopez de Castilla, D., Finberg, R. W., Dierberg, K., Tapson, V., Hsieh, L., Patterson, T. F., Paredes, R., Sweeney, D. A., Short, W. R., … Lane, H. C. (2020). Remdesivir for the Treatment of Covid-19—Final Report. *New England Journal of Medicine*, *383*(19), 1813–1826. https://doi.org/10.1056/NEJMoa2007764
97. Commissioner, O. of the. (2022, March 25). *Coronavirus (COVID-19) Update: FDA Limits Use of Certain Monoclonal Antibodies to Treat COVID-19 Due to the Omicron Variant*. FDA; FDA. https://www.fda.gov/news-events/press-announcements/coronavirus-covid-19-update-fda-limits-use-certain-monoclonal-antibodies-treat-covid-19-due-omicron
98. Weinreich, D. M., Sivapalasingam, S., Norton, T., Ali, S., Gao, H., Bhore, R., Xiao, J., Hooper, A. T., Hamilton, J. D., Musser, B. J., Rofail, D., Hussein, M., Im, J., Atmodjo, D. Y., Perry, C., Pan, C., Mahmood, A., Hosain, R., Davis, J. D., … Yancopoulos, G. D. (2021). REGEN-COV Antibody Combination and Outcomes in Outpatients with Covid-19. *New England Journal of Medicine*, *385*(23), e81. https://doi.org/10.1056/NEJMoa2108163
99. Rossignol, J.-F., Bardin, M. C., Fulgencio, J., Mogelnicki, D., & Bréchot, C. (2022). A randomized double-blind placebo-controlled clinical trial of nitazoxanide for treatment of mild or moderate COVID-19. *EClinicalMedicine*, *45*, 101310. https://doi.org/10.1016/j.eclinm.2022.101310
100. Weisblum, Y., Schmidt, F., Zhang, F., DaSilva, J., Poston, D., Lorenzi, J. C., Muecksch, F., Rutkowska, M., Hoffmann, H.-H., Michailidis, E., Gaebler, C., Agudelo, M., Cho, A., Wang, Z., Gazumyan, A., Cipolla, M., Luchsinger, L., Hillyer, C. D., Caskey, M., … Bieniasz, P. D. (2020). Escape from neutralizing antibodies by SARS-CoV-2 spike protein variants. *ELife*, *9*, e61312. https://doi.org/10.7554/eLife.61312
101. Yuan, M., Wu, N. C., Zhu, X., Lee, C.-C. D., So, R. T. Y., Lv, H., Mok, C. K. P., & Wilson, I. A. (2020). A highly conserved cryptic epitope in the receptor binding domains of SARS-CoV-2 and SARS-CoV. *Science (New York, N.y.)*, *368*(6491), 630–633. https://doi.org/10.1126/science.abb7269
102. Ferré, E. M. N., Schmitt, M. M., Ochoa, S., Rosen, L. B., Shaw, E. R., Burbelo, P. D., Stoddard, J. L., Rampertaap, S., DiMaggio, T., Bergerson, J. R. E., Rosenzweig, S. D., Notarangelo, L. D., Holland, S. M., & Lionakis, M. S. (2021). SARS-CoV-2 Spike Protein-Directed Monoclonal Antibodies May Ameliorate COVID-19 Complications in APECED Patients. *Frontiers in Immunology*, *12*. https://doi.org/10.3389/fimmu.2021.720205
103. Orive, G., Hernández, R. M., Gascón, A. R., Calafiore, R., Chang, T. M. S., De Vos, P., Hortelano, G., Hunkeler, D., Lacík, I., Shapiro, A. M. J., & Pedraz, J. L. (2003). Cell encapsulation: Promise and progress. *Nature Medicine*, *9*(1), 104–107. https://doi.org/10.1038/nm0103-104
104. Algire, G. H. (1943). An Adaptation of the Transparent-Chamber Technique to the Mouse. *JNCI: Journal of the National Cancer Institute*, *4*(1), 1–11. https://doi.org/10.1093/jnci/4.1.1
105. Chang, T. M. S. (1964). Semipermeable Microcapsules. *Science*, *146*(3643), 524–525. https://doi.org/10.1126/science.146.3643.524
106. Lim, F., & Sun, A. M. (1980). Microencapsulated Islets as Bioartificial Endocrine Pancreas. *Science*, *210*(4472), 908–910. https://doi.org/10.1126/science.6776628
107. Calafiore, R., Basta, G., Luca, G., Lemmi, A., Montanucci, M. P., Calabrese, G., Racanicchi, L., Mancuso, F., & Brunetti, P. (2006). Microencapsulated pancreatic islet allografts into nonimmunosuppressed patients with type 1 diabetes: First two cases. *Diabetes Care*, *29*(1), 137–138. https://doi.org/10.2337/diacare.29.1.137
108. Aebischer, P., Pochon, N. A., Heyd, B., Deglon, N., Joseph, J. M., Zurn, A. D., Baetge, E. E., Hammang, J. P., Goddard, M., Lysaght, M., Kaplan, F., Kato, A. C., Schluep, M., Hirt, L., Regli, F., Porchet, F., & De Tribolet, N. (1996). Gene therapy for amyotrophic lateral sclerosis (ALS) using a polymer encapsulated xenogenic cell line engineered to secrete hCNTF. *Human Gene Therapy*, *7*(7), 851–860. https://doi.org/10.1089/hum.1996.7.7-851
109. Garcia, P., Youssef, I., Utvik, J. K., Florent-Béchard, S., Barthélémy, V., Malaplate-Armand, C.,

Kriem, B., Stenger, C., Koziel, V., Olivier, J.-L., Escanye, M.-C., Hanse, M., Allouche, A., Desbène, C., Yen, F. T., Bjerkvig, R., Oster, T., Niclou, S. P., & Pillot, T. (2010). Ciliary neurotrophic factor cell-based delivery prevents synaptic impairment and improves memory in mouse models of Alzheimer's disease. *The Journal of Neuroscience: The Official Journal of the Society for Neuroscience*, *30*(22), 7516–7527. https://doi.org/10.1523/JNEUROSCI.4182-09.2010
110. Kuramoto, S., Yasuhara, T., Agari, T., Kondo, A., Jing, M., Kikuchi, Y., Shinko, A., Wakamori, T., Kameda, M., Wang, F., Kin, K., Edahiro, S., Miyoshi, Y., & Date, I. (2011). BDNF-secreting capsule exerts neuroprotective effects on epilepsy model of rats. *Brain Research*, *1368*, 281–289. https://doi.org/10.1016/j.brainres.2010.10.054
111. Luo, X.-M., Lin, H., Wang, W., Geaney, M. S., Law, L., Wynyard, S., Shaikh, S. B., Waldvogel, H., Faull, R. L. M., Elliott, R. B., Skinner, S. J. M., Lee, J. E., & Tan, P. L.-J. (2013). Recovery of neurological functions in non-human primate model of Parkinson's disease by transplantation of encapsulated neonatal porcine choroid plexus cells. *Journal of Parkinson's Disease*, *3*(3), 275–291. https://doi.org/10.3233/JPD-130214
112. Dubrot, J., Portero, A., Orive, G., Hernández, R. M., Palazón, A., Rouzaut, A., Perez-Gracia, J. L., Hervás-Stubbs, S., Pedraz, J. L., & Melero, I. (2010). Delivery of immunostimulatory monoclonal antibodies by encapsulated hybridoma cells. *Cancer Immunology, Immunotherapy*, *59*(11), 1621–1631. https://doi.org/10.1007/s00262-010-0888-z
113. Hortelano, G., Al-Hendy, A., Ofosu, F. A., & Chang, P. L. (1996). Delivery of Human Factor IX in Mice by Encapsulated Recombinant Myoblasts: A Novel Approach Towards Allogeneic Gene Therapy of Hemophilia B. *Blood*, *87*(12), 5095–5103. https://doi.org/10.1182/blood.V87.12.5095.bloodjournal87125095
114. Wen, J., Vargas, A. G., Ofosu, F. A., & Hortelano, G. (2006). Sustained and therapeutic levels of human factor IX in hemophilia B mice implanted with microcapsules: Key role of encapsulated cells. *The Journal of Gene Medicine*, *8*(3), 362–369. https://doi.org/10.1002/jgm.852
115. Orive, G., De Castro, M., Ponce, S., Hernández, R. M., Gascón, A. R., Bosch, M., Alberch, J., & Pedraz, J. L. (2005). Long-Term Expression of Erythropoietin from Myoblasts Immobilized in Biocompatible and Neovascularized Microcapsules. *Molecular Therapy*, *12*(2), 283–289. https://doi.org/10.1016/j.ymthe.2005.04.002
116. Orive, G., Echave, M. C., Pedraz, J. L., Golafshan, N., Dolatshahi-Pirouz, A., Paolone, G., & Emerich, D. (2019). Advances in cell-laden hydrogels for delivering therapeutics. *Expert Opinion on Biological Therapy*, *19*(12), 1219–1222. https://doi.org/10.1080/14712598.2019.1654452
117. Elliott, R. B., Escobar, L., Tan, P. L. J., Muzina, M., Zwain, S., & Buchanan, C. (2007). Live encapsulated porcine islets from a type 1 diabetic patient 9.5 yr after xenotransplantation. *Xenotransplantation*, *14*(2), 157–161. https://doi.org/10.1111/j.1399-3089.2007.00384.x
118. Löhr, M., Hoffmeyer, A., Kröger, J., Freund, M., Hain, J., Holle, A., Karle, P., Knöfel, W. T., Liebe, S., Müller, P., Nizze, H., Renner, M., Saller, R. M., Wagner, T., Hauenstein, K., Günzburg, W. H., & Salmons, B. (2001). Microencapsulated cell-mediated treatment of inoperable pancreatic carcinoma. *Lancet (London, England)*, *357*(9268), 1591–1592. https://doi.org/10.1016/s0140-6736(00)04749-8
119. Orive, G., Santos-Vizcaino, E., Pedraz, J. L., Hernandez, R. M., Vela Ramirez, J. E., Dolatshahi-Pirouz, A., Khademhosseini, A., Peppas, N. A., & Emerich, D. F. (2019). 3D cell-laden polymers to release bioactive products in the eye. *Progress in Retinal and Eye Research*, *68*, 67–82. https://doi.org/10.1016/j.preteyeres.2018.10.002
120. Soon-Shiong, P., Heintz, R. E., Merideth, N., Yao, Q. X., Yao, Z., Zheng, T., Murphy, M., Moloney, M. K., Schmehl, M., Harris, M., Mendez, R., Mendez, R., & Sandford, P. A. (1994). Insulin independence in a type 1 diabetic patient after encapsulated islet transplantation. *The Lancet*, *343*(8903), 950–951. https://doi.org/10.1016/S0140-6736(94)90067-1
121. Shapiro, A. M., Lakey, J. R., Ryan, E. A., Korbutt, G. S., Toth, E., Warnock, G. L., Kneteman, N. M., & Rajotte, R. V. (2000). Islet transplantation in seven patients with type 1 diabetes mellitus using a glucocorticoid-free immunosuppressive regimen. *The New England Journal of Medicine*, *343*(4), 230–238. https://doi.org/10.1056/NEJM200007273430401
122. Alagpulinsa, D. A., Cao, J. J. L., Driscoll, R. K., Sîrbulescu, R. F., Penson, M. F. E., Sremac, M., Engquist, E. N., Brauns, T. A., Markmann, J. F., Melton, D. A., & Poznansky, M. C. (2019). Alginate-microencapsulation of human stem cell–derived β cells with CXCL12 prolongs their survival and function

in immunocompetent mice without systemic immunosuppression. *American Journal of Transplantation*, *19*(7), 1930–1940. https://doi.org/10.1111/ajt.15308
123. Pradeu, T., & Cooper, E. L. (2012). The danger theory: 20 years later. *Frontiers in Immunology*, *3*, 287. https://doi.org/10.3389/fimmu.2012.00287
124. Kono, H., & Rock, K. L. (2008). How dying cells alert the immune system to danger. *Nature Reviews. Immunology*, *8*(4), 279–289. https://doi.org/10.1038/nri2215
125. Ashimova, A., Yegorov, S., Negmetzhanov, B., & Hortelano, G. (2019). Cell Encapsulation Within Alginate Microcapsules: Immunological Challenges and Outlook. *Frontiers in Bioengineering and Biotechnology*, *7*, 380. https://doi.org/10.3389/fbioe.2019.00380
126. Reyes-Sandoval, A., & Ertl, H. C. J. (2004). CpG Methylation of a Plasmid Vector Results in Extended Transgene Product Expression by Circumventing Induction of Immune Responses. *Molecular Therapy*, *9*(2), 249–261. https://doi.org/10.1016/j.ymthe.2003.11.008
127. Hortelano, G., Xu, N., Vandenberg, A., Solera, J., Chang, P. L., & Ofosu, F. A. (1999). Persistent delivery of factor IX in mice: Gene therapy for hemophilia using implantable microcapsules. *Human Gene Therapy*, *10*(8), 1281–1288. https://doi.org/10.1089/10430349950017969
128. Hortelano, G., Wang, L., Xu, N., & Ofosu, F. A. (2001). Sustained and therapeutic delivery of factor IX in nude haemophilia B mice by encapsulated C2C12 myoblasts: Concurrent tumourigenesis. *Haemophilia: The Official Journal of the World Federation of Hemophilia*, *7*(2), 207–214. https://doi.org/10.1046/j.1365-2516.2001.00492.x
129. Dufrane, D., & Gianello, P. (2012). Pig islet for xenotransplantation in human: Structural and physiological compatibility for human clinical application. *Transplantation Reviews (Orlando, Fla.)*, *26*(3), 183–188. https://doi.org/10.1016/j.trre.2011.07.004
130. Barkai, U., Rotem, A., & de Vos, P. (2016). Survival of encapsulated islets: More than a membrane story. *World Journal of Transplantation*, *6*(1), 69–90. https://doi.org/10.5500/wjt.v6.i1.69
131. Santos, E., Zarate, J., Orive, G., Hernández, R. M., & Pedraz, J. L. (2010). Biomaterials in Cell Microencapsulation. In J. L. Pedraz & G. Orive (Eds.), *Therapeutic Applications of Cell Microencapsulation* (Vol. 670, pp. 5–21). Springer New York. https://doi.org/10.1007/978-1-4419-5786-3_2
132. Schmidt, J. J., Rowley, J., & Kong, H. J. (2008). Hydrogels used for cell-based drug delivery. *Journal of Biomedical Materials Research Part A*, *87A*(4), 1113–1122. https://doi.org/10.1002/jbm.a.32287
133. de Vos, P., Faas, M. M., Strand, B., & Calafiore, R. (2006). Alginate-based microcapsules for immunoisolation of pancreatic islets. *Biomaterials*, *27*(32), 5603–5617. https://doi.org/10.1016/j.biomaterials.2006.07.010
134. Orive, G., De Castro, M., Kong, H.-J., Hernández, R. M., Ponce, S., Mooney, D. J., & Pedraz, J. L. (2009). Bioactive cell-hydrogel microcapsules for cell-based drug delivery. *Journal of Controlled Release*, *135*(3), 203–210. https://doi.org/10.1016/j.jconrel.2009.01.005
135. Weber, L. M., Hayda, K. N., Haskins, K., & Anseth, K. S. (2007). The effects of cell–matrix interactions on encapsulated β-cell function within hydrogels functionalized with matrix-derived adhesive peptides. *Biomaterials*, *28*(19), 3004–3011. https://doi.org/10.1016/j.biomaterials.2007.03.005
136. de Vos, P., Lazarjani, H. A., Poncelet, D., & Faas, M. M. (2014). Polymers in cell encapsulation from an enveloped cell perspective. *Advanced Drug Delivery Reviews*, *67–68*, 15–34. https://doi.org/10.1016/j.addr.2013.11.005
137. Hu, S., & de Vos, P. (2019). Polymeric Approaches to Reduce Tissue Responses Against Devices Applied for Islet-Cell Encapsulation. *Frontiers in Bioengineering and Biotechnology*, *7*. https://www.frontiersin.org/articles/10.3389/fbioe.2019.00134
138. Gasperini, L., Mano, J. F., & Reis, R. L. (2014). Natural polymers for the microencapsulation of cells. *Journal of the Royal Society, Interface*, *11*(100), 20140817. https://doi.org/10.1098/rsif.2014.0817
139. Lee, K. Y., & Mooney, D. J. (2012). Alginate: Properties and biomedical applications. *Progress in Polymer Science*, *37*(1), 106–126. https://doi.org/10.1016/j.progpolymsci.2011.06.003
140. Murua, A., Portero, A., Orive, G., Hernández, R. M., de Castro, M., & Pedraz, J. L. (2008). Cell microencapsulation technology: Towards clinical application. *Journal of Controlled Release*, *132*(2), 76–83. https://doi.org/10.1016/j.jconrel.2008.08.010
141. Orive, G., Tam, S., Pedraz, J., & Halle, J. (2006). Biocompatibility of alginate–poly-l-lysine microcapsules for cell therapy☆. *Biomaterials*, *27*(20), 3691–3700.

https://doi.org/10.1016/j.biomaterials.2006.02.048
142. Bhujbal, S. V., de Haan, B., Niclou, S. P., & de Vos, P. (2014). A novel multilayer immunoisolating encapsulation system overcoming protrusion of cells. *Scientific Reports*, *4*(1), Article 1. https://doi.org/10.1038/srep06856
143. Paredes-Juarez, G. A., De Haan, B. J., Faas, M. M., & De Vos, P. (2014). A Technology Platform to Test the Efficacy of Purification of Alginate. *Materials*, *7*(3), Article 3. https://doi.org/10.3390/ma7032087
144. Becker, T. A., & Kipke, D. R. (2002). Flow properties of liquid calcium alginate polymer injected through medical microcatheters for endovascular embolization. *Journal of Biomedical Materials Research*, *61*(4), 533–540. https://doi.org/10.1002/jbm.10202
145. de Vos, P., Hoogmoed, C. G., & Busscher, H. J. (2002). Chemistry and biocompatibility of alginate-PLL capsules for immunoprotection of mammalian cells. *Journal of Biomedical Materials Research*, *60*(2), 252–259. https://doi.org/10.1002/jbm.10060
146. Kendall, W. F., & Opara, E. C. (2017). Polymeric Materials for Perm-Selective Coating of Alginate Microbeads. *Methods in Molecular Biology (Clifton, N.J.)*, *1479*, 95–109. https://doi.org/10.1007/978-1-4939-6364-5_7
147. Tam, S. K., Dusseault, J., Bilodeau, S., Langlois, G., Hallé, J.-P., & Yahia, L. (2011). Factors influencing alginate gel biocompatibility. *Journal of Biomedical Materials Research Part A*, *98A*(1), 40–52. https://doi.org/10.1002/jbm.a.33047
148. van Hoogmoed, C. G., Busscher, H. J., & de Vos, P. (2003). Fourier transform infrared spectroscopy studies of alginate–PLL capsules with varying compositions. *Journal of Biomedical Materials Research Part A*, *67A*(1), 172–178. https://doi.org/10.1002/jbm.a.10086
149. Hajifathaliha, F., Mahboubi, A., Nematollahi, L., Mohit, E., & Bolourchian, N. (2020). Comparison of different cationic polymers efficacy in fabrication of alginate multilayer microcapsules. *Asian Journal of Pharmaceutical Sciences*, *15*(1), 95–103. https://doi.org/10.1016/j.ajps.2018.11.007
150. Paredes Juárez, G. A., Spasojevic, M., Faas, M. M., & de Vos, P. (2014). Immunological and Technical Considerations in Application of Alginate-Based Microencapsulation Systems. *Frontiers in Bioengineering and Biotechnology*, *2*. https://www.frontiersin.org/articles/10.3389/fbioe.2014.00026
151. Liu, Y., Tong, Y., Wang, S., Deng, Q., & Chen, A. (2013). Influence of different divalent metal ions on the properties of alginate microcapsules and microencapsulated cells. *Journal of Sol-Gel Science and Technology*, *67*(1), 66–76. https://doi.org/10.1007/s10971-013-3051-4
152. Mørch, Ý. A., Donati, I., Strand, B. L., & Skjåk-Bræk, G. (2006). Effect of Ca^{2+}, Ba^{2+}, and Sr^{2+} on Alginate Microbeads. *Biomacromolecules*, *7*(5), 1471–1480. https://doi.org/10.1021/bm060010d
153. Baruch, L., & Machluf, M. (2006). Alginate–chitosan complex coacervation for cell encapsulation: Effect on mechanical properties and on long-term viability. *Biopolymers*, *82*(6), 570–579. https://doi.org/10.1002/bip.20509
154. Shen, Y., Zhukovskaya, N. L., Guo, Q., Florián, J., & Tang, W.-J. (2005). Calcium-independent calmodulin binding and two-metal–ion catalytic mechanism of anthrax edema factor. *The EMBO Journal*, *24*(5), 929–941. https://doi.org/10.1038/sj.emboj.7600574
155. Calafiore, R., & Basta, G. (2014). Clinical application of microencapsulated islets: Actual prospectives on progress and challenges. *Advanced Drug Delivery Reviews*, *67–68*, 84–92. https://doi.org/10.1016/j.addr.2013.09.020
156. Paredes-Juarez, G. A., de Haan, B. J., Faas, M. M., & de Vos, P. (2013). The role of pathogen-associated molecular patterns in inflammatory responses against alginate based microcapsules. *Journal of Controlled Release*, *172*(3), 983–992. https://doi.org/10.1016/j.jconrel.2013.09.009
157. Tam, S. K., Dusseault, J., Polizu, S., Ménard, M., Hallé, J.-P., & Yahia, L. (2006). Impact of residual contamination on the biofunctional properties of purified alginates used for cell encapsulation. *Biomaterials*, *27*(8), 1296–1305. https://doi.org/10.1016/j.biomaterials.2005.08.027
158. Chung, C., & Burdick, J. A. (2009). Influence of three-dimensional hyaluronic acid microenvironments on mesenchymal stem cell chondrogenesis. *Tissue Engineering. Part A*, *15*(2), 243–254. https://doi.org/10.1089/ten.tea.2008.0067
159. Nicodemus, G. D., & Bryant, S. J. (2008). The role of hydrogel structure and dynamic loading on chondrocyte gene expression and matrix formation. *Journal of Biomechanics*, *41*(7), 1528–1536. https://doi.org/10.1016/j.jbiomech.2008.02.034
160. Paredes Juárez, G. A., Spasojevic, M., Faas, M. M., & de Vos, P. (2014). Immunological and

Technical Considerations in Application of Alginate-Based Microencapsulation Systems. *Frontiers in Bioengineering and Biotechnology*, *2*. https://www.frontiersin.org/articles/10.3389/fbioe.2014.00026
161. Garcia-Martin, C., Chuah, M. K., Vandendriessche, T., Ofosu, F. A., & Hortelano, G. (2000). Therapeutic levels of human factor VIII in mice implanted with encapsulated recombinant myoblasts: Potential for gene therapy of hemophilia A. *Transfusion*, *40*(10). https://lirias.kuleuven.be/2878573
162. Wen, J., Xu, N., Li, A., Bourgeois, J., Ofosu, F. A., & Hortelano, G. (2007). Encapsulated human primary myoblasts deliver functional hFIX in hemophilic mice. *The Journal of Gene Medicine*, *9*(11), 1002–1010. https://doi.org/10.1002/jgm.1098
163. Janssens, D. H., Wu, S. J., Sarthy, J. F., Meers, M. P., Myers, C. H., Olson, J. M., Ahmad, K., & Henikoff, S. (2018). Automated in situ chromatin profiling efficiently resolves cell types and gene regulatory programs. *Epigenetics & Chromatin*, *11*(1), 74. https://doi.org/10.1186/s13072-018-0243-8
164. Klein, R. S., & Rubin, J. B. (2004). Immune and nervous system CXCL12 and CXCR4: Parallel roles in patterning and plasticity. *Trends in Immunology*, *25*(6), 306–314. https://doi.org/10.1016/j.it.2004.04.002
165. Liekens, S., Schols, D., & Hatse, S. (2010). CXCL12-CXCR4 Axis in Angiogenesis, Metastasis and Stem Cell Mobilization. *Current Pharmaceutical Design*, *16*(35), 3903–3920. https://doi.org/10.2174/138161210794455003
166. Susek, K. H., Karvouni, M., Alici, E., & Lundqvist, A. (2018). The Role of CXC Chemokine Receptors 1–4 on Immune Cells in the Tumor Microenvironment. *Frontiers in Immunology*, *9*. https://www.frontiersin.org/articles/10.3389/fimmu.2018.02159
167. Yu, X., Wang, D., Wang, X., Sun, S., Zhang, Y., Wang, S., Miao, R., Xu, X., & Qu, X. (2019). CXCL12/CXCR4 promotes inflammation-driven colorectal cancer progression through activation of RhoA signaling by sponging miR-133a-3p. *Journal of Experimental & Clinical Cancer Research*, *38*(1), 32. https://doi.org/10.1186/s13046-018-1014-x
168. Dharshanan, S., Chong, H., Cheah, S. H., & Zamrod, Z. (2014). Stable expression of H1C2 monoclonal antibody in NS0 and CHO cells using pFUSE and UCOE expression system. *Cytotechnology*, *66*(4), 625–633. https://doi.org/10.1007/s10616-013-9615-x
169. Fus-Kujawa, A., Prus, P., Bajdak-Rusinek, K., Teper, P., Gawron, K., Kowalczuk, A., & Sieron, A. L. (2021). An Overview of Methods and Tools for Transfection of Eukaryotic Cells in vitro. *Frontiers in Bioengineering and Biotechnology*, *9*. https://www.frontiersin.org/articles/10.3389/fbioe.2021.701031
170. DeLuca, K. F., Mick, J. E., & DeLuca, J. G. (2022). Production and purification of recombinant monoclonal antibodies from human cells based on a primary sequence. *STAR Protocols*, *3*(4), 101915. https://doi.org/10.1016/j.xpro.2022.101915
171. Schlatter, S., Stansfield, S. H., Dinnis, D. M., Racher, A. J., Birch, J. R., & James, D. C. (2005). On the optimal ratio of heavy to light chain genes for efficient recombinant antibody production by CHO cells. *Biotechnology Progress*, *21*(1), 122–133. https://doi.org/10.1021/bp049780w
172. Zhang, R. Y., & Shen, W. D. (2012). Monoclonal antibody expression in mammalian cells. *Methods in Molecular Biology (Clifton, N.J.)*, *907*, 341–358. https://doi.org/10.1007/978-1-61779-974-7_20
173. Carton, J. M., Sauerwald, T., Hawley-Nelson, P., Morse, B., Peffer, N., Beck, H., Lu, J., Cotty, A., Amegadzie, B., & Sweet, R. (2007). Codon engineering for improved antibody expression in mammalian cells. *Protein Expression and Purification*, *55*(2), 279–286. https://doi.org/10.1016/j.pep.2007.05.017
174. *Coronavirus disease (COVID-19) pandemic*. (n.d.). Retrieved February 14, 2023, from https://www.who.int/europe/emergencies/situations/covid-19
175. *Therapeutics and COVID-19: Living guideline*. (n.d.). Retrieved April 16, 2022, from https://www.who.int/publications-detail-redirect/WHO-2019-nCoV-therapeutics-2022.2
176. Jiang, S., Zhang, X., Yang, Y., Hotez, P. J., & Du, L. (2020). Neutralizing antibodies for the treatment of COVID-19. *Nature Biomedical Engineering*, *4*(12), 1134–1139. https://doi.org/10.1038/s41551-020-00660-2
177. *Monoclonal antibodies for COVID-19 therapy and SARS-CoV-2 detection—PMC*. (n.d.). Retrieved February 14, 2023, from https://www.ncbi.nlm.nih.gov/pmc/articles/PMC8724751/
178. Plichta, J., Kuna, P., & Panek, M. (2022). Monoclonal Antibodies as Potential COVID-19 Therapeutic Agents. *COVID*, *2*(5), Article 5. https://doi.org/10.3390/covid2050045
179. Lopez-Mendez, T. B., Santos-Vizcaino, E., Pedraz, J. L., Hernandez, R. M., & Orive, G. (2021). Cell microencapsulation technologies for sustained drug delivery: Clinical trials and companies. *Drug*

Discovery Today, *26*(3), 852–861. https://doi.org/10.1016/j.drudis.2020.11.019
180. Walls, A. C., Park, Y.-J., Tortorici, M. A., Wall, A., McGuire, A. T., & Veesler, D. (2020). Structure, Function, and Antigenicity of the SARS-CoV-2 Spike Glycoprotein. *Cell*, *181*(2), 281-292.e6. https://doi.org/10.1016/j.cell.2020.02.058
181. Thakur, A., Sengupta, R., Matsui, H., Lillicrap, D., Jones, K., & Hortelano, G. (2010). Characterization of viability and proliferation of alginate-poly-L-lysine-alginate encapsulated myoblasts using flow cytometry. *Journal of Biomedical Materials Research. Part B, Applied Biomaterials*, *94*(2), 296–304. https://doi.org/10.1002/jbm.b.31648
182. Hortelano, G., Wang, L., Xu, N., & Ofosu, F. A. (2001). Sustained and therapeutic delivery of factor IX in nude haemophilia B mice by encapsulated C2C12 myoblasts: Concurrent tumourigenesis. *Haemophilia*, *7*(2), 207–214. https://doi.org/10.1046/j.1365-2516.2001.00492.x
183. ter Meulen, J., van den Brink, E. N., Poon, L. L. M., Marissen, W. E., Leung, C. S. W., Cox, F., Cheung, C. Y., Bakker, A. Q., Bogaards, J. A., van Deventer, E., Preiser, W., Doerr, H. W., Chow, V. T., de Kruif, J., Peiris, J. S. M., & Goudsmit, J. (2006). Human monoclonal antibody combination against SARS coronavirus: Synergy and coverage of escape mutants. *PLoS Medicine*, *3*(7), e237. https://doi.org/10.1371/journal.pmed.0030237
184. Wang, C., Li, W., Drabek, D., Okba, N. M. A., van Haperen, R., Osterhaus, A. D. M. E., van Kuppeveld, F. J. M., Haagmans, B. L., Grosveld, F., & Bosch, B.-J. (2020). A human monoclonal antibody blocking SARS-CoV-2 infection. *Nature Communications*, *11*(1), Article 1. https://doi.org/10.1038/s41467-020-16256-y
185. Huo, J., Zhao, Y., Ren, J., Zhou, D., Duyvesteyn, H. M. E., Ginn, H. M., Carrique, L., Malinauskas, T., Ruza, R. R., Shah, P. N. M., Tan, T. K., Rijal, P., Coombes, N., Bewley, K. R., Tree, J. A., Radecke, J., Paterson, N. G., Supasa, P., Mongkolsapaya, J., … Stuart, D. I. (2020). Neutralization of SARS-CoV-2 by Destruction of the Prefusion Spike. *Cell Host & Microbe*, *28*(3), 445-454.e6. https://doi.org/10.1016/j.chom.2020.06.010
186. Taylor, P. C., Adams, A. C., Hufford, M. M., de la Torre, I., Winthrop, K., & Gottlieb, R. L. (2021). Neutralizing monoclonal antibodies for treatment of COVID-19. *Nature Reviews Immunology*, *21*(6), Article 6. https://doi.org/10.1038/s41577-021-00542-x
187. Ashimova, A., Yegorov, S., Negmetzhanov, B., & Hortelano, G. (2019). Cell Encapsulation Within Alginate Microcapsules: Immunological Challenges and Outlook. *Frontiers in Bioengineering and Biotechnology*, *7*, 380. https://doi.org/10.3389/fbioe.2019.00380
188. Razonable, R. R., Pawlowski, C., O'Horo, J. C., Arndt, L. L., Arndt, R., Bierle, D. M., Borgen, M. D., Hanson, S. N., Hedin, M. C., Lenehan, P., Puranik, A., Seville, M. T., Speicher, L. L., Tulledge-Scheitel, S. M., Venkatakrishnan, A. J., Wilker, C. G., Badley, A. D., & Ganesh, R. (2021). Casirivimab–Imdevimab treatment is associated with reduced rates of hospitalization among high-risk patients with mild to moderate coronavirus disease-19. *EClinicalMedicine*, *40*. https://doi.org/10.1016/j.eclinm.2021.101102
189. *Effect of Subcutaneous Casirivimab and Imdevimab Antibody Combination vs Placebo on Development of Symptomatic COVID-19 in Early Asymptomatic SARS-CoV-2 Infection: A Randomized Clinical Trial | Infectious Diseases | JAMA | JAMA Network*. (n.d.). Retrieved March 4, 2022, from https://jamanetwork.com/journals/jama/fullarticle/2788256
190. Chang, P. L., Hortelano, G., Awrey, D. E., & Tse, M. (1994). Growth of recombinant fibroblasts in alginate microcapsules. *Biotechnology and Bioengineering*, *43*(10), 925–933. https://doi.org/10.1002/bit.260431005
191. Sayyar, B., Dodd, M., Wen, J., Ma, S., Marquez-Curtis, L., Janowska-Wieczorek, A., & Hortelano, G. (2012). Encapsulation of factor IX–engineered mesenchymal stem cells in fibrinogen–alginate microcapsules enhances their viability and transgene secretion. *Journal of Tissue Engineering*, *3*(1), 2041731412462018. https://doi.org/10.1177/2041731412462018
192. García-Martín, C., Chuah, M. K. L., Van Damme, A., Robinson, K. E., Vanzieleghem, B., Saint-Remy, J.-M., Gallardo, D., Ofosu, F. A., Vandendriessche, T., & Hortelano, G. (2002). Therapeutic levels of human factor VIII in mice implanted with encapsulated cells: Potential for gene therapy of haemophilia A. *The Journal of Gene Medicine*, *4*(2), 215–223. https://doi.org/10.1002/jgm.248
193. Montanucci, P., Cari, L., Basta, G., Pescara, T., Riccardi, C., Nocentini, G., & Calafiore, R. (2019). Engineered Alginate Microcapsules for Molecular Therapy Through Biologic Secreting Cells. *Tissue Engineering. Part C, Methods*, *25*(5), 296–304. https://doi.org/10.1089/ten.TEC.2018.0329

194. Abani, O., Abbas, A., Abbas, F., Abbas, M., Abbasi, S., Abbass, H., Abbott, A., Abdallah, N., Abdelaziz, A., Abdelfattah, M., Abdelqader, B., Abdul, B., Abdul Rasheed, A., Abdulakeem, A., Abdul-Kadir, R., Abdullah, A., Abdulmumeen, A., Abdul-Raheem, R., Abdulshukkoor, N., … Zyengi, S. (2022). Casirivimab and imdevimab in patients admitted to hospital with COVID-19 (RECOVERY): A randomised, controlled, open-label, platform trial. *The Lancet*, *399*(10325), 665–676. https://doi.org/10.1016/S0140-6736(22)00163-5
195. Milone, M. C., & O'Doherty, U. (2018). Clinical use of lentiviral vectors. *Leukemia*, *32*(7), Article 7. https://doi.org/10.1038/s41375-018-0106-0
196. Zheng, C., Wang, S., Bai, Y., Luo, T., Wang, J., Dai, C., Guo, B., Luo, S., Wang, D., Yang, Y., & Wang, Y. (2018). Lentiviral Vectors and Adeno-Associated Virus Vectors: Useful Tools for Gene Transfer in Pain Research. *Anatomical Record (Hoboken, N.j. : 2007)*, *301*(5), 825–836. https://doi.org/10.1002/ar.23723
197. Cheng, S.-Y., Constantinidis, I., & Sambanis, A. (2006). Insulin secretion dynamics of free and alginate-encapsulated insulinoma cells. *Cytotechnology*, *51*(3), 159–170. https://doi.org/10.1007/s10616-006-9025-4
198. Sayyar, B., Dodd, M., Marquez-Curtis, L., Janowska-Wieczorek, A., & Hortelano, G. (2014). Cell-matrix Interactions of Factor IX (FIX)-engineered human mesenchymal stromal cells encapsulated in RGD-alginate vs. Fibrinogen-alginate microcapsules. *Artificial Cells, Nanomedicine, and Biotechnology*, *42*(2), 102–109. https://doi.org/10.3109/21691401.2013.794354
199. Huo, J., Zhao, Y., Ren, J., Zhou, D., Duyvesteyn, H. M. E., Ginn, H. M., Carrique, L., Malinauskas, T., Ruza, R. R., Shah, P. N. M., Tan, T. K., Rijal, P., Coombes, N., Bewley, K. R., Tree, J. A., Radecke, J., Paterson, N. G., Supasa, P., Mongkolsapaya, J., … Stuart, D. I. (2020). Neutralization of SARS-CoV-2 by Destruction of the Prefusion Spike. *Cell Host & Microbe*, *28*(3), 445-454.e6. https://doi.org/10.1016/j.chom.2020.06.010
200. Orive, G., Ponce, S., Hernández, R. M., Gascón, A. R., Igartua, M., & Pedraz, J. L. (2002). Biocompatibility of microcapsules for cell immobilization elaborated with different type of alginates. *Biomaterials*, *23*(18), 3825–3831. https://doi.org/10.1016/S0142-9612(02)00118-7
201. Hall, K. K., Gattás-Asfura, K. M., & Stabler, C. L. (2011). Microencapsulation of islets within alginate/poly(ethylene glycol) gels cross-linked via Staudinger ligation. *Acta Biomaterialia*, *7*(2), 614–624. https://doi.org/10.1016/j.actbio.2010.07.016
202. Orive, G., Hernández, R. M., Gascón, A. R., Calafiore, R., Chang, T. M. S., Vos, P. D., Hortelano, G., Hunkeler, D., Lacík, I., Shapiro, A. M. J., & Pedraz, J. L. (2003). Cell encapsulation: Promise and progress. *Nature Medicine*, *9*(1), 104–107. https://doi.org/10.1038/nm0103-104
203. Thakur, A., Sengupta, R., Matsui, H., Lillicrap, D., Jones, K., & Hortelano, G. (2010). Characterization of viability and proliferation of alginate-poly-L-lysine-alginate encapsulated myoblasts using flow cytometry. *Journal of Biomedical Materials Research. Part B, Applied Biomaterials*, *94*(2), 296–304. https://doi.org/10.1002/jbm.b.31648
204. Wen, J., Vargas, A. G., Ofosu, F. A., & Hortelano, G. (2006). Sustained and therapeutic levels of human factor IX in hemophilia B mice implanted with microcapsules: Key role of encapsulated cells. *The Journal of Gene Medicine*, *8*(3), 362–369. https://doi.org/10.1002/jgm.852
205. Vaithilingam, V., Fung, C., Ratnapala, S., Foster, J., Vaghjiani, V., Manuelpillai, U., & Tuch, B. E. (2013). Characterisation of the Xenogeneic Immune Response to Microencapsulated Fetal Pig Islet-Like Cell Clusters Transplanted into Immunocompetent C57BL/6 Mice. *PLOS ONE*, *8*(3), e59120. https://doi.org/10.1371/journal.pone.0059120
206. Cousens, L. P., Najafian, N., Mingozzi, F., Elyaman, W., Mazer, B., Moise, L., Messitt, T. J., Su, Y., Sayegh, M., High, K., Khoury, S. J., Scott, D. W., & De Groot, A. S. (2013). In Vitro and In Vivo Studies of IgG-derived Treg Epitopes (Tregitopes): A Promising New Tool for Tolerance Induction and Treatment of Autoimmunity. *Journal of Clinical Immunology*, *33*(Suppl 1), 43–49. https://doi.org/10.1007/s10875-012-9762-4
207. Castaman, G., & Matino, D. (2019). Hemophilia A and B: Molecular and clinical similarities and differences. *Haematologica*, *104*(9), 1702–1709. https://doi.org/10.3324/haematol.2019.221093
208. Gomez, K., Klamroth, R., Mahlangu, J., Mancuso, M. E., Mingot, M. E., & Ozelo, M. C. (2014). Key issues in inhibitor management in patients with haemophilia. *Blood Transfusion*, *12*(Suppl 1), s319–s329. https://doi.org/10.2450/2013.0246-12

209. Caspi, R. R., Silver, P. B., Luger, D., Tang, J., Cortes, L. M., Pennesi, G., Mattapallil, M. J., & Chan, C.-C. (2008). Mouse Models of Experimental Autoimmune Uveitis. *Ophthalmic Research*, *40*(3–4), 169–174. https://doi.org/10.1159/000119871
210. De Groot, A. S., Moise, L., McMurry, J. A., Wambre, E., Van Overtvelt, L., Moingeon, P., Scott, D. W., & Martin, W. (2008). Activation of natural regulatory T cells by IgG Fc-derived peptide "Tregitopes." *Blood*, *112*(8), 3303–3311. https://doi.org/10.1182/blood-2008-02-138073
211. Saraiva, M., & O'Garra, A. (2010). The regulation of IL-10 production by immune cells. *Nature Reviews. Immunology*, *10*(3), 170–181. https://doi.org/10.1038/nri2711
212. Sanjabi, S., Zenewicz, L. A., Kamanaka, M., & Flavell, R. A. (2009). Anti-inflammatory and pro-inflammatory roles of TGF-beta, IL-10, and IL-22 in immunity and autoimmunity. *Current Opinion in Pharmacology*, *9*(4), 447–453. https://doi.org/10.1016/j.coph.2009.04.008
213. *The primary mechanism of the IL-10-regulated antiinflammatory response is to selectively inhibit transcription—PubMed*. (n.d.). Retrieved February 14, 2023, from https://pubmed.ncbi.nlm.nih.gov/15937121/
214. Asadullah, K., Sterry, W., & Volk, H. D. (2003). Interleukin-10 therapy—Review of a new approach. *Pharmacological Reviews*, *55*(2), 241–269. https://doi.org/10.1124/pr.55.2.4
215. Lykken, J. M., Candando, K. M., & Tedder, T. F. (2015). Regulatory B10 cell development and function. *International Immunology*, *27*(10), 471–477. https://doi.org/10.1093/intimm/dxv046
216. O'Garra, A., Barrat, F. J., Castro, A. G., Vicari, A., & Hawrylowicz, C. (2008). Strategies for use of IL-10 or its antagonists in human disease. *Immunological Reviews*, *223*, 114–131. https://doi.org/10.1111/j.1600-065X.2008.00635.x
217. Finn, J. D., Ozelo, M. C., Sabatino, D. E., Franck, H. W. G., Merricks, E. P., Crudele, J. M., Zhou, S., Kazazian, H. H., Lillicrap, D., Nichols, T. C., & Arruda, V. R. (2010). Eradication of neutralizing antibodies to factor VIII in canine hemophilia A after liver gene therapy. *Blood*, *116*(26), 5842–5848. https://doi.org/10.1182/blood-2010-06-288001
218. Ballow, M. (2014). Mechanisms of immune regulation by IVIG. *Current Opinion in Allergy and Clinical Immunology*, *14*(6), 509–515. https://doi.org/10.1097/ACI.0000000000000116
219. Levast, B., Li, Z., & Madrenas, J. (2015). The role of IL-10 in microbiome-associated immune modulation and disease tolerance. *Cytokine*, *75*(2), 291–301. https://doi.org/10.1016/j.cyto.2014.11.027
220. Afraz, S., Stevic, I., Matino, D., Wen, J., Atkinson, H., Chan, A. K. C., & Hortelano, G. (2022). Co-administration of FVIII with IVIG reduces immune response to FVIII in hemophilia A mice. *Scientific Reports*, *12*(1), Article 1. https://doi.org/10.1038/s41598-022-19392-1